CO_2 Capture from Flue Gas Using Solid Molecular Basket Sorbents

(DOE Project DE-FE0000458)

Final Technical Report

For the Period of Sept. 1st, 2009 – Aug. 31st, 2012

Eric Fillerup, Zhonghua Zhang, Emanuela Peduzzi, Dongxiang Wang, Jiahua Guo, Xiaoliang Ma, Xiaoxing Wang, and Chunshan Song* (PI)

The Pennsylvania State University

EMS Energy Institute and Department of Energy and Mineral Engineering

C211 CUL, University Park, PA 16802

*E- Mail: csong@psu.edu / Tel: 814-863-4466 / Fax: 814-865-3573

November 30th, 2012

DISCLAIMER

This report was prepared as an account of work sponsored by an agency of the United States Government. Neither the United States Government nor any agency thereof, or any of their employees, makes any warranty, expressed or implied, or assumes any legal liability or responsibility for the accuracy, completeness, or usefulness of any information, apparatus, product, or process disclosed, or represents that its use would not infringe privately owned rights. Reference herein to any specific commercial product, process, or service by trade name, trademark, manufacturer, or otherwise does not necessarily constitute or imply its endorsement, recommendation, or favoring by the United States Government or any agency thereof. The views and opinions of authors expressed herein do not necessarily state or reflect those of the United States Government or any agency thereof.

ACKNOWLEDGEMENTS

We gratefully acknowledge the support of this work by the US Department of Energy, National Energy Technology Laboratory through the grant DE-FE0000458. We would like to thank the DOE-NETL Project Manager, B. Andrew O'Palko, and the members of NETL team attending our project review meetings for helpful discussions.

Table of Contents

Page

1. List of Tables and Figures …… 3
2. Executive Summary …… 6
3. Introduction …… 9
4. Technical Progress …… 9
4.1. Experimental …… 9
4.2. Development of a new generation of MBS for CO_2 capture and separation (Task 2) …… 10
4.2.1. Exploring to improve the CO_2 sorption performance of MBS …… 10
4.2.1.1. Mesocellular silica Foam based MBS (MCF-MBS) …… 10
4.2.1.2. Hexagonal Mesoporous Silica based MBS (HMS-MBS) …… 12
4.2.2. Exploring low cost support for MBS …… 13
4.2.2.1. Silica-gel-based MBS …… 13
4.2.2.2. Fume-silica-based MBS …… 16
4.2.2.3. Carbon-based MBS …… 18
4.2.3. CO_2 sorption mechanism study by TPD method …… 21
4.3. Computational chemistry approaches (Task 3) …… 22
4.3.1. Computational Methods …… 22
4.3.2. Effect of cross-linking on PEI structure …… 23
4.3.3. CO_2 sorption over PEI and cross-linked PEI …… 23
4.4. Thermal stability improvement (Task 4) …… 23
4.4.1. Effect of Regeneration Temperature for MBS-2 with PEI(Mn, 423) …… 23
4.4.2. The use of PEI with high molecular weight …… 24
4.4.3. Improvement of MBS-2 sorbent via cross-linking …… 28
4.4.4. Improvement of FS-MBS sorbent via cross-linking …… 33
4.5. Scaling up the sorption process (Task 5) …… 35
4.5.1. Proposed process design for CO_2 capture based on PEI/SBA-15 sorbent …… 35
4.5.2. Scale-up test on PEI/SBA-15 sorbent …… 35
4.5.3. Scale-up test on PEI/FS sorbent …… 37
4.6. Conducting a preliminary techno-economic analysis (Task 6) …… 39
4.6.1. Energy consumption estimation …… 39
4.6.2. Material cost estimation …… 40
5. Reference …… 41
6. Publications and Presentations …… 42
7. Milestone Status Report …… 44
8. Milestone Status Description …… 45
9. Appendix – Supporting Figures …… 46

1. List of Tables and Figures

Tables

Page

Table 1. Porous properties of MCF, HMS, SBA-15 and MCM-41 ……..…….. **11**
Table 2. Orthogonal experiment design and results …….…...….. **13**
Table 3. Porous properties of Fumed Silica M5, HS5, EH5 and SBA-15 ……..…….. **16**
Table 4. Pore properties of carbon materials used in this study …….……..….. **18**
Table 5. CO_2 capacity of CB-MBS in comparison with PEI-50/SBA-15 and PEI-50/MCM-41 measured by TGA at 75 °C under a pure CO_2 flow at a flow rate of 100 ml/min ….…….. **19**
Table 6. Textural characterization of C4 and PEI/C4 with different PEI loading ……..…….. **20**
Table 7. Calculated heat of formation for each cross-linked PEIs ……..... **23**
Table 8. The sorption energies of CO_2 on PEI and cross-linked PEIs …….. **23**
Table 9. CO_2 sorption capacity of MBS-2 (423) with cycles at desorption temperatures …… **24**
Table 10. CO_2 sorption capacity of MBS-2 (423) with cycles at elevated temperatures using the stripping N_2 gas containing ~2% H_2O …….……..... **24**
Table 11. CO_2 sorption capacity with cycles and the calculated capacity loss percentages after cycles over the MBS-2 prepared with different PEI molecular weight under dry conditions ……... **27**
Table 12. Table 12. CO_2 sorption capacity with cycles and the calculated capacity loss percentages after cycles over the MBS-2 prepared with different PEI molecular weight under wet conditions **28**
Table 13. CO_2 sorption capacity with cycles and the calculated capacity loss percentages after cycles over the MBS-2 prepared with different PEI molecular weight and cross-linked with diacid compound under dry conditions …….……..….. **31**
Table 14. CO_2 sorption capacity with cycles and the calculated capacity loss percentages after cycles over the MBS-2 prepared with different PEI molecular weight and cross-linked with diacid compound under wet conditions …….……...….. **32**
Table 15. Sorption capacity of MBS-M5 samples with and without OA addition within 5 CO_2 sorption-desorption cycles measured by TGA …….…….. **34**
Table 16. Sorption capacity of MBS-HS5 samples with and without OA addition for 5 cycles of CO_2 sorption-desorption tests measured by TGA …….…….. **34**
Table 17. Operational and thermal data used for heat requirements estimates …….…….. **40**

Figures and Schemes

Figure 1. Typical TGA profiles obtained on PEI(50)/MCF and PEI(50)/SBA-15 during CO_2 sorption and desorption process …….. **11**
Figure 2. CO_2 sorption capacity as a function of PEI loading on the SBA-15-based MBS and MCF-based MBS sorbent …….…….. **11**
Figure 3. Effect of PEI Loading on the CO_2 Sorption Performance of HMS-MBS (red) and MBS-2 (black). Conditions: Temp., 75 °C; CO_2 concentration, 100%; Flow rate, 100 mL/min …...**12**
Figure 4. Effect of Sorption Temperature on the CO_2 Sorption Performance of HMS-MBS ……..**12**
Figure 5. Breakthrough curves of PEI-50/SBA-15 and PEI-50/SG for CO_2 capture from the simulated flue gas (15 v% CO_2, 4.5 v% O_2 in N_2) in presence/absence of moisture at 75 °C and 207 h^{-1} GHSV in the fixed-bed flow sorption system …….……... **15**
Figure 6. Recovery percentage of the CO_2 capacity as a function of sorption-desorption cycle number. Data were from TGA at 75 °C with pure CO_2 gas for sorption and desorption at 75 and 100 °C, respectively, with pure N_2 gas for desorption …….…….. **15**

Figure 7. The CO_2 mass-based and volume-based sorption capacities of PEI-50/SBA-15 and PEI-50/SG measured in TGA with pure CO_2 gas and the fixed-bed flow system with the simulated flue gas both at 75 °C ……. **16**
Figure 8. Gravimetric and volumetric capacity of different fumed silica, silica gel and SBA-15 supported PEI sorbents with 50 wt% PEI loading ……. **16**
Figure 9. Gravimetric and volumetric sorption capacity of PEI/FS-M5 sorbents as a function of PEI loading amount …… **17**
Figure 10. CO_2 sorption capacity as a function of sorption temperature over (■) the PEI-50/FS-M5 and (●) the PEI-50/SG sorbent measured by TGA method …….. **17**
Figure 11. Breakthrough curves of PEI-50/SBA-15 and PEI-50/FS-M5 for CO_2 capture from the simulated flue gas (15 v% CO_2, 4.5 v% O_2 in N_2) in presence/absence of moisture at 75 °C and 207 h^{-1} GHSV in the fixed-bed flow sorption system …….. **18**
Figure 12. The regenerability behavior of MBS (i.e., PEI-50/SBA-15) and PEI-50/FS-M5 measured by TGA for 5 cycles …….. **18**
Figure 13. Effect of PEI loading on CO_2 sorption capacity of PEI/C4 ……... **20**
Figure 14. CO_2 sorption isotherms of PEI-50/C4 measured at 25, 75, and 100 °C …….. **20**
Figure 15. TGA curve and CO_2 sorption capacity for 10 sorption-desorption cycles of PEI(50)/C4 at 75 ºC ……..**21**
Figure 16. Typical CO_2-TPD profile with peak de-convolution and fitting curves ……..**22**
Figure 17. CO_2 uptake as a function of sorption temperature and sorption time over 50 wt% PEI/SBA-15 …….. **22**
Figure 18. TGA profiles for multiple regeneration cycles of MBS-2 (423) at elevated desorption temperatures …….. **24**
Figure 19. TGA profiles for multiple regeneration cycles of MBS-2 (423) at elevated temperatures using the stripping N_2 gas containing ~2 v% H_2O …….. **24**
Figure 20. (A) TGA and (B) DTGA profiles of 50 wt% PEI/SBA-15 with different PEI molecular weight …….. **25**
Figure 21. TGA profiles for multiple regeneration cycles of MBS-2 with PEI molecular weight (Mw) of 600 at elevated temperatures using dry N_2 as the stripping gas for desorption …….. **25**
Figure 22. TGA profiles for multiple regeneration cycles of MBS-2 with PEI molecular weight (Mw) of 1200 at elevated temperatures using dry N_2 as the stripping gas for desorption ……..**25**
Figure 23. Desorption curves of MBS-2 with PEI Mw of 600 at elevated temperatures. ……. **26**
Figure 24. Desorption rates of MBS-2 with different Mw PEI in the regime I and II as a function of desorption temperature …….. **26**
Figure 25. The CO_2 sorption capacity as a function of sorption-desorption cycles over the MBS-2 prepared with PEI molecular weight of (●) 423, (■) 600 and (▲) 1800 under dry conditions measured by TGA …….. **27**
Figure 26. The CO_2 sorption capacity as a function of sorption-desorption cycles over the MBS-2 prepared with PEI molecular weight of (●) 423, (■) 600 and (▲) 1800 under wet conditions measured by TGA …….. **27**
Figure 27. CO_2 breakthrough curves obtained over MBS-2 and BPA/MBS-2 sorbents for CO_2 separation from the model flue gas containing 15% CO_2 and 4.5% O_2 in N_2 at 75 °C …. **29**
Figure 28. CO_2 breakthrough curves obtained over MBS-2 and OA/MBS-2 sorbents for CO_2 separation from the model flue gas containing 15% CO_2 and 4.5% O_2 in N_2 at 75 °C …….. **29**
Figure 29. TGA profiles of SBA-15, 15% PEI/SBA-15, 50% PEI/SBA-15 (i.e., MBS-2) and 1% OA/MBS-2 …….. **30**
Figure 30. FTIR spectra of oxalic acid cross-linked MBS-2 under N_2 flow at different temperatures …….. **30**
Figure 31. The CO_2 sorption capacity as a function of sorption-desorption cycles over the MBS-2(423), 5%OA-MBS-2(423), MBS-2(600) and 5%OA-MBS-2(600) samples under dry conditions measured by TGA …….. **31**

Figure 32. The CO_2 sorption capacity as a function of sorption-desorption cycles over the MBS-2(600), 5%OA-MBS-2(600), and 5%TPA-MBS-2(600) samples under dry conditions measured by TGA …….. **31**
Figure 33. The CO_2 sorption capacity as a function of sorption-desorption cycles over the MBS-2(423), 5%OA-MBS-2(423), MBS-2(600) and 5%OA-MBS-2(600) samples under wet conditions measured by TGA …….…….…….. **32**
Figure 34. The CO_2 sorption capacity as a function of sorption-desorption cycles over the MBS-2(600), 5%OA-MBS-2(600), and 5%TPA-MBS-2(600) samples under dry conditions measured by TGA ……..…….…….. **32**
Figure 35. TGA profiles of MBS-M5 samples with and without OA addition within 5 cyclic CO_2 sorption-desorption tests ……..……..…….. **34**
Figure 36. TGA profiles of MBS-HS5 samples with and without OA addition for 5 cycles of CO_2 sorption-desorption tests …….…….. **34**
Figure 37. TGA profiles of MBS-HS5 samples with and without OA addition under N_2 flow …….. **35**
Figure 38. Appearance of PEI/SBA-15 in powder and pellet (10-18 mesh, i.e., 1-2 mm) form and the 200 mL column in GC oven used in the scale-up test …….…….. **36**
Figure 39. Breakthrough curves of CO_2 over the PEI/SBA-15 sorbent pellets (10-18 mesh, or 1-2 mm, 2 mL in total) at 75 °C for CO_2 capture from model flue gas containing 14% CO_2 in N_2 with a flow rate of 100 mL/min (a GHSV of ~3000 h^{-1}) …….…….. **36**
Figure 40. Breakthrough curves of CO_2 over the PEI/SBA-15 sorbent pellets (10-18 mesh, or 1-2 mm, 200 mL in total) at 75 °C for CO_2 capture model flue gas containing about 15% CO_2 and 4.5% O_2 in N_2 with a flow rate of 400 mL/min (a GHSV of ~120 h^{-1}) …….. **36**
Figure 41. Breakthrough curves of CO_2 over the PEI/FS sorbent in fine powder (Black line) and in pellets (10-18 mesh, or 1-2 mm, Red line) at 75 °C for CO_2 capture from model flue gas containing 15% CO_2 in N_2 …….…….…….. **38**
Figure 42. Breakthrough curves of CO_2 over the PEI/SBA-15 sorbent pellets (10-18 mesh, or 1-2 mm, 200 mL in total) at 75 °C for CO_2 capture model flue gas containing about 15% CO_2 and 4.5% O_2 in N_2 with a flow rate of 400 mL/min (a GHSV of ~120 h^{-1}). …….……... **38**
Figure 43. Breakthrough curves of CO_2 uptake as a function of cycle number during scale-up test over PEI/FS sorbent. …….…….…….. **39**
Figure 44. Appearance of PEI/FS pellets (10-18 mesh, i.e., 1-2 mm) (a) before and (b) after 10 cycles of CO_2 sorption-desorption. …….……..…….. **39**
Figure 45. Heat requirements for the regeneration of the sorbents. ……..…..…….. **40**
Figure 46. Weight (black), heat-flow (blue) and temperature (red) profiles during CO_2 sorption and desorption over PEI-50/FS-M5 sorbent. ……...….…….. **40**
Figure 47. The comparison in the CO_2 sorption capacity and estimated material cost of the early generation and the new generation MBS developed in this project. ……..…….. **41**
Scheme 1. Proposed sorption process using MBS for CO_2 capture from flue gas. ……... **35**

2. Executive Summary

The objective of this project is to develop a new generation of solid, regenerable polymeric molecular basket sorbent (MBS) for more cost-efficient capture and separation of CO_2 from flue gas of coal-fired power plants. The primary goal is to develop a cost-effective MBS sorbent with better thermal stability. To improve the cost-effectiveness of MBS, we have explored commercially available and inexpensive support to replace the more expensive mesoporous molecular sieves like MCM-41 and SBA-15. In addition, we have developed some advanced sorbent materials with 3D pore structure such as hexagonal mesoporous silica (HMS) to improve the CO_2 working capacity of MBS, which can also reduce the cost for the whole CO_2 capture process. During the project duration, the concern regarding the desorption rate of MBS sorbents has been raised, because lower desorption rate increases the desorption time for complete regeneration of the sorbent which in turn leads to a lower working capacity if the regeneration time is limited. Thus, the improvement in the thermal stability of MBS became a vital task for later part of this project. The improvement in the thermal stability was performed via increasing the polymer density either using higher molecular weight PEI or PEI cross-linking with an organic compound. Moreover, we have used the computational approach to estimate the interaction of CO_2 with different MBSs for the fundamental understanding of CO_2 sorption, which may benefit the development, design and modification of the sorbents and the process.

The major achievements and results are highlighted below:

- A new MBS prepared using mesocellular silica foam (MCF) which has larger spherical cell and bigger pore volume compared to other mesoporous materials was used as the support. The CO_2 sorption capacity of PEI(50)/MCF is 151 mg/g, much higher than that of PEI(50)/SBA-15 (136 mg/g). Over MCF-based MBS, the 65 wt% PEI loading gave the highest carbon CO_2 capacity of 206 mg/g.
- Another highly porous, 3-D channel mesoporous silica material with wormhole-like pore channels, hexagonal mesoporous silica (HMS) has also been applied as the support for MBS preparation. The CO_2 sorption capacity of PEI/HMS varied from 73 to 182 mg-CO_2/g-sorbent with PEI loading from 30 to 65 wt%, much higher than MBS-1 and MBS-2.
- A series of silica gel based MBS has been developed and studied for CO_2 capture from flue gas. Among the studied silica gel samples, the one with pore size of 15 nm, particle size of 200-245 meshes was the best for supporting PEI for CO_2 sorption. The effects of PEI loading, sorption temperature and moisture have been studied. For best sorption capacity, the optimized PEI loading was 50 wt% and the sorption temperature was 75 °C. The presence of moisture enhanced the sorption capacity of silica gel based MBS. Compared to MBS-2, the PEI-50/SG gave similar gravimetric capacity but a much higher volumetric capacity (80 mg/ml versus 30 mg/ml). The regeneration with repeated cycles, however, showed about 11.6% loss in capacity for 10 cycles at 100 °C desorption, indicating that the thermal stability of silica gel based MBS requires further improvement.
- Commercially available fumed silica samples including M5, HS5 and EH5 have been studied for MBS preparation and their performance for CO_2 capture has been examined. The sorption capacity for PEI-50/FS-M5, PEI-50/FS-HS5, and PEI-50/FS-EH5 is about 132, 145 and 159 mg/g, respectively, with the volumetric capacity of 57, 80, and 68 mg/ml, all much higher than MBS-2 (~24 mg/ml). The CO_2 capacity increased with the increase of PEI loading and reached the maximum of 141 mg/g at PEI loading of 45 wt%. The best sorption capacity was also obtained at 75 °C. Compared to MBS-2 and PEI-50/SG sorbent, the FS-MBS showed higher capacity at 25 °C, suggesting that the FS-MBS may be more effective for CO_2 capture at low temperature. In addition, FS-MBS showed a higher working capacity. The promotion effect of moisture was also observed over fumed silica based MBS for CO_2 sorption.

- Three activated carbons (ACs) and two carbon black (CB) samples have been studied for MBS preparation in this project. The sorption capacity of carbon based MBS varied largely due likely to the characteristic pore structure of carbon samples. Among all tested CB-MBS samples, PEI-50/C4 gave the highest CO_2 sorption capacity of 135 mg/g, significantly higher than that of PEI-50/MCM-41 (110 mg/g) and almost the same as that of PEI-50/SBA-15 (138 mg/g).
- The CO_2 sorption capacity of the PEI/C4 samples with different PEI loadings was evaluated. It was found that the CO_2 sorption capacity increased with increasing PEI loading amount when the PEI loading was < 65 wt%. PEI-65/C4 gave the highest CO_2 sorption capacity of 154 mg/g. The presence of moisture improved the CO_2 sorption capacity of CB-MBS. The sorption isotherm study showed that a combination of TSA and pressure-swing adsorption (PSA) or using steam as a carrier gas may be necessary. The regenerability of PEI-50/C4 was also evaluated. About 92% of the initial CO_2 sorption capacity can be recovered after 10 cycles.
- The CO_2 sorption mechanism over MBS-2 has been studied by CO_2 temperature programmed desorption method, which indicates two sorption regions for CO_2 sorption including surface region and PEI bulk region.
- We have applied the computational approach to assist in improvement of the thermal stability of MBS. Via calculation of the binding bonds and formation energy, it showed that the addition of diacid to cross-link PEI polymer help stabilize the polymer and improve the thermal stability. It supports that the cross-linking is feasible approach to promote the thermal stability of MBS.
- We proposed two methods to improve the thermal stability of PEI based MBS material: increasing the PEI molecular weight and applying the cross-linking using organic diacid compounds including oxalic acid and terephthalic acid. We have assessed the effectiveness of these two methods in improving the thermal stability by extending the cycle number from 5 to 20 cycles.
- We studied the effect of PEI molecular weight on the sorption capacity and thermal stability of MBS-2 sorbent under dry and wet conditions. The results showed that the use of PEI with high molecular weight is highly beneficial in terms of improving the thermal stability of MBS-2 materials for CO_2 capture under both dry and wet conditions. Within 10 and 20 repeated cycles, a reduction of about 80% and 90% in the loss of the sorbent capacity was successfully obtained by using PEI polymer with molecular weight of 1800 and wet conditions for CO_2 sorption and regeneration.
- As for the cross-linking method using a diacid compound including oxalic acid (OA) and terephthalic acid (TPA), it was found that under dry conditions, the addition of OA and TPA does not promote the thermal stability of the MBS-2 sorbent within repeated cycles. However, under wet conditions, the addition of OA did promote the thermal stability of the MBS-2 sorbent within 10 repeated cycles. The capacity loss was only 4.9% after 10 repeated cycles. The results also imply that oxalic acid is a better cross-linking agent for PEI than terephthalic acid in terms of better thermal stability both under the dry and wet conditions.
- We have proposed a conceptual process using MBS for CO_2 capture. Then we scaled up the test from 5 ml to 200 ml for both MBS-2 and FS-MBS to provide more reliable and accurate parameters for the engineering design of the process and feasible study. At that scale, the MBS sorbent can still work effectively to remove CO_2 from flue gas down to very low level and show a high capacity.
- We have conducted a preliminary techno-economical assessment on the developed MBS in terms of energy consumption and materials cost. The estimation showed that the heat requirement for solid MBS is about 2 fold lower than that for liquid 30 wt% MEA solution.

Compared to our early generation of MBS, the new MBS developed in this project has a significant reduction in cost, as much as 90% reduction.

- Through the project research work, we have published 6 journal papers and 6 conference proceedings. We have also delivered 12 presentations (10 oral and 2 posters) at national and international related conferences.

We have conducted two progress review meetings at PSU in June 2010 and at Pittsburgh in May 2011, respectively. The technical progress reports and annual reports have been submitted timely. As shown in this final report, all the tasks, milestones and the objectives have been completed and achieved.

3. Introduction

The primary objective of the proposed research project is to develop a new generation of solid and regenerable polymeric molecular basket sorbent (MBS) for more efficient capture and separation of CO_2 from flue gas of coal-fired power plants to support the DOE NETL CO_2 capture program mission. This research project is based on the concept of "molecular basket" sorbent (MBS) which has been invented and developed in our laboratory. The key idea of MBS is to immobilize CO_2-philic polymers, such as polyethylenimine (PEI), on to high-surface-area mesoporous (nano-porous) materials to prepare the molecular basket sorbent (MBS), which can greatly increase the number of approachable sorption sites on/in the sorbent, and enhance the sorption/desorption rate by increasing the gas-sorbent contacting interfacial area and by improving the mass transfer in the sorption/desorption process.

The specific goals for this project include: 1) to develop a new generation of MBS which has a regenerable working sorption capacity higher than 70 mg-CO_2/g-S; 2) to lower the cost by using commercially available and inexpensive support material for MBS preparation, which can be significantly cheaper than the early generations of MBS-1 and MBS-2 (i.e., PEI/MCM-41 and PEI/SBA-15); 3) to improve the thermal stability of PEI-based MBS for the CO_2 capture process and the consequent regeneration process, thus reducing the process operation cost.

To improve the cost-effectiveness for CO_2 capture from flue gas, two approaches have been studied and applied for this project. One approach is to examine cheaper porous materials to replace expensive mesoporous molecular sieves like MCM-41 and SBA-15. For example, fumed silica (FS) is commercially available and relatively cheap (~ $18/kg). Another is to improve the CO_2 working capacity of MBS, which can also reduce the cost for the whole CO_2 capture process. Using an advanced material with 3D pore structure such as hexagonal mesoporous silica (HMS) may be promising for achieving a higher CO_2 sorption capacity. Additionally, fundamentally understanding of the CO_2 sorption process over the MBS will be beneficial to further improve the sorption capacity and develop a better sorbent.

In this project, the concern regarding to the desorption rate of MBS sorbents has been raised, because lower desorption rate increases the desorption time for complete regeneration of the sorbent which in turn leads to a lower working capacity if the regeneration time is limited. It is found that increasing desorption temperature can increase desorption rate significantly. However, increasing desorption temperature could result in a significant loss in the sorption capacity of MBS materials. In addition, the use of cheaper supports instead of SBA-15 which has uniform pore structure may result in a worse stability in sorption-regeneration cycles. Thus, the improvement in the thermal stability of MBS is also a vital task for this project.

Consequently, the approaches we have taken in this research project include 1) optimizing the combination of CO_2-phylic polymers and nanoporous materials to further enhance CO_2 sorption capacity; 2) searching for inexpensive and commercially-available materials, such as silica gel, fumed silica and carbon materials to replace expensive mesoporous molecular sieves such as MCM-41 and SBA-15, for preparation of new generation of MBS to significantly reduce the sorbent cost; 3) evaluating the sorption performance of the developed MBSs for CO_2 capture, including the sorption capacity, regenerability and stability; and determining the best conditions for sorption and desorption; 4) using the computational approach to estimate the interaction of CO_2 with different MBSs for the fundamental understanding of CO_2 sorption, which may benefit the development, design and modification of the sorbents and the process; 5) improving the thermal stability of the developed MBSs, especially for the stability of MBS during the repeated regeneration via increasing the polymer density either using higher molecular weight PEI or PEI cross-linking with an organic compound; 6) scaling up the sorption process and conducting the preliminary and simplified techno-economical assessment on the development sorbent materials.

The technical results obtained in this project are reported in detail as follows.

4. Technical Progress

4.1. Experimental

The preparation of Molecular Basket Sorbent (MBS) follows the procedures described in literature [1,2], with the exception of the substitution of the support material. A suitable support was then

added to the solution, which was then stirred for an additional 4 hrs. After that, methanol was removed at 40 °C overnight followed by 24 hrs in a vacuum oven at 100 °C. Commercially available carbon materials, fumed silica, and silica gel were applied in this project. Other advanced mesoporous materials with 3D structure were prepared according to the literature or purchased from Aldrich. The incorporation of organic diacid was similarly done by impregnation of SBA-15 or fumed silica with an oxalic acid and PEI solution in methanol, which was prepared by dissolution of PEI in methanol followed by addition of the desired amount of an oxalic acid, then stirred for 1 hour.

The CO_2 sorption performance, thermal stability and regenerability of the developed MBS samples were tested by thermogravimetric analysis (TGA) method using a TA Q600 TGA/DSC. In a typical experiment unless otherwise indicated, as shown in **Figure S1**, about 10 mg of the sample was loaded on the sample pan, increase the temperature at a rate of 10 ºC /min from 30 ºC to 100 ºC under a N_2 flow at a rate of 100 ml/min. Keep the sample at 100 ºC for 100 min to remove moisture, solvent or other adsorbates from the sample. Then, cool the sample to 75 ºC, change the flow gas from N_2 to CO_2 and hold temperature at 75 ºC for 100 min for CO_2 sorption. After CO_2 sorption, increase the temperature to 100 ºC, and switch the flow gas from CO_2 to N_2 for desorption at 100 ºC. This cycle was repeated 5 to 20 times to study the regenerability and stability of the sorbent material. The sorption and desorption capacity is calculated on the basis of the weight loss and gain during the sorption and desorption process. For thermal stability, the sample was heated at 5 °C/min to 500 °C under 100 mL/min N_2 (UHP).

In addition, a fixed-bed flow tubular reactor system with an electrical furnace was also assembled to evaluate the sorbent. The molecular basket sorbent was completely filled in the reactor tube, which was made of stainless steel with outer diameter of ca. 9.5 mm, inner diameter of ca. 7.0 mm and about 150 mm in length. The volume of sorbent was about 5.8 ml. Before sorption, the sorbent bed was heated to 100 °C in helium at a flow rate of 50 ml/min and held overnight to ensure that it was 'clean' prior to the adsorption. When the bed was cooled down to room temperature, a model flue gas containing 15% CO_2 and 4.5% O_2 in N_2 was introduced into the sorption column under atmospheric pressure. The pressure drop across the sorbent column was monitored by a small-range pressure gauge. When the outlet CO_2 concentration reached the initial feed concentration, i.e., the sorbent was saturated by CO_2, the gas line was switched to helium at a flow rate of 100 ml/min and the column temperature was increased to 100 °C and held at this temperature to perform the desorption. The outlet CO_2 concentration in the effluent gas was detected by an on-line SRI 8610C gas chromatography (GC) equipped with a molecular sieve 5A column and a silica-gel column, and a thermal conductive detector (TCD). The detector limitation of the GC was ca. 500 ppmv.

The breakthrough capacity (denoted as Cap (BT), mg-CO_2/g, STP) was calculated according to the following equation:

$$Cap(BT) = \frac{BT \times FR \times C^{in}{}_{CO_2} \times 10^{-6}}{V_{mol} \times W}$$

where BT is the breakthrough time, the time (min) when the CO_2 concentration in the effluent reaches 500 ppmv; FR is the total flow rate (mL/min); V_{mol} is the molar volume (24.4 mL/mmol at standard conditions); W is the weight of the sample (in grams) and $C^{in}{}_{CO_2}$ is the CO_2 concentration in the feed gas, generally 15%. The saturation capacity (denoted as Cap(S), mg-CO_2/g, STP) was calculated by integration of the area between the breakthrough curve and the initial CO_2 line (15%).

4.2. Development of a new generation of MBS for CO_2 capture and separation (Task 2)

4.2.1. Exploring to improve the CO_2 sorption performance of MBS

4.2.1.1. Mesocellular silica Foam based MBS (MCF-MBS)

In this study, a new type of mesoporous material, mesocellular silica foam (MCF) was purchased from Aldrich and used for preparation of MBS for CO_2 capture. MCF has larger spherical cell and bigger pore volume compared to other mesoporous materials. The diameter of spherical cell is about 10-50nm, these cells are connected to each other by windows to form continuous three dimension pore system. The size of the window is about 10-20 nm. In addition, the three dimension pore structure of MCF will

facilitate the diffusion of CO_2 during the sorption process. Thus, these characteristics make MCF an attractive candidate for the MBS preparation.

Table 1 lists the surface area and pore volume of MCF, SBA-15 and MCM-41. As it can be seen, MCF exhibits the highest pore size and pore volume and comparable surface area among them. The spherical cell of MCF is 18 nm, with a window size of 13 nm (pore opening), which is about 2 times and 5 times than that of SBA-15 and MCM-41, respectively. Total pore volume of MCF is 2.31 ml/g, which is about 2 times of SBA-15 and MCM-41. MCF exhibits the highest pore size and pore volume.

Table 1. Porous properties of MCF, HMS, SBA-15 and MCM-41.

Sample source	S_{BET} (m^2/g)	V_{total} (ml/g)	V_{micro} (ml/g)	V_{meso} (ml/g)	Average pore (cell) size (nm)	Window size (nm)
MCF	950	2.4	-	2.4	18	13
HMS	1012	1.12		1.12	2.6	
SBA-15	950	1.31	-	1.31	6.6	-
MCM-41	1229	1.15	-	1.15	2.7	-

A series of MCF-MBS samples were prepared by loading different PEI amount in a range from 30 to 90 wt%. For comparison, the SBA-15-based MBS with different PEI loading was also prepared. The solid form of prepared MBS at different PEI loadings has been examined. For MCF-MBS, a sorbent in good powder state could still be obtained even at PEI loading as high as 80 wt%. Further Increasing PEI content to 90 wt% resulted in a paste-like slurry sorbent, indicating that some loaded PEI is covering the external surface of MCF material. However, over SBA-15, 70 wt% PEI loading leaded to the paste-like slurry sorbent, indicating that MCF is more suitable to disperse the loaded PEI.

MCF-MBS was evaluated for CO_2 sorption via TGA. Figure 1 shows the typical TGA profile over PEI(50)/MCF sorbent during the CO_2 sorption and desorption. The TGA profile obtained on PEI(50)/SBA-15 is also presented for comparison. Based the TGA data, the CO_2 sorption capacity of PEI(50)/MCF is 151 mg/g, which is higher than that of PEI(50)/SBA-15 (136 mg/g), although both have the same PEI loading (50 wt%).

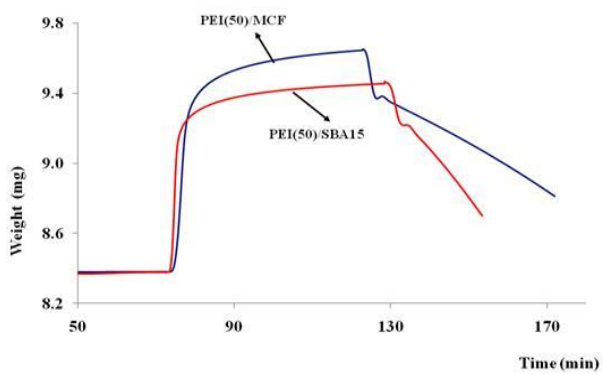

Figure 1. Typical TGA profiles obtained on PEI(50)/MCF and PEI(50)/SBA-15 during CO_2 sorption and desorption process.

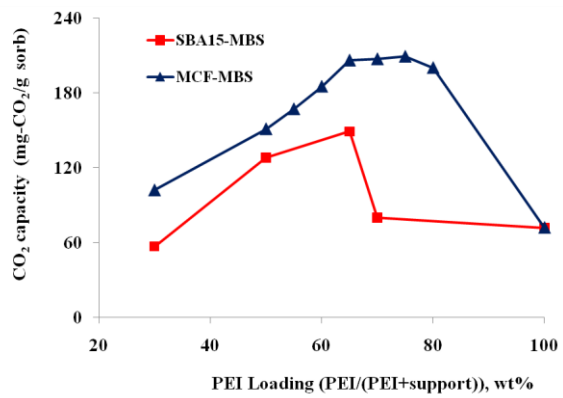

Figure 2. CO_2 sorption capacity as a function of PEI loading on the SBA-15-based MBS and MCF-based MBS sorbent.

Figure 2 shows the CO_2 sorption capacity as a function of PEI loading over PEI/MCF and PEI/SBA-15 sorbents measured by TGA method. As can be seen, after PEI loading, the obtained CO_2 sorption capacity was better than that of the pure PEI, suggesting that PEI and MCF support have a synergetic effect on the CO_2 sorption performance. The CO_2 sorption capacity increased with the increase of PEI loading over both SBA-15-based and MCF-based MBS sorbents when PEI loading was below 65 wt%. Over MCF-based MBS, the sample with 65% PEI loading gave the highest carbon CO_2 capacity,

reaching 206 mg/g. Further increasing the PEI loading amount to 70-75 wt%, the CO_2 sorption capacity doesn't show much change. However, when PEI loading was 80%, the CO_2 sorption capacity slightly decreased. For SBA-15-based MBS, 65% PEI loading also gave the highest CO_2 sorption capacity of 149 mg/g. In contrast to MCF, when the PEI loading amount was increased to 70 wt%, the CO_2 sorption capacity significantly dropped.

4.2.1.2. Hexagonal Mesoporous Silica based MBS (HMS-MBS)

HMS is another highly porous, 3-D channel mesoporous silica material with wormhole-like pore channels. The wormhole channel motif is an important structural feature that can favor CO_2 sorption process, and more sorption sites can be exposed to CO_2. Thus, in this project, HMS has been synthesized and applied as a support for MBS preparation. The measured BET surface area, pore volume and pore size for HMS is 1012 m^2/g, 1.12 ml/g and 2.6 nm, which is almost the same as those of MCM-41 (Table 1). Although the N_2 physisorption shows that HMS has similar pore properties to MCM-41, HMS contains wormhole-like pore channels arrayed in 3D while MCM-41 only has tubular pore channels arrayed in 1-D. Thus, it is expected that HMS-based MBS may have better CO_2 sorption performance that MCM-41-based MBS.

Figure 3 shows the effect of PEI loading amount on CO_2 sorption capacity of HMS-MBS. The CO_2 sorption capacity increased with the increase of PEI loading. For examples, the CO_2 sorption capacity of PEI/HMS increased from 73 to 160 mg-CO_2/g-sorbent when PEI loading was increased from 30 to 50 wt%. PEI/HMS with 65 wt% PEI loading gave the highest CO_2 capacity, reaching to 182 mg-CO_2/g-sorbent. Interestingly, HMS, which has close pore size and pore volume to that of MCM-41 exhibited much higher CO_2 sorption capacity than that of MCM-41 based MBS under same conditions. This result could be attributed to the contribution of 3-D wormhole-like pore structure of HMS. Further increasing the PEI loading amount to 70 wt%, the CO_2 sorption capacity decreased to 163 mg-CO_2/g-sorbent. It may be because extra PEI is coating on the external surface of HMS at such a high level of PEI loading.

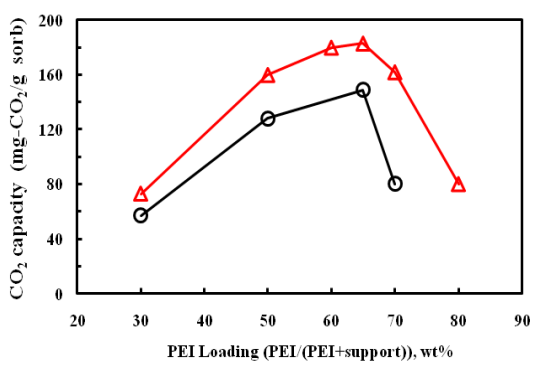

Figure 3. Effect of PEI Loading on the CO_2 Sorption Performance of HMS-MBS (red) and MBS-2 (black). Conditions: Temp., 75 °C; CO_2 concentration, 100%; Flow rate, 100 mL/min.

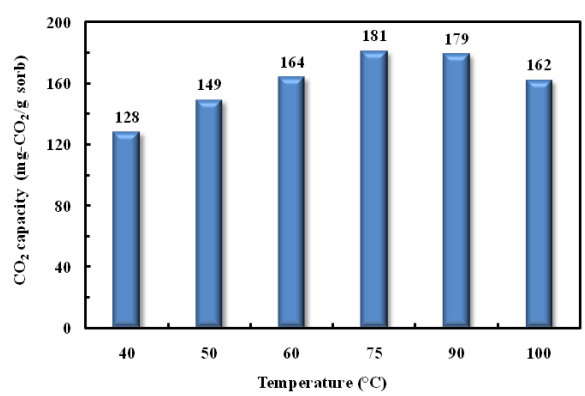

Figure 4. Effect of Sorption Temperature on the CO_2 Sorption Performance of HMS-MBS.

For comparison, Figure 3 also presents the CO_2 sorption capacity of PEI/SBA-15 sorbent (MBS-2) as a function of PEI loading. For PEI/SBA15 sorbents, it exhibited a similar trend in CO_2 sorption capacity with the increase of PEI loading, as observed for PEI/HMS sorbents. 65 wt% PEI loading gave the highest CO_2 sorption capacity of 149 mg/g among PEI loading studied. Interestingly, the HMS-MBS showed higher sorption capacity than PEI/SBA-15 at all the PEI loadings studied, although the pore volume and pore size of HMS is less than that of SBA-15. Recalling the 3-D wormhole-like pore structure of HMS, the better CO_2 sorption capacity may be attributed to its unique pore structure feature. Over the HMS-MBS, the amine efficiency increases with the increase of PEI loading, reaches the maximum at ca. 50 wt% PEI loading and then decreases again. The maximum amine efficiency is 0.31 mol-CO_2 per mol-amine.

Figure 4 shows the effect of sorption temperature on the CO_2 sorption capacity of HMS-MBS. At 40 °C, a CO_2 capacity of 128 mg/g was obtained. When the temperature was increased to 50 and 60 °C, the amount of sorbed CO_2 increased to 149 and 164 mg/g, respectively. The highest CO_2 sorption capacity was attained at 75°C, being 182 mg/g. According to our earlier studies, at higher temperature, the PEI molecules become more flexible and more CO_2 affinity sites are exposed, leading to a higher CO_2 sorption capacity of MBS. Further increasing the temperature to 90 °C, the CO_2 sorption capacity slightly decreased. And bigger drop in sorption capacity was observed when the temperature was raised to 100 °C. At a much higher temperature, the CO_2 sorption over amine is mainly controlled by thermodynamics, which favors the desorption at such a high temperature (e.g., 100 °C), resulting in an apparent drop in the sorption capacity.

4.2.2. Exploring low cost support for MBS

4.2.2.1. Silica-gel-based MBS

In this project, a series of silica gel (SG) samples with different pore size and different particle size was purchased from Aldrich. Before using, silica gel samples were dried in a vacuum oven at 100 °C overnight. PEI with average molecule weight (Mn) of 423, 25000 (branched), and 50000 (branched) were also purchased from Aldrich. The silica-gel-supported PEI sorbents were prepared by a wet impregnation method. The silica-gel-supported PEI sorbents with different PEI loading were denoted as PEI-*x*/SG, where *x* is the percentage of PEI-loading amount in the sorbent. The CO_2 sorption capacity of the prepared sorbents was evaluated and measured by TGA at 75 °C under pure CO_2 atmosphere with a CO_2 flow rate of 100 ml/min. In order to reduce the number of experiments, the orthogonal experiment was designed to determine the best combination of the factors for preparation of the silica-gel-based MBS. Each factor has three levels: pore size (40Å, 60Å, 150Å), particle size (35~60 mesh, 100~200 mesh, 200~425 mesh), PEI loading percentage (40%, 50%, 60%), and molecule weight of PEI (423, 25,000, 50,000), as listed in Table 2.

Table 2. Orthogonal experiment design and results.

	Factor				Cap.
N	Pore size (Å)	Particle Size (mesh)	PEI Loading (%)	Mw	mg/g
1	40	35~60	40	423	5.6
2	40	100~200	50	25000	12.0
3	40	200~425	60	50000	8.2
4	150	35~60	50	50000	22.5
5	150	100~200	60	423	76.0
6	150	200~425	40	25000	77.5
7	60	35~60	60	25000	7.8
8	60	100~200	40	50000	11.4
9	60	200~425	50	423	60.6
K1	8.6	12.0	31.5	47.4	Best design
K2	58.7	33.1	31.7	32.4	150Å
K3	26.6	48.8	30.6	14.0	200~425 mesh
R	50.1	36.8	1.1	33.4	50%
S	3863	2044	1.9	1676	423

According to the orthogonal experiment design, total 9 experiments, as listed in Table 2**,** were conducted, and the results are also shown in Table 2**.** The measured K values indicate that the pore size, particle size and molecular weight have strong effect on the sorption performance of the prepared sorbent. The PEI loading in the range from 40 wt % to 60 wt % only showed slightly effect on the sorption performance. Increase in the pore size of silica gel and decrease in both the particle size of silica gel and molecular weight of PEI were beneficial for increase of the CO_2 sorption capacity. 50 wt% PEI loading

was the best for preparation of the silica-gel-based MBS. The results suggested that the best combination of the various parameters for preparation of the silica-gel-based MBS is to use silica gel with 150 Å pore size and 200~425 mesh particle size by loading 50%wt PEI with molecule weight of 423.

In order to further examine the effect of PEI loading, a series of PEI/SG samples were prepared by using the best SG sample and PEI (423 g/mol) at different PEI loading of 10, 30, 50, and 60 wt%, respectively. The surface area, pore volume and pore-size distribution of the prepared PEI/SG samples were measured by the nitrogen adsorption/desorption. The pore volume and the surface area of the silica gel support were 1.03 cm^3/g and 260 m^2/g, respectively. With increase of the PEI loading, both the pore volume and the surface area of PEI/SG decreased continuously. The pore volume and surface area of PEI-50/SG were 0.17 cm^3/g and 35 m^2/g, respectively. At PEI loading of 60 wt%, almost no pore volume and surface area were measurable. The trend indicated that PEI was loaded inside the pores and the excessive PEI may be coated on the external surface of the silica gel particles, leading to the agglomeration of the silica gel particles. SEM images of silica gel, PEI-10/SG, PEI-50/SG, and PEI-60/SG showed that almost no PEI or very little of PEI was observed on the external surface of the particles in PEI-10/SG, PEI(50)/SG, while some PEI coated on the external surface of PEI(60)/SG particles, leading to the partial agglomeration of the particles, confirming that the most of PEI was filled into the silica gel pores in PEI(50)/SG sample.

The effect of PEI loading on the CO_2 sorption capacity at 75 °C was further examined by TGA. The silica gel alone gave a CO_2 adsorption capacity of 5.1 mg/g, indicating that there is also a weaker interaction between CO_2 and the silica gel. When PEI loading amount increased from zero to 50 wt%, the CO_2 sorption capacity increased to the maximum of 131.1 mg/g. After this point, the CO_2 sorption capacity decreased with increase of the PEI loading amount. This trend is similar to the result observed in our previous study of the PEI/SBA-15 samples. It is clearly shown that loading of PEI on the silica gel increases the CO_2 sorption capacity significantly. This is because PEI contains a great number of the potential CO_2-philic sites and the silica gel makes these sites accessible through improving the dispersion of PEI. When the PEI loading is higher than 50 wt %, the excessive PEI is coated on the external surface of the silica gel particles, resulting in the agglomeration of the particles and, thus, the number of the accessible sorption sites is reduced.

Effect of the sorption temperature on the sorption capacity of PEI-50/SG was examined using TGA with pure CO_2 gas at 25, 50, 65, 75, 85 and 100 °C, respectively. The CO_2 sorption capacity of PEI-50/SG increased with increasing temperature from 85.6 mg/g at 25 °C to the highest capacity of 131.1 mg/g at 75 °C, then decreased to 124.5 mg/g at 100 °C. The best sorption temperature was similar to the results observed for PEI-50/MCM-41 and PEI-50/SBA-15. The results indicate that at the temperature range from 25 to 75 °C, the diffusion of CO_2 in the PEI may be a sorption rate-control step. Consequently, elevating temperature results in increase of the number of accessible amine sites in the sorbent, and, thus, increases the CO_2 sorption capacity. When the temperature is higher than 75 °C, the thermodynamics may play a more important role, thus, resulting in decrease of the sorption capacity with increasing temperature.

Effect of moisture on the CO_2 sorption capacity of PEI-50/SG was examined in the fixed-bed flow system using a simulated flue gas with 15 v% CO_2, 4.5 v% O_2 in N_2. About 3.0 v% of H_2O was added to the simulated flue gas by bubbling the gas through water. The sorption breakthrough curves of PEI-50/SG in the absence/presence of moisture are shown in Figure 5. The breakthrough capacity of PEI-50/SG was 138 mg/g in the absence of moisture, while in the presence of moisture in the flue gas the breakthrough capacity of PEI-50/SG increased to 185 mg/g. This result confirms that the presence of moisture improves the sorption capacity of the supported PEI sorbents.

In addition of the high CO_2 capacity and selectivity, regeneration and stability of sorbent in cycles are crucial for practical application of the sorbent, as they are directly related to the cost of the sorption/desorption process. In this study, desorption was performed by switching the flue gas to pure N_2 gas. The 10 sorption-desorption cycles of PEI-50/SG were conducted by TGA. The sorption was at 75 °C and the desorption was at 75 and 100 °C, respectively, for comparison. The measured sorption capacities as a function of the cycle number are shown in Figure 6. For desorption at 100 °C, a slight decrease of the

sorption capacity with increasing cycle number was observed. The sorption capacity decreased from 131 mg/g for the fresh sorbent to 116 mg/g for the regenerated sorbent after 10 cycles. The sorption capacity was reduced by about 11.6% after 10 cycles. For desorption at 75 °C, a less decrease of the sorption capacity with increasing cycle number was observed. The sorption capacity of the regenerated sorbent after 10 cycles was 125 mg/g, indicating that 95.4% of the sorption capacity was recovered after 10 cycles. The results suggest that desorption at 75 °C is better than that at 100 °C for keeping the sorption capacity in the cycles. The detailed analysis of the sorption capacity as a function of the cycle number further shows that the degradation of the sorbent became insignificant with increasing cycle number.

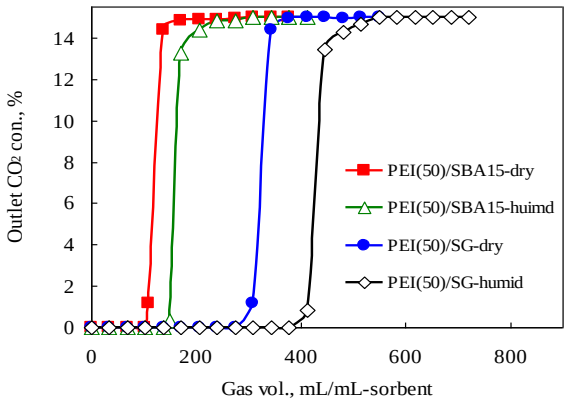

Figure 5. Breakthrough curves of PEI-50/SBA-15 and PEI-50/SG for CO_2 capture from the simulated flue gas (15 v% CO_2, 4.5 v% O_2 in N_2) in presence/absence of moisture at 75 °C and 207 h^{-1} GHSV in the fixed-bed flow sorption system.

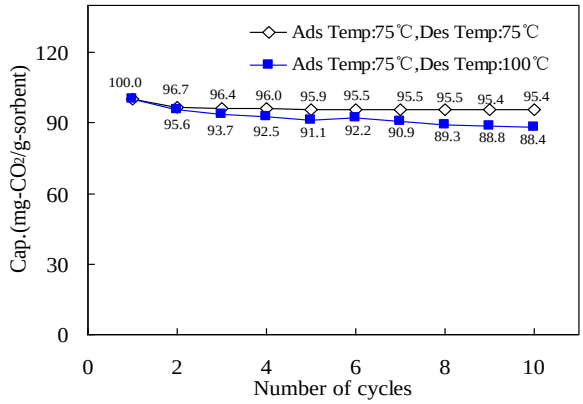

Figure 6. Recovery percentage of the CO_2 capacity as a function of sorption-desorption cycle number. Data were from TGA at 75 °C with pure CO_2 gas for sorption and desorption at 75 and 100 °C, respectively, with pure N_2 gas for desorption.

The thermal stability of the silica gel, PEI and PEI/SG with different PEI loading were also examined by TGA. The silica gel was stable at the temperature less than 600 °C with only mass loss of 3.9 wt%. The PEI lost about 1.0 wt% at 100 °C, which is probably due to the moisture and other low-boiling compounds in PEI. PEI began to lose the weight significantly at above 120 °C, and a sharp weight loss was observed at 300 °C for decomposition of PEI. When the temperature increased to above 375 °C, the weight of PEI sample became zero, indicating that PEI decomposed and/or evaporated completely. PEI/SG samples began to lose the weight around 120 °C and ended the loss of the weight around 375 °C with the sharp weight loss at 300 °C, similar to the pure PEI. It indicates that there is almost no change in the thermal stability of PEI after loading PEI on the silica gel, and PEI-50/SG should be stable at a temperature less than 120 °C.

Comparison of PEI-50/SG with PEI-50/SBA-15. In order to compare the sorption capacity of PEI-50/SG with PEI-50/SBA-15, both were evaluated at the same conditions by using both the TGA and the fixed-bed flow sorption system. The breakthrough curves of PEI-50/SBA-15 at 75 °C with the simulated flue gas (15 v% CO_2, 4.5 v% O_2 in N_2) in the presence/absence of moisture are also shown in Figure 5. The sorption capacities measured for the two sorbents in different tested systems are shown in Figure 7 for comparison. On the basis of the TGA results, the mass-based CO_2 sorption capacity of PEI-50/SG is 131 mg/g, which is less than, but very close to that of PEI-50/SBA-15. The mass-based CO_2 sorption capacity of PEI-50/SG measured in the fixed-bed flow system is 138 mg/g, which is almost the same as that 140 mg/g of PEI-50/SBA-15. It indicates that the mass-based sorption capacity of PEI-50/SG is comparable with that of PEI-50/SBA-15. In addition, the volume based sorption capacity of PEI-50/SG and PEI-50/SBA-15 is 83 and 32 mg/ml, respectively, on the basis of the tests in the fixed-bed flow system. The higher volume-based capacity of PEI-50/SG is due to its higher packing density (0.60 g/ml) than that of PEI-50/SBA-15 by 173%. This difference in the packing density results in the greater volume-based sorption capacity of PEI-50/SG than that of PEI-50/SBA-15 by a factor of 2.6. In comparison with the result from Zhu et al., [3] the

CO_2 capacity (86 mg/g) of PEI-50/SG developed in this study is higher than that reported by Zhu et al. [3] by more than 85% at the same temperature (25 °C). The significantly higher capacity of PEI-50/SG can be attributed to the optimization of PEI/SG formulation in this study.

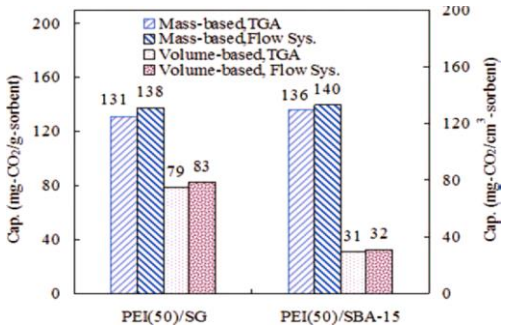

Figure 7. The CO_2 mass-based and volume-based sorption capacities of PEI-50/SBA-15 and PEI-50/SG measured in TGA with pure CO_2 gas and the fixed-bed flow system with the simulated flue gas both at 75 °C.

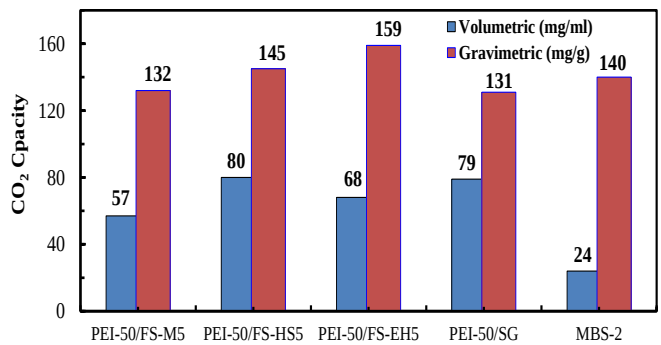

Figure 8. Gravimetric and volumetric capacity of different fumed silica, silica gel and SBA-15 supported PEI sorbents with 50 wt% PEI loading.

4.2.2.2. Fume-silica-based MBS

Different types of fumed silica (FS) from Cabot including FS-M5, FS-EH5, and FS-HS5 were used as the support for preparation of new MBS via a wet impregnation method with polyethylenimine (PEI, Aldrich, Mn, ~423). The fumed silica-supported PEI sorbents were denoted as PEI-*x*/FS, where *x* is the weight percentage of PEI in the sorbent. The porous properties of fumed silica used in this project were examined by N_2 physisorption at -196 °C on a Micromeritics ASAP 2020 analyzer. Before measurement, the sample was degassed at 200 °C under vacuum for 24h. Based on the isotherm, the BET surface, pore volume and BJH pore size can calculated, which are listed in Table 1. The surface area and pore volume of the used fumed silica samples range from 200-300 m^2/g and 0.5-0.6 ml/g, respectively, smaller than those of SBA-15. However, the pore size of fumed silica samples (about 13-14 nm) is larger than that of SBA-15 (around 6.6 nm).

Table 3. Porous properties of Fumed Silica M5, HS5, EH5 and SBA-15

Sample	S_{BET}, m^2/g	Pore Volume, ml/g	Pore Diameter, nm
FS-M5	214	0.55	14.0
FS-HS5	265	0.63	13.3
FS-EH5	315	0.61	13.0
SBA-15	950	1.31	6.0

The fumed silica based sorbents with 50wt% PEI loading have been evaluated via TGA. Figure 8 shows the obtained gravimetric and volumetric sorption capacity. The MBS-2 (PEI-50/SBA-15) has a gravimetric capacity of 140 mg/g. With fumed silica as the support, a similar or even higher gravimetric sorption capacity can be attained. It is about 132 mg/g for PEI-50/FS-M5, 145 mg/g for PEI-50/FS-HS5 and 159 mg/g for PEI-50/FS-EH5. As for the volumetric sorption capacity, all the fumed silica based sorbents exhibit much higher value than MBS-2. It is about 57 mg/ml for PEI-50/FS-M5, 80 mg/ml for PEI-50/FS-HS5 and 68 mg/ml for PEI-50/FS-EH5, much higher than MBS-2, whose volumetric sorption capacity is only about 24 mg/ml, due likely to higher density of fumed silica based sorbents. The densities of PEI-50/FS-M5 and of PEI-50/FS-HS5 are ca. 0.6 g/ml while the density of MBS-2 is only about 0.2 g/ml. The results clearly show that the use of fume silica can greatly improve the volumetric sorption capacity of MBS material compared to SBA-15, which is important for real applications where the

volume of a sorber is limited. Fumed silica based MBS showed similar volumetric capacity to silica gel based MBS, but a higher gravimetric capacity.

Figure 9 shows the CO_2 gravimetric and volumetric sorption capacity as a function of PEI loading over PEI/FS-M5 sorbents measured by TGA method. Pure PEI gives a sorption capacity of 60 mg/g at the current conditions. After loading onto the FS-M5 support, the obtained CO_2 sorption capacity was better, except the one with 25 wt% PEI loading, which showed a sorption capacity of 59 mg/g, almost the same as pure PEI. It suggests that PEI and nanoporous fumed silica have a synergetic effect on the CO_2 sorption performance. The CO_2 capacity increased with the increase of PEI loading and reached the maximum of 141 mg/g at PEI loading of 45 wt%. Further Increasing PEI loading resulted in the decrease of the sorption capacity. It is 132 and 106 mg/g for PEI-50/FS-M5 and PEI-60/FS-M5, respectively. Thus, the best PEI loading for FS-M5 support is about 45 wt%. While for the MBS-2, the optimum PEI loading over SBA-15 is about 50-60 wt%. However, for the volumetric sorption capacity of PEI/FS-M5 sorbents, it increases with the increase of PEI loading. It should be noted that both the density of PEI/FS-M5 sorbents and the gravimetric sorption capacity determined the volumetric capacity. Although, at high PEI loadings, the gravimetric sorption capacity decreases, the density of the sorbent increases much, resulting in the increasing trend.

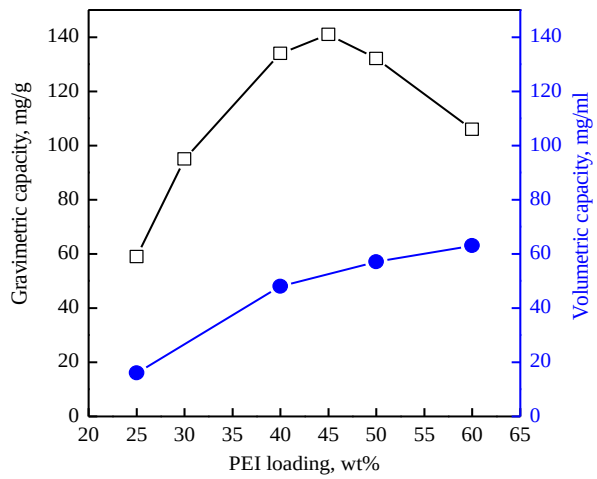

Figure 9. Gravimetric and volumetric sorption capacity of PEI/FS-M5 sorbents as a function of PEI loading amount.

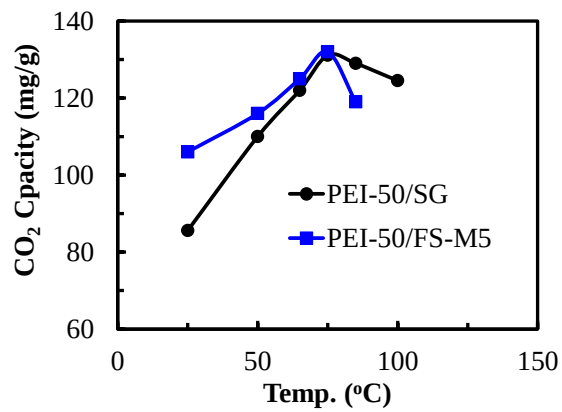

Figure 10. CO_2 sorption capacity as a function of sorption temperature over (■) the PEI-50/FS-M5 and (●) the PEI-50/SG sorbent measured by TGA method.

The effect of temperature on the sorption capacity of the PEI-50/FS-M5 sorbent has been studied and the result is reported in Figure 10. As it can be seen, the CO_2 sorption capacity increases with the increase of sorption temperature. The best sorption capacity was achieved at 75 °C. Further increasing temperature to 85 °C, a decrease of 13 mg/g in the sorption capacity is observed. The current result is consistent with our previous observation on MBS-2, which also showed 75 °C as the best sorption temperature. It should be pointed out that the developed PEI-50/FS-M5 sorbent shows a high CO_2 sorption capacity at 25 °C, being about 106 mg/g. For MBS-2 and PEI-50/SG sorbent, it is only about 60 and 85.6 mg/g, respectively at such a low temperature. It indicates that the PEI-50/FS-M5 is more effective for CO_2 capture at low temperature than MBS-2, and may be more applicable and promising for low temperature operation. In addition, compared to silica gel based MBS, the fumed silica based MBS showed a higher working capacity for sorption at 75 °C and desorption at 85 °C.

Effect of moisture on the CO_2 sorption capacity of PEI-50/FS-M5 was examined in the fixed-bed flow system using a simulated flue gas with 15 v% CO_2, 4.5 v% O_2 in N_2. About 3.0 v% of H_2O was added to the simulated flue gas by bubbling the gas through water. The sorption breakthrough curves of PEI-50/FS-M5 in the absence/presence of moisture are shown in Figure 11. Clearly, the breakthrough

capacity increased with the presence of moisture, confirming that the presence of moisture improves the sorption capacity of the supported PEI sorbents.

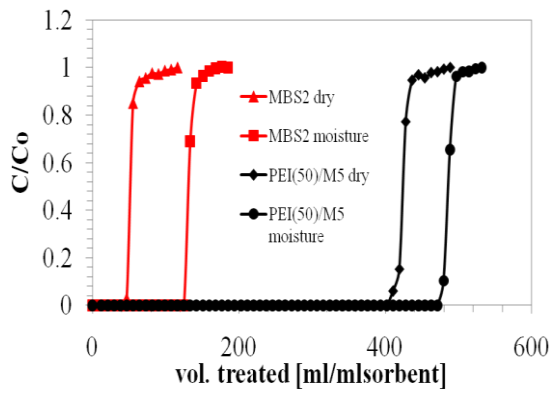

Figure 11. Breakthrough curves of PEI-50/SBA-15 and PEI-50/FS-M5 for CO_2 capture from the simulated flue gas (15 v% CO_2, 4.5 v% O_2 in N_2) in presence/absence of moisture at 75 °C and 207 h^{-1} GHSV in the fixed-bed flow sorption system.

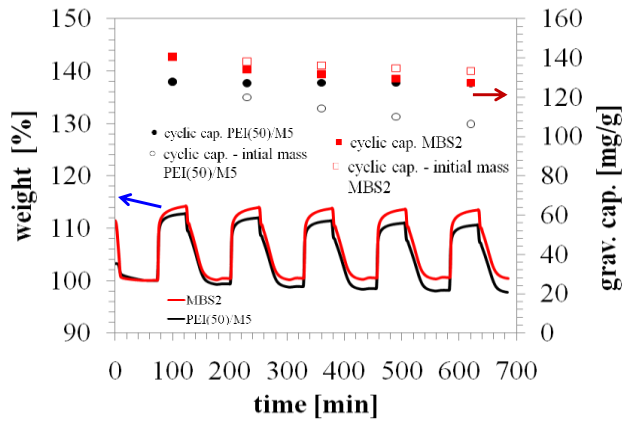

Figure 12. The regenerability behavior of MBS (i.e., PEI-50/SBA-15) and PEI-50/FS-M5 measured by TGA for 5 cycles.

The regenerability of fumed silica based MBS has also been studied by TGA method for 5 cycles in this project, which is shown in Figure 12. An obvious baseline change was observed over the PEI-50/FS-M5 sample. After 5 cycles, the baseline dropped about 2%. As for the sorption capacity, both samples showed the decrease in capacity with sorption cycles, suggesting that the improvement in the thermal stability of MBS sorbents is needed. The capacity loss for PEI-50/FS-M5 was about 16.9%, while it is about 5.1% for the MBS-2. The results indicate that compared to MBS-2, the fumed silica based MBS is less stable, which leads to our further task for this project to improve the thermal stability.

Table 4. Pore properties of carbon materials used in this study

Sample source ID	Source	S_{BET} (m^2/g)	S_{micro} (m^2/g)	S_{meso} (m^2/g)	V_{total} (ml/g)	V_{micro} (ml/g)	V_{meso} (ml/g)	Pore size (nm)
C1	AC from coal	1151	910	241	0.64	0.442	0.20	2.22
C2	AC from wood	1495	1000	495	1.21	0.55	0.66	2.91
C3	AC from wood	2320	1397	923	1.64	0.79	0.84	2.85
C4	CB from coal	1486	575	911	2.69	0.50	2.19	7.26
C5	CB from coal	1121	380	741	2.47	0.47	2.00	6.95
SBA-15		950			1.31	0	1.31	6.59
MCM-41		1229			1.15	0	1.15	2.74

4.2.2.3. Carbon-based MBS

As another widely used and inexpensive material is commercial carbon, which has been applied for MBS preparation and studied for their CO_2 sorption performance in this project. Table 4 lists the porous properties of the carbon materials including three activated carbons (ACs) and two carbon black (CB) used. As can be seen**,** C1 has mainly microporous structure. C2 has dominantly mesorpore. C3 has the similar volume of the micropores and mesopores. C4 and C5 have dominantly mesoporous structure with the highest pore volume in these carbon samples. Carbon-based MBSs (CB-MBS) were prepared by wet impregnation method, as described above. The prepared CB-MBS samples were denoted as PEI-*x*/*y*, where *x* is the PEI loading percentage and *y* is the ID of the support material.

A series of CB-MBS prepared by using different carbon materials with 50 wt% PEI loading was evaluated by TGA. The results are shown in Table 5 in comparison with MBS-1 (PEI-50/MCM-41) and MBS-2 (PEI-50/SBA-15). The measured capacities of CB-MB samples were quite different. PEI-50/C1

gave the least capacity of 33 mg/g and appeared to be sticky slurry, while others were a solid powder. It is probably because excessive amount of PEI was coated on the external surface. In all tested CB-MBS samples, PEI-50/C4 gave the highest CO_2 sorption capacity of 135 mg/g, significantly higher than that of PEI-50/MCM-41 (110 mg/g) and almost the same as that of PEI-50/SBA-15 (138 mg/g). The measured CO_2 sorption capacity of PEI-50/C5 was 126 mg/g, which is slightly lower than that of PEI-50/C4, but considerably higher than other CB-MBS samples.

Table 5. CO_2 capacity of CB-MBS in comparison with PEI-50/SBA-15 and PEI-50/MCM-41 measured by TGA at 75 °C under a pure CO_2 flow at a flow rate of 100 ml/min.

Sample source ID	Packing density (g/ml)	Mass-based CO_2 capacity (mg-CO_2/g-sorb)	Volume-based CO_2 Capacity (mg-CO_2/ml-sorb)
PEI-50/C1		33	
PEI-50/C2	0.52	63	33
PEI-50/C3	0.61	59	36
PEI-50/C4	0.35	135	47
PEI-50/C5	0.22	126	28
PEI-50/SBA-15	0.22	138	30
PEI-50/MCM-41	0.27	110	30

Interestingly, it was also found that PEI-50/C2, PEI-50/C3, and PEI-50/C4 had a much higher packing density – 0.52, 0.61, and 0.35 g/mL, respectively – in comparison with those of MBS-1 (0.27 g/mL) and MBS-2 (0.22 g/mL). According to the packing density, the volume based CO2 capacity was also estimated. As shown in Table 5, PEI-50/C2, PEI-50/C3, and PEI-50/C5 have a volume based capacity similar to those of MBS-1 and MBS-2, and PEI-50/C4 even has a volume based capacity as high as 47 mg/mL-sorb, which is higher than that of MBS-2 by 57%. For a large scale CO_2 sorption process, higher volume-based CO_2 sorption capacity is very important because it will reduce the sorbent bed size and, thus, reduce the infrastructure investment for mass CO_2 capture. Therefore, the high volume-based sorption capacity is another significant advantage of PEI-50/C4 over MBS-2.

There are oxygen-containing functional groups on the activated carbon, such as, carboxylic groups, phenolic hydroxyl groups, etc. These weak acidic groups might consume some amine groups in PEI, resulting in the reduced CO_2 sorption capacity. In order to examine the effect of the surface oxygen-containing functional groups on the sorption performance of CB-MBS, the oxygen-containing functional groups on C3 surface was tailored by heating at 500, 600, 700, and 800 °C, respectively, under a N_2 flow. The characterization of the pore structure of the treated samples indicates that the pore volume and surface area of the samples were almost no changes. A temperature programmed desorption method was used to characterize the surface oxygen-containing functional groups. [4] The results indicate that more than 75% of the oxygen-containing functional groups on the surface of C3 were removed after the heat treatment at 700 °C for 2 h. However, the CO_2 sorption capacities of PEI-50/heat-treated-C3 increased by only 5% in comparison with that of PEI-50/C3. A little change in capacity was also observed the samples treated at other temperatures. The results indicate that the oxygen-containing functional groups on the surface of carbon materials may have some effect, but they are not a key factor in determining the sorption performance of the activated-carbon-supported PEI sorbent.

The amount of loaded PEI might play an important role in determining the CO_2 sorption capacity of CB-MBS. Since the C4 has the highest pore size and pore volume among all carbon materials tested in the present study, a series of PEI/C4 samples with different PEI loading amounts were prepared, and their textural structures were characterized by N_2 physical adsorption. Table 6 lists the surface area and pore volume of the parent C4 and PEI/C4 with different PEI loading. A significant reduction in the surface area and total pore volume with increasing amine loading was observed. For instance, the surface area and the total pore volume of C4 were 1486 m^2/g and 2.69 mL/g, respectively. With 30 wt% PEI loading, the surface area and the total pore volume decreased to 321 m^2/g and 1.31 mL/g. When the PEI loading was 50 wt%, the surface area and total pore volume further decreased to 37 m^2/g and 0.33 mL/g, respectively.

Continuous increase in the PEI loading to 65 wt% caused the further decrease in the surface area and the total pore volume to 27 m^2/g and 0.29 mL/g, respectively. The decrease in the BET surface area and pore volume of PEI/C4 samples with increasing PEI loading suggests that the loaded PEI was filled into the pores of the carbon support, as also indicated by the pore size distribution (see **Figure S2**) measured by the N_2 adsorption with DFT method.

Table 6. Textural characterization of C4 and PEI/C4 with different PEI loading.

Sample source ID	S_{BET} (m^2/g)	S_{micro} (m^2/g)	S_{meso} (m^2/g)	V_{total} (ml/g)	V_{micro} (ml/g)
C4	1486	575	911	2.69	0.50
PEI(30)/C4	321	5.40	315.60	1.31	0.14
PEI(50)/C4	37	0.60	36.40	0.33	0.02
PEI(65)/C4	27	0.45	26.55	0.29	0.01

The CO_2 sorption capacity of the PEI/C4 samples with different PEI loadings was evaluated by using TGA, and the results are shown in Figure 13. It was found that the CO_2 sorption capacity increased with increasing PEI loading amount when the PEI loading was < 65 wt%. PEI-65/C4) gave the highest CO_2 sorption capacity of 154 mg/g. Upon further increasing the PEI loading amount, a significant decrease of the CO_2 capacity was observed. The CO_2 sorption capacity of PEI-70/C4 was reduced to only about 60 mg/g. This is because the 70 wt% PEI loading is beyond the saturation pore volume of C4, and the extra PEI was coated on the external surface of the C4 particles, which results in the agglomeration of the particles, as also visibly observed. The agglomeration of the particles could reduce the total number of accessible amine sites as a result of an increase in the diffusion resistance of CO_2 into the bulk of the PEI in the pores. Therefore, the maximum CO_2 sorption capacity of 154 mg/g was obtained for the PEI/C4 sorbent with 65 wt% PEI loading. It needs to be mentioned that the best PEI loading on C4 (65 wt%) is higher than the best PEI loading on MCM-41 and SBA-15 (50 wt%). This can be ascribed to the larger pore volume of C4 than those of MCM-41 and SBA-15.

The influence of moisture on the CO_2 sorption capacity of PEI(50)/C4 was examined in a fixed-bed flue system by passing the simulated flue gas, which contain 15 vol % CO_2 and 4.5 vol % O_2 in N_2, with and without moisture. The moisture concentration in the simulated flue gas was about 3 v%. In the absence of H_2O, PEI-50/C4 was saturated by CO_2 at 137 mg/g. In the presence of moisture, it became 147 mg/g. The results show that moisture has a positive effect on PEI-50/C4 sorbent for CO_2 sorption.

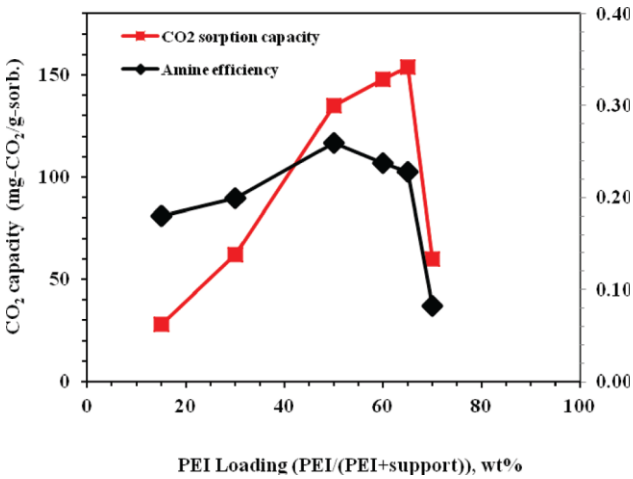

Figure 13. Effect of PEI loading on CO_2 sorption capacity of PEI/C4

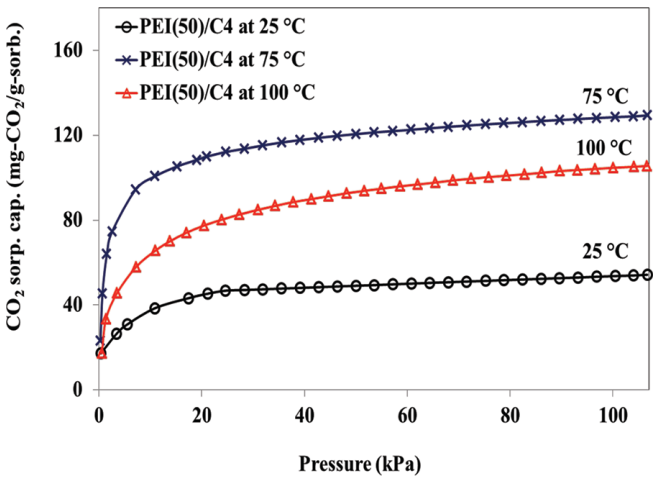

Figure 14. CO_2 sorption isotherms of PEI-50/C4 measured at 25, 75, and 100 °C.

The sorption isotherms at 25, 75, and 100 °C were measured by using the modified Micromeritics ASAP 2020 analyzer which is shown in Figure 14. The PEI-50/C4 exhibited a CO_2 sorption capacity of 64 mg/g at 25 °C and 100 kPa. With increasing temperature to 75 °C, the measured CO_2 capacity of became higher and reached a capacity of 129 mg/g at 75 °C. Upon further increasing temperature to 100 °C, the measured CO_2 capacity decreased to106 mg/g. The observed sorption isotherms of PEI-50/C4 at different temperatures also provide another important message: for regeneration of the spent MBS, using the thermal-swing adsorption (TSA) alone is not sufficient because an increase in the temperature from 75 to 100 °C can desorb only ~18% of the sorbed CO_2. The regeneration of the spent PEI-50/C4 at higher temperature may cause decomposition or degradation of PEI. Thus, a combination of TSA and pressure-swing adsorption (PSA) or using steam as a carrier gas may be necessary. More investigation in regeneration of CB-MBS is required for practical application.

The regenerability of PEI-50/C4 was also evaluated by conducting the CO_2 sorption/desorption cycles using TGA. The obtained TGA curve and CO_2 sorption capacity as a function of the cycle number are shown in Figure 15. A slight reduction of the CO_2 sorption capacity was observed with an increasing sorption/desorption cycle number, but such a drop trend becomes insignificant with an increasing cycle number. About 92% of the initial CO_2 sorption capacity can be recovered after 10 cycles. As is well-known, the flue gas also contains moisture and O_2. The effects of both moisture and O_2 were also examined. It was found that the presence of O_2 had almost no effect on the sorption performance of PEI-50/C4, while the presence of moisture in the model gas had even a positive effect. Further investigations in finding a major reason for the sorbent degradation and how to improve the stability of CB-MBS are necessary.

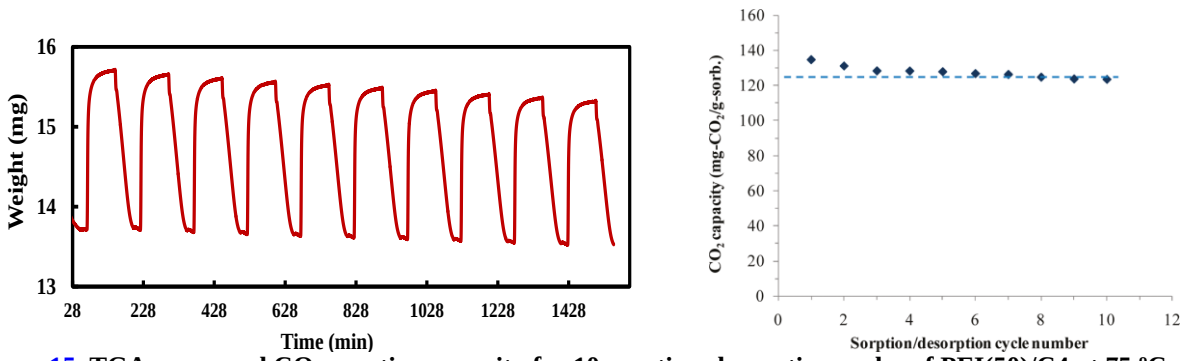

Figure 15. TGA curve and CO_2 sorption capacity for 10 sorption-desorption cycles of PEI(50)/C4 at 75 ºC.

4.2.3. CO_2 sorption mechanism study by TPD method

To further improve the sorption capacity and develop a better sorbent, it is necessary to fundamentally understand the CO_2 sorption process over the MBS. Thus, we have also used temperature programmed desorption (TPD) method to study the CO_2 sorption mechanism. Figure 16 shows CO_2-TPD profile obtained over PEI-50/SBA-15. It can be de-convoluted into two components: a major peak at ca. 80 °C, and a much smaller peak at ca. 95 °C, which may hint the presence of two different regions for CO_2 sorption. Figure 17 shows the effects of sorption temperature and time on the sorption capacity of PEI-50/SBA-15 sorbent examined by TPD. With the increase of the sorption temperature, the sorption capacity increased and reached the maximum at about 90 °C, then decreased with further increasing temperature. For the effect of sorption time, two distinct regions can be observed. When the sorption temperature was below or equal to 90 °C, prolonging the sorption time can favor the sorption of CO_2 over the sorbent. However, if the sorption temperature was over 90 °C, there was no beneficial of extending sorption time on the sorption capacity. It either did not change, or even decreased with increase of sorption time.

Combining TPD profile and the trends in sorption temperature and time, the CO_2 sorption model or mechanism over PEI/SBA-15 can be proposed. Over the 50 wt% PEI/SBA-15 sample, there are two regions, i.e., surface region and PEI bulk region, for CO_2 sorption. At low temperature, due to high

diffusion barrier and the activation energy required for PEI bulk region, most CO_2 is sorbed in the surface region, showing low sorption capacity and one high temperature desorption peak. However, when CO_2 sorption is carried out at high temperature, e.g., 75 °C, both the surface region and PEI bulk region can work for CO_2 sorption. Thus, high sorption capacity is attained. In the desorption process, the sorbed CO_2 evolved from PEI bulk region to surface region and then away from the surface region. In other words, sorbed CO_2 molecules first dissociate in the PEI bulk region, then diffuse to the surface region, and finally further dissociate to leave the sorbent. As suggested by the isosteric heat of sorption, this desorption occurred at low temperature. With the depletion of the sorbed CO_2 and the decrease of CO_2 loading, the residue in the surface region gives a high temperature desorption peak.

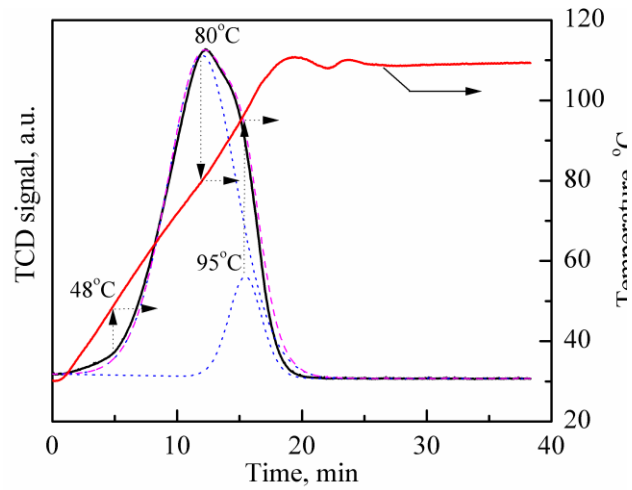

Figure 16. Typical CO_2-TPD profile with peak de-convolution and fitting curves.

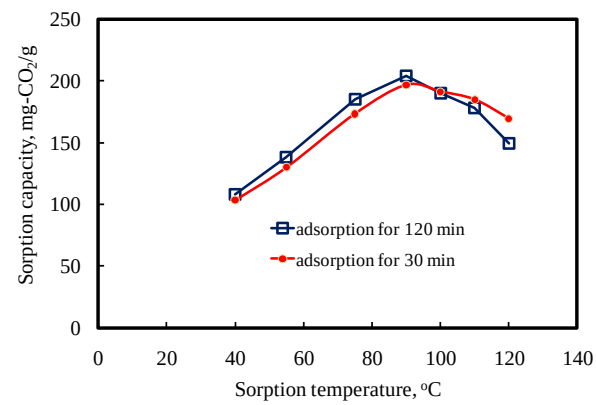

Figure 17. CO_2 uptake as a function of sorption temperature and sorption time over 50 wt% PEI/SBA-15.

4.3. Computational chemistry approaches (Task 3)

In this project, we have studied the sorption of CO_2 molecule on cross-linked polyethylenimine (PEI) using AM1*, a semi-empirical method to assist the study on the improvement of the thermal stability of MBS. The calculation showed that C atom in CO_2 molecule bonds with N-atom in PEI when CO_2 is sorbed on PEI (The PEI was built as NH_2-$(CH_2CH_2NH)_8$-H, see **Figure S3** in the Appendix). The bonding length is 2.84 Å and the sorption energy is -2.8 kcal/mol. Besides the N-C binding, H-bonding may also contribute to the sorption. The studied cross-linking agent includes oxalic acid (HOOC-COOH), malonic acid (HOOC-CH_2-COOH), succinic acid (HOOC-CH_2-CH_2-COOH), and DL-malic acid (HOOC-CH_2-CHOH-COOH).

4.3.1. Computational Methods

All the calculations in this work were performed with Material Studios. The sorption was initially calculated by using the module of adsorption locator, which is a preparatory and screening tool for adsorption study in Material Studios. The calculations generate sorption configurations automatically with a ranking of the energies for each generated configuration, indicating the preferred sorption sites. Then the configurations with high rankings will be subsequently used as starting points for further semi-empirical quantum studies, with AM1* method in the module of VAMP in Material Studios.

The stability of the cross-linked PEI was compared via the calculation as:

$$\Delta E_{\text{cross-link}} = E_{\text{acid+2PEI}} - E_{\text{acid}} - E_{\text{PEI}};$$

The more negative $\Delta E_{\text{cross-link}}$ is, the more stable the cross-linked structure is.

The sorption energies were calculated as: $\Delta E_{\text{sorption}} = E_{\text{CO2+PEI}} - E_{\text{CO2}} - E_{\text{PEI}}$

Since sorption is always an exothermic process, E_{sorption} is negative. The more negative $\Delta E_{\text{sorption}}$ is, the stronger the sorption happens.

4.3.2. Effect of cross-linking on PEI structure

Table 7 lists the heat of formation calculated when PEI is cross-linked with the four acid molecules (The structure for each configuration can be found in **Figure S4**). Based on the bonding lengths given in **Figure S4** and the calculated heats of formation, cross-linking molecules could bind two PEI strongly via hydrogen bonding in a parallel mode.

Table 7. Calculated heat of formation for each cross-linked PEIs

	Heat of formation (kcal/mol)
Oxalic acid - 2PEI	-7.66
Malonic acid - 2PEI	-8.89
Succinic acid - 2PEI	-7.94
DL-malic - 2PEI	-5.51

Among these acid molecules studied, oxalic acid has 2 carbon atoms in the chain; malonic acid has 3 carbons in the chain; succinic acid and DL-malic acid both have 4 carbons. The cross-linking molecule using malonic acid is the most stable one with the largest negative heat of formation, indicating that the cross-linking molecule should have a proper length: neither too long nor too short.

4.3.3. CO_2 sorption over PEI and cross-linked PEI

The configurations of CO_2 sorption on PEI and the cross-linked PEIs were computed and presented in **Figure S5**. In these cases, we are interested in whether the sorption energies could be enhanced at the linking sites. Consequently, the sorption energies of CO_2 were calculated and listed in Table 8.

Table 8. The sorption energies of CO_2 on PEI and cross-linked PEIs.

	CO_2 sorption energy (kcal/mol)
PEI	-2.83
Oxalic acid - 2PEI	-3.10
Malonic acid - 2PEI	-3.21
Succinic acid - 2PEI	-3.66
DL-malic acid - 2PEI	-5.10

Different from the trends in heat of adsorption, CO_2 sorption energy becomes stronger when the cross-linking molecule is longer in length. The larger space among PEI and acid molecules for CO_2 sorption could be one of the reasons for the stronger sorption. Also as the least stable cross-linked PEIs, DL-malic acid PEIs may have higher activity for sorption.

4.4. Thermal stability improvement (Task 4)

4.4.1. Effect of Regeneration Temperature for MBS-2 with PEI(Mn, 423)

Analysis of the stability of MBS-2 (423) at desorption temperatures above 100°C is shown in Figure 18. The corresponding CO_2 sorption capacity is listed in Table 9. As can be seen, the deactivation of PEI including PEI volatilization and the formation of carbamides, became increasingly pronounced as temperatures increase. This is evidenced by the observation of the change in baseline and peak maxima of the multiple regeneration cycles and the changes in CO_2 capacity. At 100 °C, there is very little change either in the polymer mass or the loss in capacity due to carbamides formation. As temperatures rise to 120 and 130 °C, the shift of the baseline is observed, which is interpreted as the formation of carbamides, Additionally, the peak maxima is also decreasing, which is interpreted as a concurrent loss in polymer mass.

This trend is more evident when the wet (~2% H_2O) stripping gas is used for desorption and regeneration. Figure 19 shows TGA profiles of MBS-2 (423) regenerated at elevated temperatures under the wet stripping gas. The corresponding CO_2 capacities are presented in Table 10. When the wet

stripping gas is used, a similar trend for the loss of polymer mass is observed with increasing temperatures. The carbamides formation however is inhibited by the presence of H_2O in the stripping gas. It elucidates the use of wet stripping gas does not affect the impact of polymer loss at higher temperatures, but could mitigate the impact of carbamide formation. As also seen in Figure 19, the loss in mass at lower temperatures is more pronounced in presence of H_2O than that under dry stripping gas (as evidenced by the dropping baseline). As desorption temperatures rise, more polymer is getting lost.

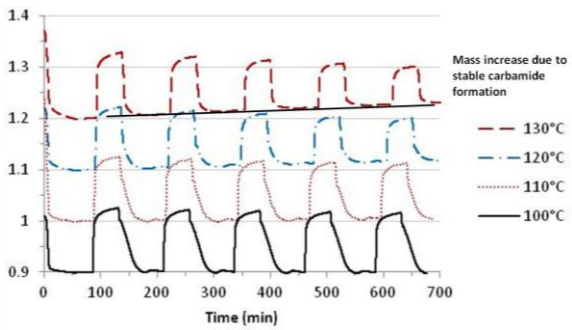

Figure 18.TGA profiles for multiple regeneration cycles of MBS-2 (423) at elevated desorption temperatures.

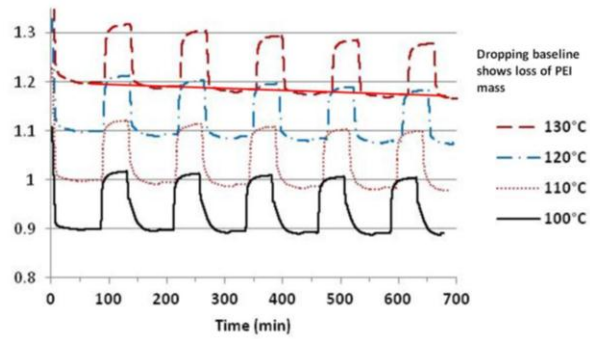

Figure 19. TGA profiles for multiple regeneration cycles of MBS-2 (423) at elevated temperatures using the stripping N_2 gas containing ~2 v% H_2O.

Table 9. CO_2 sorption capacity of MBS-2 (423) with cycles at desorption temperatures.

Cycle Number	Sorption capacity at desorption temperature, mg-CO_2/g-sorbent			
	100 °C	110 °C	120 °C	130 °C
1	125.6	126.8	122.9	128.2
2	121.5	119.0	110.1	113.4
3	119.7	114.5	101.7	98.0
4	118.5	112.4	92.0	85.9
5	115.7	108.5	85.0	74.9

Table 10. CO_2 sorption capacity of MBS-2 (423) with cycles at elevated temperatures using the stripping N_2 gas containing ~2% H_2O.

Cycle Number	Sorption capacity at desorption temperature, mg-CO_2/g-sorbent			
	100 °C	110 °C	120 °C	130 °C
1	117.6	122.1	112.6	117.8
2	115.7	120.0	110.2	113.5
3	114.9	117.6	108.0	110.1
4	114.4	116.6	105.8	107.1
5	114.4	116.2	103.7	104.9

4.4.2. The use of PEI with high molecular weight

In this project, we have investigated how the use of PEI with higher molecular weight influences thermal stability of MBS. Figure 20 shows (A) the thermal gravimetric analysis (TGA) and (B) the differential thermal gravimetric analysis (DTGA) profiles of 50 wt% PEI/SBA-15 samples with different PEI molecular weight. Before 100 °C There was a slight weight loss observed over all these samples due probably to the desorption of the adsorbed moisture and/or other gases like CO_2. After that, the samples exhibited thermal behavior with the increase of temperature. If taking 10% weight loss as the comparing point, it can be clearly seen that the temperature required increases gradually with the increase of PEI molecular weight. The one using a molecular weight of 1800 required a much higher temperature compared to the one with a lower molecular weight of 423, indicating that the use of a higher molecular weight PEI appears to be beneficial to the thermal stability of the final MBS material.

As shown in Figure 20. (A) TGA and (B) DTGA profiles of 50 wt% PEI/SBA-15 with different PEI molecular weight.Figure 20B, the peak temperature shifting with PEI molecular weight is clear. For the sample with a PEI molecular weight of 423, the decomposition peak temperature was ca. 270 °C. With increasing PEI molecular weight, the peak temperature progressively shifted to 300 °C for the one with a PEI molecular weight of 600, to 310 °C for the one with a PEI molecular weight of 1200 and further to 365 °C for the one with a PEI molecular weight of 1800. With the increase of molecular weight, the chain length increases. Consequently, the interaction between inter-molecules and intra-molecules becomes stronger. As a result, the decomposition peak temperature increased.

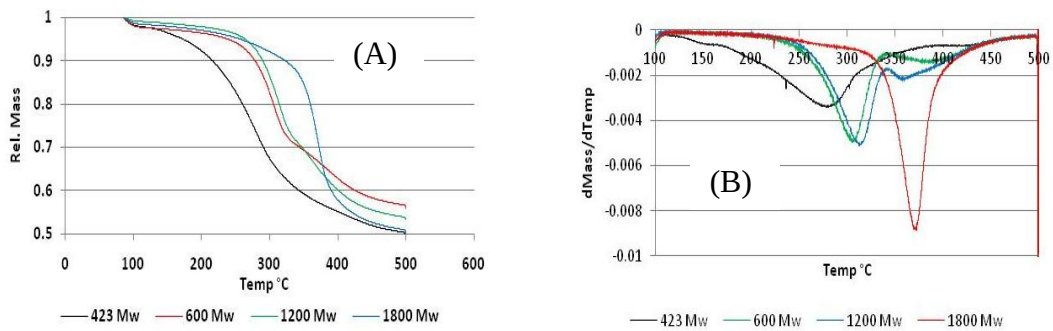

Figure 20. (A) TGA and (B) DTGA profiles of 50 wt% PEI/SBA-15 with different PEI molecular weight.

As shown, the time required to fully remove CO_2 from MBS sorbents is a limiting factor in the working capacity. TGA analysis shows that complete removal of CO_2 can be a slow process. As shown in Figure 21, at 100 ˚C, the complete removal of CO_2 from sorbent takes on the order of 45 min. Increasing the desorption temperature could shorten that process, as evidenced by the decrease in the desorption time for the complete CO_2 removal. When the desorption temperature is about 110 ˚C, the time for the complete CO_2 removal is reduced to 35 min. It further decreases to 25 min at 120 ˚C and significantly down to about 5 min at 130 ˚C. When the desorption temperature is higher than 130 ˚C, however, the time needed for the complete CO_2 removal from the sorbent does not change much. Considering that higher desorption temperature could greatly impact the stability of the sorbent material, the result implies that for MBS sorbents, the optimized desorption temperature is about 130 ˚C.

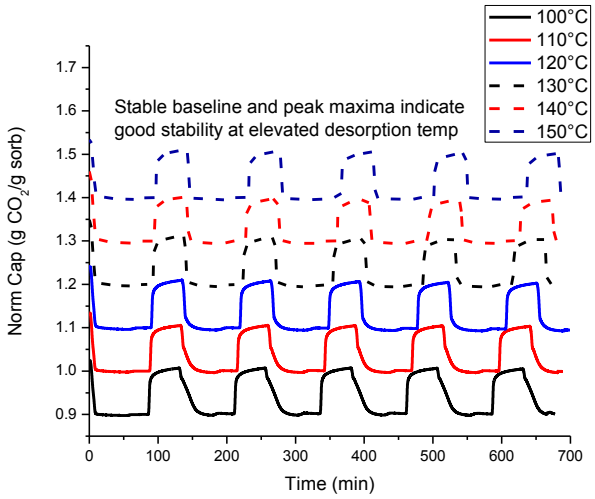

Figure 21. TGA profiles for multiple regeneration cycles of MBS-2 with PEI molecular weight (Mw) of 600 at elevated temperatures using dry N_2 as the stripping gas for desorption.

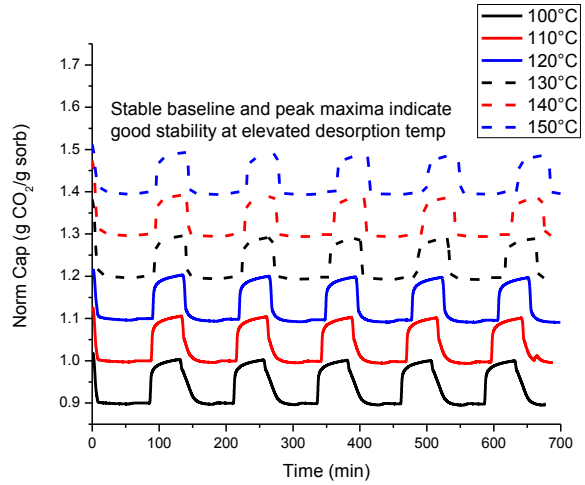

Figure 22. TGA profiles for multiple regeneration cycles of MBS-2 with PEI molecular weight (Mw) of 1200 at elevated temperatures using dry N_2 as the stripping gas for desorption.

This trend has also been seen in all four MBS samples with different Mw PEI including 600, 800, 1200 and 1800. As the desorption temperature rises, the time required to remove all CO_2 from the sorbent is reduced. Figure 22 shows a similar set of experiments over MBS-2 prepared by using PEI with Mw of 1200. Similar to the sample with PEI Mw of 600, the time required for full regeneration of the sorbent is greatly reduced as desorption temperature rises. 130 °C appears to be the best desorption temperature for this MBS sample with PEI Mw of 1200, in consideration of the desorption kinetics and the sorbent stability at high temperatures.

To examine the change in the desorption rate with the increase of the desorption temperature, we have stacked the desorption curves for the MBS sample with PEI Mw of 600, which is shown in Figure 23. As it can be seen, two desorption kinetic regimes can be easily identified in the desorption curves under all the desorption temperatures studied. One of which appears to be temperature dependent, which leads to a significant increase in desorption rate at these higher temperatures.

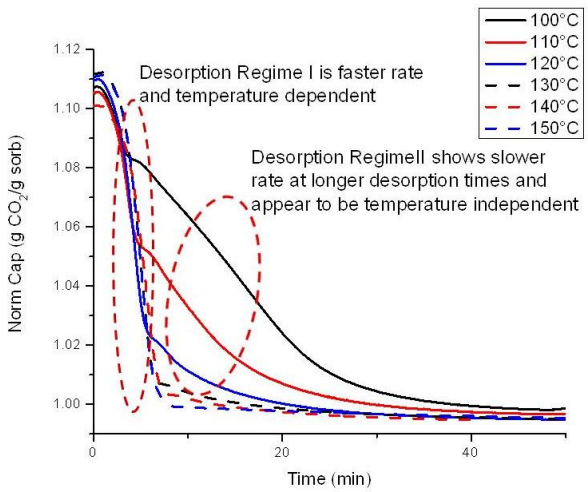

Figure 23. Desorption curves of MBS-2 with PEI Mw of 600 at elevated temperatures.

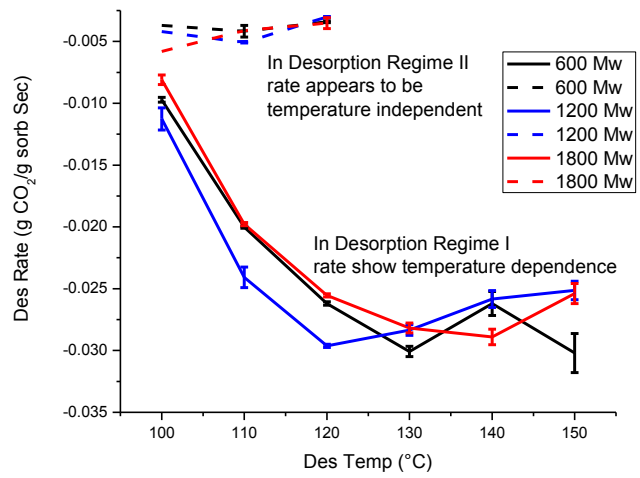

Figure 24. Desorption rates of MBS-2 with different Mw PEI in the regime I and II as a function of desorption temperature.

Upon close inspection of the desorption curves of MBS-2 with PEI Mw of 600 at temperatures of 100, 110 and 120 °C shown in Figure 23, it is noted that there are two portions of the desorption curve which are linear. These are denoted as regime I and regime II. Here, we use the linear part of the desorption curve to calculate the CO_2 desorption rate at different temperatures. The calculated desorption rates within the two regimes as a function of desorption temperature are presented in Figure 24**.** As seen, the desorption rate changes little with the desorption temperature in the regime II, while it varies greatly in the regime I, indicating that the desorption rate in the regime I is temperature dependent while it is temperature independent in the regime II. The desorption rate in the regime I is roughly double that of the regime II at 100 °C. As the temperature rises to 130 °C and higher, the desorption rate in the regime I rises to roughly 3 times of that at the desorption rate of 100 °C.

Therefore, increasing the desorption temperature is an effective way to enhance CO_2 desorption over the MBS-2 sorbents and 130 °C could be the optimized temperature for desorption. Furthermore, a higher working capacity with shortened desorption time may be achieved at elevated desorption temperature, such as 130 °C.

Figure 25 shows the CO_2 sorption capacity as a function of the sorption-desorption cycles (20 cycles) over the MBS-2 prepared by using PEI with molecular weight of 423, 600 and 1800 (termed as MBS-2(423), MBS-2(600) and MBS-2(1800), respectively) under dry conditions. The CO_2 sorption was conducted at 75 ˚C and the CO_2 desorption was performed at 120 ˚C with UHP N_2 as the purge gas. The CO_2 sorption capacity at the 1st, 10th and 20th cycle and the corresponding capacity loss after the 10th and 20th cycle are calculated and presented in Table 11. For the initial sorption capacity, the MBS-2 with low

PEI molecular weight gave a higher value. It was 106.3, 84.2, and 78.0 mg-CO_2/g-sorb for the MBS-2 with the PEI molecular weight of 423, 600 and 1800, respectively. With the increase of the cycle number, a significant drop in CO_2 capacity was observed over the MBS-2(423) sample. The CO_2 capacity became 66.8 mg-CO_2/g-sorb after 10 cycles and further decreased to 30.9 mg-CO_2/g-sorb after 20 cycles. The capacity loss reached to 37.1% for 10 cycles and as high as 70.9% for 20 cycles. The result clearly showed that the stability of MBS-2(423) is a big concern even it has a high initial capacity for CO_2.

Table 11. CO_2 sorption capacity with cycles and the calculated capacity loss percentages after cycles over the MBS-2 prepared with different PEI molecular weight under dry conditions.

Sample	Cap. under dry conditions (mg/g)			Cap. loss after 10 cycles (%)	Cap. loss after 20 cycles (%)
	1st	10th	20th		
MBS-2(423)	106.3	66.8	30.9	37.1	70.9
MBS-2(600)	84.2	71.6	63.3	14.9	24.7
MBS-2(1800)	78.0	71.9	64.9	7.8	16.7

Compared to MBS-2(423), the use of the PEI with higher molecular weight could improve the stability of the formed MBS-2 samples. The observed capacity loss with the increase of the cycle number was much less than that for MBS-2(423) sample. As for the MBS-2(600) sample, the CO_2 capacity became 71.6 mg-CO_2/g-sorb after 10 cycles and further decreased to 63.3 mg-CO_2/g-sorb after 20 cycles, corresponding to the capacity loss of 14.9% for 10 cycles and 24.7% for 20 cycles. The loss in capacity was only half of that for the MBS-2(423) sample. When the PEI molecular weight increased to 1800, the loss in capacity became even less within the same cycles. It was 7.8% for 10 cycles and 16.7% for 20 cycles, which is about 20% of those observed for the MBS-2(423) sample. The results highlight that the use of PEI with high molecular weight is highly beneficial in terms of improving the thermal stability of MBS-2 materials for CO_2 capture.

Further, we have also investigated the effect of moisture on the improvement of the stability of MBS-2 material for CO_2 capture. Moisture was introduced via a water bubbler using a UHP nitrogen stream then mixing with the CO_2 stream for sorption and with N_2 for desorption. The introduced moisture content was about 1.5%. Figure 26 shows the CO_2 sorption capacity as a function of the sorption-desorption cycles (20 cycles) over the MBS-2(423), MBS-2(600) and MBS-2(1800) samples under wet conditions. The CO_2 sorption was conducted at 75 ˚C and the CO_2 desorption was performed at 120 ˚C with UHP N_2 containing 1.5% moisture as the purge gas. The CO_2 sorption capacity at the 1st, 10th and 20th cycle and the corresponding capacity loss after the 10th and 20th cycle are calculated and presented in Table 12.

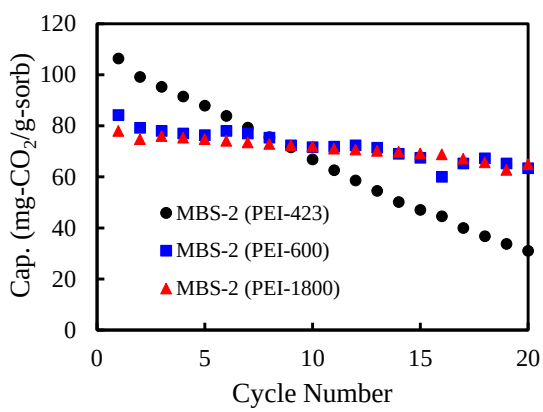

Figure 25. The CO_2 sorption capacity as a function of sorption-desorption cycles over the MBS-2 prepared with PEI molecular weight of (●) 423, (■) 600 and (▲) 1800 under dry conditions measured by TGA.

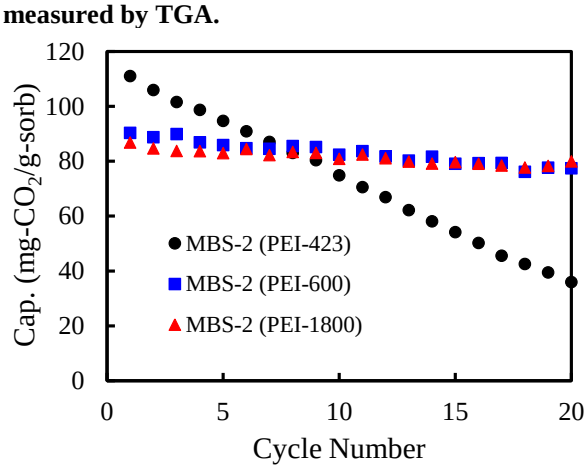

Figure 26. The CO_2 sorption capacity as a function of sorption-desorption cycles over the MBS-2 prepared with PEI molecular weight of (●) 423, (■) 600 and (▲) 1800 under wet conditions measured by TGA.

For the initial sorption capacity, the MBS-2 with low PEI molecular weight gave a higher value. It was 111.0, 90.3, and 86.8 mg-CO_2/g-sorb for the MBS-2(423), MBS-2(600) and MBS-2(1800) samples, respectively. All were slightly better than those under dry conditions, implying that the presence of moisture has a promotion effect on the CO_2 sorption capacity of MBS materials, as reported by Xu et al. [5]. With the increase of the cycle number, a significant drop in CO_2 capacity was still observed over the MBS-2(423) sample. The CO_2 capacity became 74.8 mg-CO_2/g-sorb after 10 cycles and further decreased to 35.9 mg-CO_2/g-sorb after 20 cycles. The capacity loss reached to 32.6% for 10 cycles and as high as 67.6% for 20 cycles. Compared to the loss under dry conditions, it suggests that the presence of moisture does not improve the stability of MBS-2(423) sample.

Table 12. CO_2 sorption capacity with cycles and the calculated capacity loss percentages after cycles over the MBS-2 prepared with different PEI molecular weight under wet conditions.

Sample	Cap. under wet conditions (mg/g)			Cap. loss after 10 cycles (%)	Cap. loss after 20 cycles (%)
	1st	10th	20th		
MBS-2(423)	111.0	74.8	35.9	32.6	67.6
MBS-2(600)	90.3	82.3	77.4	8.8	14.3
MBS-2(1800)	86.8	80.9	79.9	6.8	7.9

As for the samples with high PEI with higher molecular weight, however, a good improvement was observed. Over the MBS-2(600) sample under wet conditions, the CO_2 capacity became 82.3 mg-CO_2/g-sorb after 10 cycles and further decreased to 77.4 mg-CO_2/g-sorb after 20 cycles, corresponding to the capacity loss of 8.8% for 10 cycles and 14.3% for 20 cycles. Compared to the loss under the dry conditions which was 14.9% for 10 cycles and 24.7% for 20 cycles, the capacity loss under wet conditions was much less, becoming only half of that, indicating that the addition of moisture could greatly improve the thermal stability of the MBS-2(600) sample for CO_2 capture. A similar promotion effect on the thermal stability was also observed over the MBS-2(1800) sample. The capacity loss became 6.8% for 10 cycles and 7.9% for 20 cycles.

As shown above, compared to the initial MBS-2(423) sample, the thermal stability has been significantly improved by using the PEI with molecular weight of 1800 and adding moisture in the purge gas for desorption. Within 10 and 20 repeated cycles, a reduction of about 80% and 90% in the loss of the sorbent capacity was successfully obtained by using PEI polymer with molecular weight of 1800 and wet conditions for CO_2 sorption and regeneration.

4.4.3. Improvement of MBS-2 sorbent via cross-linking

The cross-linking method may help the PEI attach each other and thus promote its thermal stability and regeneration stability. Since the crosslinking occurs on the amine sites, the sorption capacity may be less due to the consumption by the crosslinking agent. On the other hand, we found in our early work that the amine usage of MBS-2 still less than the theoretical value. The crosslinking may expand the PEI molecules, thus more and unused amine sites can be exposed for CO_2 sorption. Consequently, the CO_2 sorption capacity may even increase.

PEI cross-linking modification was done using one of two cross-linking agents: bisphenol A diglycidyl ether (BPA) or oxalic acid (OA). Preparation of the BPA cross-linked sample was done by impregnation of SBA-15 with BPA cross-linked PEI solution. BPA cross-linked PEI solutions were prepared by addition of the desired amount of BPA/acetone solution (50/50 v%) to PEI/acetone solution (0.13 g/mL) with further stirring for 1 hrs. Then the BPA cross-linked PEI solution was added to SBA-15/acetone slurry (0.13 g/mL). The slurry was then stirred for another 4 hrs. After that, the solvent was removed at 40 °C under vacuum overnight. Oxalic acid (OA) cross-linked samples were similarly prepared by impregnation of SBA-15 with an OA cross-linked solution. This OA cross-linked PEI

solution was prepared by addition of the desired amount of an oxalic acid/MeOH solution (50/50 v%) to 2 g PEI in methanol (0.25 g/mL) with continuous stirring for 1 hour. The OA cross-linked PEI solution was then added to SBA-15/acetone slurry (0.25 g/mL), stirred for 4 hrs, and then dried at 40 °C under vacuum overnight.

Figure 27 shows the CO_2 breakthrough curves on BPA-crosslinked MBS-2 samples for CO_2 separation from the model flue gas containing 15% CO_2 and 4.5% O_2 in N_2 at 75 °C. The original MBS-2 sorbent exhibited a good performance for CO_2 capture. The addition of BPA to crosslink PEI resulted in the decrease of CO_2 sorption capacity of MBS-2 sorbent. Even with 0.5 wt% BPA crosslinking PEI, CO_2 broke through much earlier in comparison with MBS-2. Similar breakthrough curve was obtained over the 1 wt% BPA/MBS-2 sample. Further increasing the crosslinking amount by introducing more BPA to 2.5 wt% and 5 wt%, CO_2 broke through even earlier. Based on the breakthrough curves, the corresponding sorption capacity can be calculated to be 140.5, 92.8, 96.7, 80.1 and 77.9 mg-CO_2/g-sorbent for MBS-2, 0.5% BPA/MBS-2, 1% BPA/MBS-2, 2.5% BPA/MBS-2, and 5% BPA/MBS-2, respectively. Clearly, using BPA as the crosslinking agent to modify the MBS-2 sorbent results in the decrease of CO_2 sorption capacity of MBS-2.

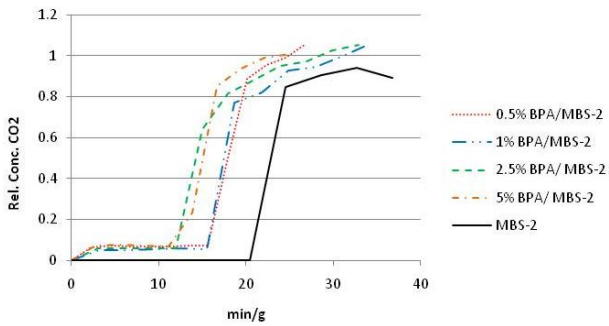

Figure 27. CO_2 breakthrough curves obtained over MBS-2 and BPA/MBS-2 sorbents for CO_2 separation from the model flue gas containing 15% CO_2 and 4.5% O_2 in N_2 at 75 °C.

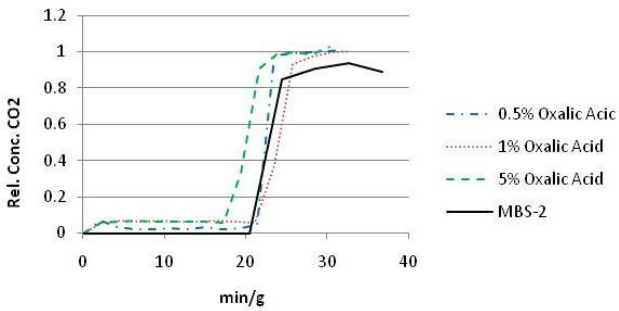

Figure 28. CO_2 breakthrough curves obtained over MBS-2 and OA/MBS-2 sorbents for CO_2 separation from the model flue gas containing 15% CO_2 and 4.5% O_2 in N_2 at 75 °C.

Figure 28 shows the CO_2 breakthrough curves on OA-crosslinked MBS-2 samples for CO_2 separation from the model flue gas containing 15% CO_2 and 4.5% O_2 in N_2 at 75 °C. For comparison, the breakthrough curve obtained on MBS-2 is also presented. Interestingly, unlike BPA as the crosslinking agent, when 0.5 and 1 wt% of OA was used to crosslink PEI in MBS-2 sorbent, almost the same breakthrough time was observed, suggesting that comparing to BPA, OA as the crosslinking agent has a minor effect on the sorption capacity of MBS-2. However, further increasing the OA amount to 5 wt%, the breakthrough of CO_2 became much earlier. The corresponding sorption capacities of these sorbents are 119, 131.1 and 105 mg-CO_2/g-sorbent for 0.5% OA/MBS-2, 1% OA/MBS-2, and 5% OA/MBS-2, respectively. Compared to BPA-crosslinked MBS-2 samples, the OA crosslinked MBS-2 samples have higher CO_2 sorption capacity, although the introduction of OA also results in the decrease of the sorption capacity of MBS-2 sorbent.

Figure 29 shows the thermal stability of MBS-2 after OA-crosslinking was examined by TGA. For comparison, the TGA profiles obtained over SBA-15, 15 wt% PEI/SBA-15 and 50 wt% PEI/SBA-15 (i.e., MBS-2) are also presented. It can be seen that there was about 12 % of weight loss observed over pure SBA-15 before 100 °C probably due to the desorption of the adsorbed moisture and/or other gases like CO_2, suggesting the SBA-15 prepared in this work has a potential to adsorb the moisture and/or other gases at room temperature. Almost no weight loss was observed when temperature higher than 100 °C till to 600 °C. When 15 wt% PEI was loaded, the weight loss before 100 °C became smaller and a sharp loss was observed at about 300 °C. In our previous work, we found that over the pure PEI, the weight loss was ca. 2 % when the temperature increased to 100 °C, and the decomposition started at above 150 °C with a

sharp weight loss appearing at about 200 °C. When the temperature was higher than 300 °C, the rate of weight loss decreased, indicating a different decomposition process. Thus, compared to pure PEI, the thermal stability of loaded PEI was promoted, probably due to surface interaction between the amine groups in PEI and the surface silanol groups which has been identified in our early *in-situ* FTIR study [2].

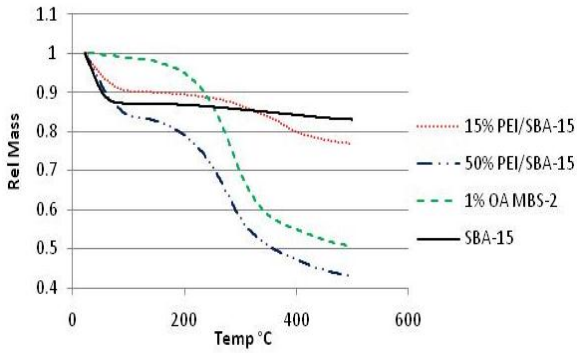

Figure 29. TGA profiles of SBA-15, 15% PEI/SBA-15, 50% PEI/SBA-15 (i.e., MBS-2) and 1% OA/MBS-2.

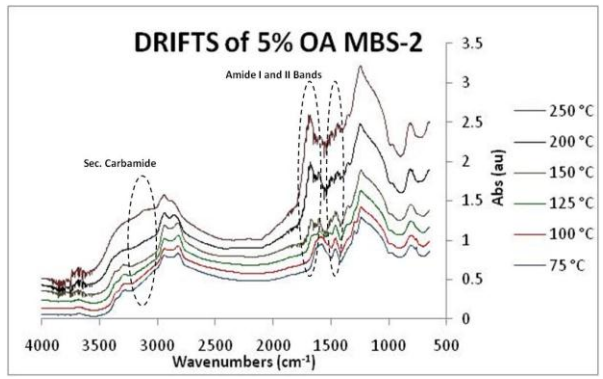

Figure 30. FTIR spectra of oxalic acid cross-linked MBS-2 under N_2 flow at different temperatures.

However, when PEI loading was increased to 50 wt%, besides the weight loss before 100 °C induced by the pre-adsorbed moisture and CO_2, a quickly weight loss starting at about 150 °C can be recognized. After OA-crosslinked, there was a very little amount of weight loss before 100 °C and the quickly weight loss starting point shifted to about 200 °C, as shown in Figure 29. This result suggests that the introduction of oxalic acid to crosslink the PEI in MBS-2 has a positive impact on thermal stability of MBS-2. The impact of OA- and/or BPA crosslinking on the regeneration stability of MBS-2 material will be further studied in the next report period.

The nature of the interactions introduced by incorporation of oxalic acid have been investigated by FTIR analysis. DRIFTS of MBS-2 and oxalic acid incorporated MBS-2 shows evidence of the formation of an ionic interaction in the form of ammonium (peaks at 3000-2800 cm^{-1} and 2000-1700 cm^{-1}) and carboxylate (broad peaks at 2700-2200 cm^{-1} and 1600 cm^{-1}) between the amines of PEI and the organic acid, especially when oxalic acid incorporated MBS-2 was heated and DRIFTS spectra taken at various temperatures, as shown in Figure 30. The appearance of peaks at (1700, 1515 and 3300-3000 cm^{-1}) indicates dehydration of the ammonium carboxylate species to the carbamide, forming a chemical bond between polymer strands. As the temperature rises above 100 °C, the amide I and II bands begin to become apparent in the DRIFTS spectra. As the temperature continues to rise above 150 °C there seems to be little change in the formation of carbamide in the sorbent. When the temperature is raised to 250 °C, the peaks consistent with cross linked PEI continue to be visible and continue in approximately the same intensity suggesting that the material remains fairly constant in composition as temperature rises.

The regenerability of the cross-linked MBS-2 sorbent has also been investigated by TGA in this work. The sample loaded with 5% of oxalic acid to the MBS-2(423) and MBS-2(600) were prepared and evaluated their performance for CO_2 sorption-desorption with repeated cycles. Figure 31 shows the CO_2 sorption capacity as a function of the sorption-desorption cycles (20 cycles) over the MBS-2(423), 5%OA-MBS-2(423), MBS-2(600) and 5%OA-MBS-2(600) samples under dry conditions. The CO_2 sorption was conducted at 75 ˚C and the CO_2 desorption was performed at 120 ˚C with UHP N_2 as the purge gas. The CO_2 sorption capacity at the 1st, 10th and 20th cycle and the corresponding capacity loss after the 10th and 20th cycle are calculated and presented in Table 13.

The MBS-2(423) sample showed the initial CO_2 sorption capacity of 106.3 mg-CO_2/g-sorb. After 5% OA was added to crosslink PEI polymer, the sorption capacity dropped, being about 78.9 mg-CO_2/g-sorb. In addition, the final sorption capacity after 10 and 20 cycles was also worse than that without OA addition. The capacity loss of the 5%OA-MBS-2(423) sorbent was 45.2 and 80.2% after 10 and 20

repeated cycles, while it was 37.1 and 70.9% for the MBS-2(423). It suggests that the addition of OA to the MBS-2 prepared by PEI polymer with molecular weight of 423 not only decreases the sorption capacity for CO_2, but also reduces the thermal stability of the sorbent material for CO_2 sorption-desorption cycles.

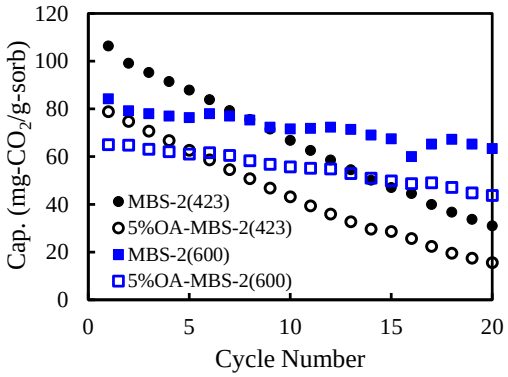

Figure 31. The CO_2 sorption capacity as a function of sorption-desorption cycles over the MBS-2(423), 5%OA-MBS-2(423), MBS-2(600) and 5%OA-MBS-2(600) samples under dry conditions measured by TGA.

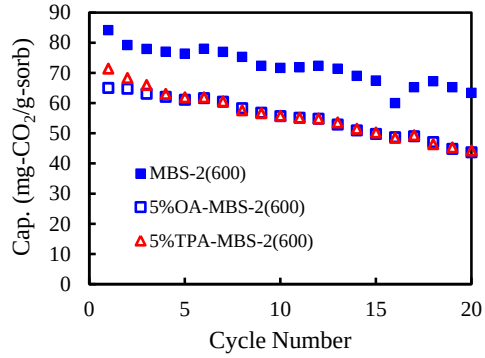

Figure 32. The CO_2 sorption capacity as a function of sorption-desorption cycles over the MBS-2(600), 5%OA-MBS-2(600), and 5%TPA-MBS-2(600) samples under dry conditions measured by TGA.

Table 13. CO_2 sorption capacity with cycles and the calculated capacity loss percentages after cycles over the MBS-2 prepared with different PEI molecular weight and cross-linked with diacid compound under dry conditions.

Sample	Cap. under dry conditions (mg/g)			Cap. loss after 10 cycles (%)	Cap. loss after 20 cycles (%)
	1st	10th	20th		
MBS-2(423)	106.3	66.8	30.9	37.1	70.9
5%OA-MBS-2(423)	78.9	43.2	15.6	45.2	80.2
MBS-2(600)	84.2	71.6	63.3	14.9	24.7
5%OA-MBS-2(600)	65.0	55.7	43.7	14.4	32.7
5%TPA-MBS-2(600)	71.4	55.8	44.3	21.9	38.0

As for the MBS-2(600) sample, a reduction in CO_2 capacity was also observed with the addition of 5% OA. The capacity dropped from 84.2 mg-CO_2/g-sorb for the MBS-2(600) sample to 65.0 mg-CO_2/g-sorb for the 5%OA-MBS-2(600) sample. After 10 cycles, the capacity loss over the 5%OA-MBS-2(600) sorbent was 14.4%, which is similar to the one for the MBS-2(600) sorbent after 10 cycles (~14.9%). When the repeated cycles increased to 20 cycles, the capacity loss for the 5%OA-MBS-2(600) sorbent became 32.7%, larger than that for the MBS-2(600) sorbent, which was about 24.7%. It shows that under dry conditions, the addition of OA does not promote the thermal stability of the MBS-2 sorbent within repeated cycles. It may also suggest that oxalic acid is not a proper cross-linking agent to improve the thermal stability of MBS-2 sorbent.

Consequently, we have investigated another diacid compound, terephthalic acid (TPA) to cross-link PEI polymer. The obtained CO_2 sorption capacity as a function of sorption-desorption cycles is shown in Figure 32. For comparison, the obtained sorption capacity for MBS-2(600) and 5%OA-MBS-2(600) sorbent is also presented. The calculated CO_2 sorption capacity at the 1st, 10th and 20th cycle and the corresponding capacity loss after the 10th and 20th cycle are also listed in Table 13. Using TPA as the cross-linking agent, the initial sorption capacity was 71.4 mg-CO_2/g-sorb, better than that of the 5%OA-MBS-2(600) sample (65.0 mg-CO_2/g-sorb), but still lower than that of the MBS-2(600) sample (84.2 mg-CO_2/g-sorb). Additionally, as shown in Figure 32, the sorption capacity curve for the 5%TPA-MBS-2(600) sample and 5%OA-MBS-2(600) sample was almost overlapped, suggesting that the two sorbents have

similar thermal stability within the studied CO_2 sorption-desorption cycles. The capacity loss was 21.9 and 38.0% after 10 and 20 cycles. The results indicate that under dry conditions, cross-linking PEI polymer with diacid (either oxalic acid or terephthalic acid) does not promote the thermal stability of the MBS-2 sorbent.

As shown above that using a wet gas stream could also promote the thermal stability of MBS-2 sorbent for CO_2 sorption-desorption. Therefore, we have further investigated the effect of diacid cross-linking on thermal stability of MBS-2 under wet conditions. Figure 33 shows the CO_2 sorption capacity as a function of the sorption-desorption cycles (20 cycles) over the MBS-2(423), 5%OA-MBS-2(423), MBS-2(600) and 5%OA-MBS-2(600) samples under wet conditions. The CO_2 sorption was conducted at 75 ˚C and the CO_2 desorption was performed at 120 ˚C with UHP N_2 containing 1.5% moisture as the purge gas. The CO_2 sorption capacity at the 1st, 10th and 20th cycle and the corresponding capacity loss after the 10th and 20th cycle are calculated and presented in Table 14.

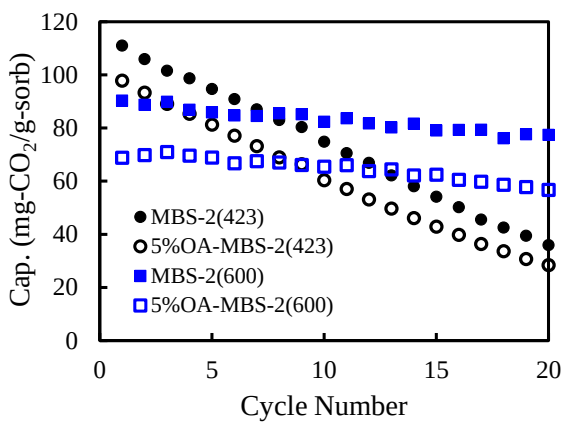

Figure 33. The CO_2 sorption capacity as a function of sorption-desorption cycles over the MBS-2(423), 5%OA-MBS-2(423), MBS-2(600) and 5%OA-MBS-2(600) samples under wet conditions measured by TGA.

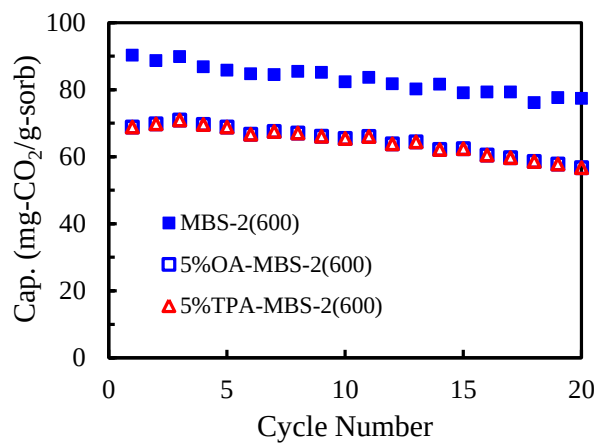

Figure 34. The CO_2 sorption capacity as a function of sorption-desorption cycles over the MBS-2(600), 5%OA-MBS-2(600), and 5%TPA-MBS-2(600) samples under dry conditions measured by TGA.

Table 14. CO_2 sorption capacity with cycles and the calculated capacity loss percentages after cycles over the MBS-2 prepared with different PEI molecular weight and cross-linked with diacid compound under wet conditions.

Sample	Cap. under wet conditions (mg/g)			Cap. loss after 10 cycles (%)	Cap. loss after 20 cycles (%)
	1st	10th	20th		
MBS-2(423)	111.0	74.8	35.9	32.6	67.6
5%OA-MBS-2(423)	97.8	60.3	28.4	38.3	70.9
MBS-2(600)	90.3	82.3	77.4	8.8	14.3
5%OA-MBS-2(600)	68.8	65.4	56.7	4.9	17.6
5%TPA-MBS-2(600)	78.6	66.3	60.6	15.7	22.9

The MBS-2(423) sample showed the initial CO_2 sorption capacity of 111.0 mg-CO_2/g-sorb. After 5% OA was added to crosslink PEI polymer, the sorption capacity dropped, being about 97.8 mg-CO_2/g-sorb. The capacity reduction due to the addition of OA was about 12% under wet conditions, which is much less than that under dry conditions (about 26%). Unfortunately, even under wet conditions, the thermal stability was not improved. The capacity loss was 38.3 and 70.9% after 10 and 20 repeated cycles. Though it is better than that under dry condition, it is still worse than the MBS-2(423) sorbent without

OA addition. Thus, it reveals that the addition of OA to the MBS-2(423) would not promote the thermal stability whether under dry or wet conditions.

As for the MBS-2(600) sample, a reduction in CO_2 capacity was also observed with the addition of 5% OA even under wet conditions. The capacity dropped from 90.3 mg-CO_2/g-sorb for the MBS-2(600) sample to 68.8 mg-CO_2/g-sorb for the 5%OA-MBS-2(600) sample. Unlike under dry conditions, a promotion effect on the thermal stability due to the addition of OA was observed under wet conditions. After 10 cycles, the capacity loss over the 5%OA-MBS-2(600) sorbent was only 4.9%, which is much less than that for the MBS-2(600) sorbent after 10 cycles (~8.8%). When the repeated cycles increased to 20 cycles, the capacity loss for the 5%OA-MBS-2(600) sorbent became 17.6%, however, slightly larger than that for the MBS-2(600) sorbent, which was about 14.3%. It shows that under wet conditions, the addition of OA did promote the thermal stability of the MBS-2 sorbent within 10 repeated cycles. After that, the thermal stability of the OA cross-linked MBS-2(600) sorbent still needs to be improved further.

Furthermore, we have also investigated the influence of adding another diacid compound, terephthalic acid (TPA) to cross-link PEI polymer under wet conditions. The obtained CO_2 sorption capacity as a function of sorption-desorption cycles is shown in Figure 34. For comparison, the obtained sorption capacity for MBS-2(600) and 5%OA-MBS-2(600) sorbent is also presented. The calculated CO_2 sorption capacity at the 1st, 10th and 20th cycle and the corresponding capacity loss after the 10th and 20th cycle are also listed in Table 14. As can be seen, using TPA as the cross-linking agent under wet conditions, the initial sorption capacity was 78.6 mg-CO_2/g-sorb, better than that of the 5%OA-MBS-2(600) sample (68.8 mg-CO_2/g-sorb), but still lower than that of the MBS-2(600) sample (90.3 mg-CO_2/g-sorb). Additionally, as shown in Figure 34, the sorption capacity curve for the 5%TPA-MBS-2(600) sample and 5%OA-MBS-2(600) sample was almost overlapped, suggesting that the two sorbents have similar thermal stability within the studied CO_2 sorption-desorption cycles under wet conditions. The capacity loss was 15.7 and 22.9% after 10 and 20 cycles, both larger than those over the 5%OA-MBS-2(600) sorbent. The results indicate that oxalic acid is a better cross-linking agent for PEI than terephthalic acid in terms of better thermal stability both under the dry and wet conditions.

4.4.4. Improvement of FS-MBS sorbent via cross-linking

As discussed above, the thermal stability of MBS-2 could be improved by adding diacids such as oxalic acid. As shown in this work, fumed silica as a support replacement for ordered silica (MCM-41, SBA-15) showed a good sorption capacity, low preparation and material cost, but also indicates a loss of capacity upon regeneration. To investigate the influence of organic diacids addition on the thermal stability of these materials, a series of MBS samples were prepared using commercially available fumed silica (Cab-o-Sil M5 and HS5 from Sigma-Aldrich), polyethylenimine (PEI) (600 Mw, Polysciences Inc.) and oxalic acid (Alfa Aesar). Same preparation procedure as MBS-2 was conducted for fumed silica based MBS preparation with OA cross-linking.

Figure 35 shows the TGA profiles of MBS-M5 and OA incorporated MBS-M5 samples for CO_2 capture within 5 cycles. In each cycle, CO_2 sorption using pure CO_2 stream and desorption by purging N_2 were performed at 75 and 100 °C, respectively. The obtained sorption capacity for each sample and each cycle was listed in Table 15. MBS-M5 without OA incorporation showed high capacity for CO_2 capture, reaching 140.5 mg-CO_2/g-sorbent. However, within 5 cycles of CO_2 sorption-desorption test, the sorption capacity of this material decreased gradually. After 5 cycles, the sorption capacity was about 97% of that for the fresh sample. Compared to MBS-M5 sample, those with OA addition showed much better cyclic stability. With 1% OA addition, only a slight decrease was observed in the first 2 cycles. After 5 cycles of sorption-desorption, the sorption capacity was 126.3 mg-CO_2/g-sorbent, about 99% of that for the fresh sample. For the samples with higher OA loadings, almost no decrease was observed during 5 cycles of CO_2 sorption-desorption operation, indicating that the addition of OA can improve the stability of MBS-M5 materials for thermal treatment and regeneration. Besides, it should also be noted that the addition of OA will result in the decrease of the CO_2 sorption capacity of MBS-M5 sorbent, although the addition of OA could promote the stability of MBS-M5 sorbent during thermal treatment and regeneration. As shown in Table 15, with 1% OA addition, the sorption capacity decreased to 127.4 mg-CO_2/g-sorbent. Further

increasing OA loadings to 5, 10%, the sorption capacity of MBS-M5 dropped to 107.4 and 83.9 mg-CO_2/g-sorbent, respectively. When the OA addition amount was increased to 25%, the sorption capacity of formed 25% OA-MBS-M5 sorbent was only 14.8 mg-CO_2/g-sorbent, significantly lower than that of MBS-M5, being only 10% of the initial capacity.

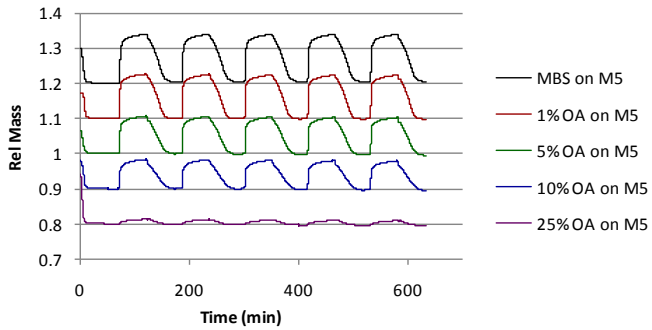

Figure 35. TGA profiles of MBS-M5 samples with and without OA addition within 5 cyclic CO_2 sorption-desorption test.

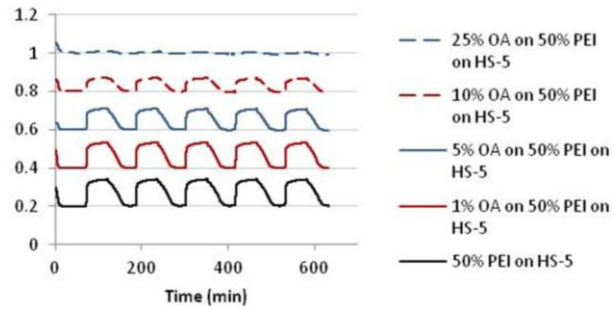

Figure 36. TGA profiles of MBS-HS5 samples with and without OA addition for 5 cycles of CO_2 sorption-desorption tests.

Table 15. Sorption capacity of MBS-M5 samples with and without OA addition within 5 CO_2 sorption-desorption cycles measured by TGA.

OA addition, %	Sorption capacity, mg-CO_2/g-sorbent				
	Cycle 1	Cycle 2	Cycle 3	Cycle 4	Cycle 5
0	140.5	137.3	136.9	136.8	136.3
1	127.4	126.6	126.5	126.3	126.3
5	107.4	107.0	106.2	107.7	107.9
10	83.9	83.1	80.9	82.8	83.7
25	14.8	14.4	14.6	14.7	14.9

Another promising fumed silica sample, Cab-O-Sil HS5 was also used as the support for MBS preparation. Figure 36 shows the TGA profiles of MBS-HS5 and OA incorporated MBS-HS5 samples for CO_2 capture within 5 cycles. In each cycle, CO_2 sorption using pure CO_2 stream and desorption by purging N_2 were performed at 75 and 100 °C, respectively. The obtained sorption capacity for each sample and each cycle was listed in Table 16. MBS-HS5 without OA incorporation showed high capacity for CO_2 capture, reaching 138.9 mg-CO_2/g-sorbent. However, within 5 cycles of CO_2 sorption-desorption test, the sorption capacity of this material decreased gradually. After 5 cycles, the sorption capacity was 135.3 mg-CO_2/g-sorbent, about 97% of that for the fresh sample.

Table 16. Sorption capacity of MBS-HS5 samples with and without OA addition for 5 cycles of CO_2 sorption-desorption tests measured by TGA.

OA addition, %	Sorption capacity, mg-CO_2/g-sorbent				
	Cycle 1	Cycle 2	Cycle 3	Cycle 4	Cycle 5
0	138.9	135.7	136.0	136.1	135.3
1	133.1	130.3	129.9	130.1	130.1
5	111.3	109.2	108.6	108.9	108.8
10	72.6	69.1	70.2	69.9	70.5
25	9.5	9.9	10.1	10.0	9.9

Compared to MBS-HS5 sample, those with OA addition showed much better cyclic stability. With 1% OA addition, only a slight decrease was observed in the first 2 cycles. After 5 cycles of sorption-desorption, the sorption capacity was ca. 130 mg-CO_2/g-sorbent, about 98% of that for the fresh sample. For the samples with higher OA loadings, almost no decrease was observed during 5 cycles of CO_2

sorption-desorption operation, indicating that the addition of OA can improve the stability of MBS-M5 materials for thermal treatment and regeneration. However, it should also be noted that the addition of OA results in the decrease of the CO_2 sorption capacity of MBS-HS5 sorbent, although the addition of OA could promote the stability of MBS-HS5 sorbent during thermal treatment and regeneration. As shown in Table 16, with 1% OA addition, the sorption capacity slightly decreased from 138.9 to 133.1 mg-CO_2/g-sorbent. Further increasing OA loadings to 5, 10%, the sorption capacity of MBS-HS5 dropped to 111.3 and 72.6 mg-CO_2/g-sorbent, respectively. When the OA addition amount was increased to 25%, the sorption capacity of formed 25% OA-MBS-HS5 sorbent was only 9.5 mg-CO_2/g-sorbent, significantly lower than that of MBS-HS5, being only 7% of the initial capacity.

Figure 37 shows the thermal stability of MBS-HS5 and MBS-HS5 with OA incorporation. The decomposition temperature for MBS-HS5 is about 310 °C. With the addition of OA, the decomposition temperature shifts to higher temperature. The more OA is added, the higher the decomposition temperature for OA-MBS-HS5 sorbent is. It clearly shows the improvement in thermal stability of MBS-HS5 via the addition of OA, which is consistent with the computational results and our earlier reports on MBS-2 and MBS-M materials.

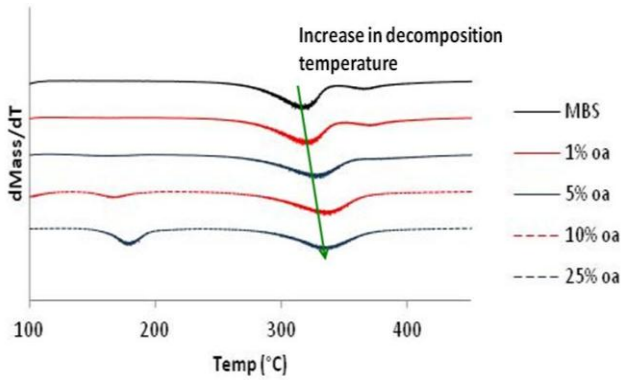

Figure 37. TGA profiles of MBS-HS5 samples with and without OA addition under N_2 flow.

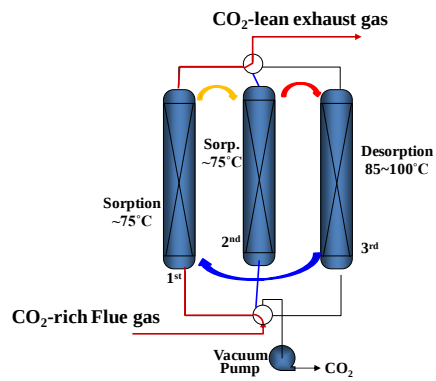

Scheme 1. Proposed sorption process using MBS for CO_2 capture from flue gas.

4.5. Scaling up the sorption process (Task 5)

4.5.1. Proposed process design for CO_2 capture based on PEI/SBA-15 sorbent

For the PEI/SBA-15 sorbent, we propose to use a fixed-bed adsorption process to continuously remove and recover CO_2, as illustrated in **Scheme** . We will use three columns in series to conduct CO_2 capture from raw flue gas at 75 °C. Because of high CO_2-affinity of PEI/SBA-15 sorbent, the CO_2-lean exhaust gas can be produced after adsorption, which is environmentally allowable. As soon as the first column is broke through, the second column will continue removing CO_2 from the pre-cleaned flue gas to secure the CO_2 concentration in the effluent, while the first column serving as a guard column, so that the sorption capacity of the sorbent in the first column can be fully utilized. As soon as the first column is saturated, it will be replaced by a completely regenerated column (3rd column in the **Scheme**). While the previous second column is now working as a guard column and will be fully used. In that way, the process can run continuously and the CO_2-rich flue gas stream can be deeply cleaned, while sorption capacity of these sorption columns could be fully utilized.

It should be pointed out that the proposed continuous fixed-bed sorption-desorption process is not the only option. Via the improvement of physical & chemical properties of the PEI/SBA-15 sorbent, other type of system such as fluidized-bed or moving-bed can be developed and applied for CO_2 capture from glue gas.

4.5.2. Scale-up test on PEI/SBA-15 sorbent

In this project, we have conducted a scale-up test on the developed PEI/SBA-15 sorbents with a sorbent bed volume of 200 mL in order to provide more reliable and accurate parameters for the engineering design of the process and feasible study. A stainless steel column (5.08 cm, O.D.; 4.12 cm, I.D.; 15 cm in Length, total volume, 200 mL) has been fabricated for this work. For a large column, the pressure drop across the column can be considerably high if a sample in powder form is used. Thus, we have made a pellet form (10-18 mesh, or 1-2 mm particles) for this study. The appearance of the prepared pellet PEI/SBA-15 sorbent in comparison with original PEI/SBA-15 sorbent in powder form and the manufactured 200 mL column within a GC oven as a heating source are shown in Figure 38. It can be seen that there is no significant change in PEI/SBA-15 after pelletizing.

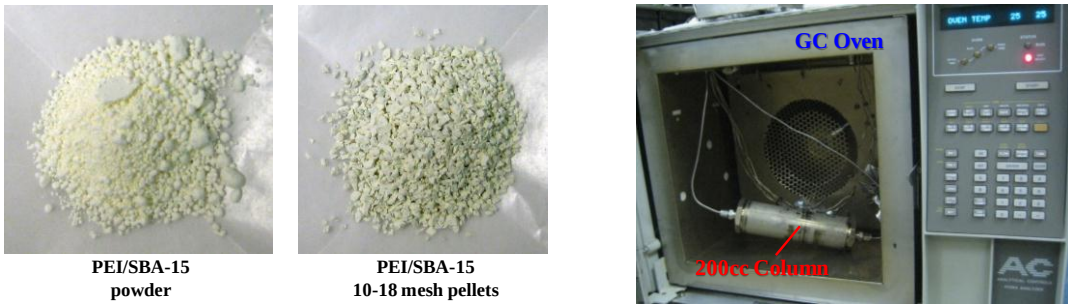

Figure 38. Appearance of PEI/SBA-15 in powder and pellet (10-18 mesh, i.e., 1-2 mm) form and the 200 mL column in GC oven used in the scale-up test.

Before the scale-up test using the 200 mL column, the pelletized PEI/SBA-15 sorbent has been evaluated for CO_2 capture from model flue gas to ensure its CO_2 sorption performance. About 1.2 g of PEI/SBA-15 pellets were packed into a small column (9.5 mm, O.D.; 7.5 cm, I.D.; 5 cm in Length, total volume, ~2 mL). After the pretreatment at 100 °C, the model flue gas contain 14% CO_2 in N_2 was introduced at 100 ml/min under 75 °C and CO_2 concentration in the effluent was recorded by on-line MKS-2030 multigas analyzer. The result is presented in Figure 39.

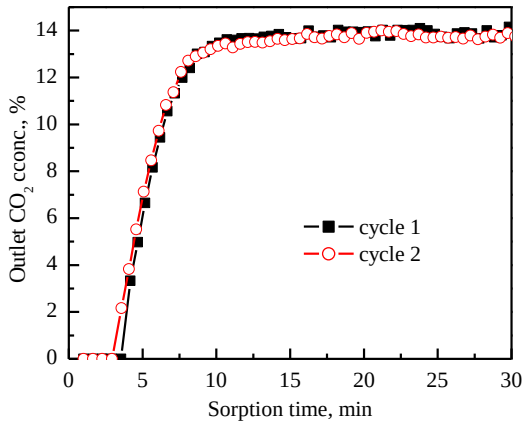

Figure 39. Breakthrough curves of CO_2 over the PEI/SBA-15 sorbent pellets (10-18 mesh, or 1-2 mm, 2 mL in total) at 75 °C for CO_2 capture from model flue gas containing 14% CO_2 in N_2 with a flow rate of 100 mL/min (a GHSV of ~3000 h^{-1}).

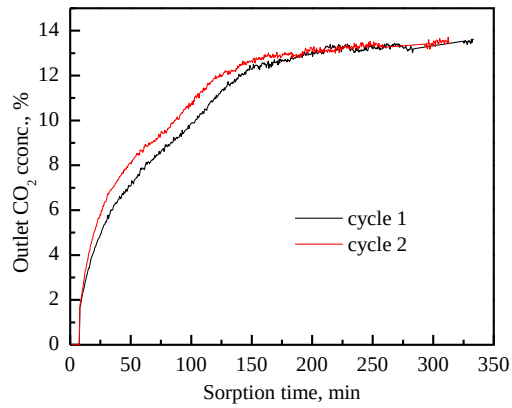

Figure 40. Breakthrough curves of CO_2 over the PEI/SBA-15 sorbent pellets (10-18 mesh, or 1-2 mm, 200 mL in total) at 75 °C for CO_2 capture model flue gas containing about 15% CO_2 and 4.5% O_2 in N_2 with a flow rate of 400 mL/min (a GHSV of ~120 h^{-1})

The PEI/SBA-15 pellets can work effectively to remove CO_2 from flue gas down to very low level and show up a high capacity. On the basis of breakthrough curve, the sorption capacity can be calculated as of 136.7 mg-CO_2/g-sorbent. The value is slightly lower than that obtained over PEI/SBA-15

sorbent in powder mode, indicating that the pelletizing process will not damage the sorption properties of the PEI/SBA-15 material. Additionally, we have also test the regenerability of the PEI/SBA-15 pellets. The spent EPI/SBA-15 sorbent in pellets was regenerated at 100 °C by flowing 100 ml/min of pure nitrogen for 2 hrs, then applied for CO_2 sorption again. The obtained CO_2 breakthrough curve is also presented in Figure 39. Consequently, the sorption capacity is calculated, being 126.0 mg-CO_2/g-sorbent, lower than that for the fresh sorbent. It may be due to the loss and/or degradation of PEI polymer or the incomplete desorption of CO_2 during the regeneration under the current conditions.

With the proved data from the small column test, the 200 ml column was packed with PEI/SBA-15 pellets. Then the column was pretreated under 100 mL/min of nitrogen at 100 °C for 24 hrs to ensure the "clean" of the packed sorbent. Before sorption, the weight of the column and the cleaned sorbent was measured. The simulated flue gas contain 15% CO_2 and 4.5% O_2 in N_2 was introduced at 400 ml/min under 75 °C and CO_2 concentration in the effluent was monitored by on-line MKS-2030 multigas analyzer.

Similar as the test in a small column, the scale-up column packed with PEI/SBA-15 pellets can also work effectively to remove CO_2 from flue gas down to very low level and show up a high capacity. On the basis of breakthrough curve, the sorption capacity can be calculated as of 135.0 mg-CO_2/g-sorbent, which is very close to the value obtained from the small scale test. This result indicates that the developed PEI/SBA-15 is able to be scaled up without losing its capacity for CO_2 capture. At this large scale, we have also test the regenerability of the PEI/SBA-15 pellets. The spent EPI/SBA-15 sorbent in pellets was regenerated at 90 °C by flowing 165 ml/min of pure nitrogen overnight, then applied for CO_2 sorption again. The obtained CO_2 breakthrough curve is also presented in Figure 40. The sorption capacity for the second cycle is about 119.2 mg-CO_2/g-sorbent, which is about 12% lower than that for the first cycle. Since it was desorbed for overnight, the decrease of the sorption capacity may be caused by the loss and/or degradation of PEI polymer during the regeneration under the studied conditions.

4.5.3. Scale-up test on PEI/FS sorbent

We have conducted a scale-up test on the developed cost-effective PEI/FS sorbents with a sorbent bed volume of 200 mL in order to provide more reliable and accurate parameters for the engineering design of the process and feasible study. Cab-O-Sil fumed silica (FS) from CABOT was used as the silica support material for preparation of new MBS. Polyethylenimine with average molecular weight of 600 was purchased from PolySciences Inc. The fumed silica supported polyethylenimine (PEI) sorbents were prepared via a wet impregnation method.

As described in the last report, we used the same stainless steel column (5.08 cm, O.D.; 4.12 cm, I.D.; 15 cm in Length, total volume, 200 mL) fabricated for this work. The primary concern in regarding to the reactor design for scale-up test is the system pressure drop caused by the packed bed with this fine powder sorbent, which can block the gas flow resulting in unreliable data. In addition, considering a very large amount of flue gas from coal-fired power plant needs to be processed, higher GHSV is preferred, which may push the fine sorbent powder in to the system, resulting in the blockage. One solution is to pack the reactor with sorbent in the form of pellet rather than in the form of fine powder, which will allow flue gas to flow easily through the sorbent, lowering the pressure-drop. Thus, we have made a pellet form (10-18 mesh, or 1-2 mm particles) of PEI/FS for this study. It should be noted that we did not apply any binding agents for pelletizing.

The appearance of the prepared pellet PEI/FS sorbent was compared with original PEI/FS sorbent in powder form and no significant change in PEI/FS after pelletizing was observed. Before the scale-up test using the 200 mL column, the pelletized PEI/FS sorbent has been evaluated for CO_2 capture from model flue gas to ensure its CO_2 sorption performance. A small column made of stainless steel with 150 mm in length and 7.7 mm in inner diameter (corresponding to a bed volume of 7.0 ml) is used for this small scale lab test. About 2 g of dry fine powder PEI/FS sorbent or pellet PEI/FS sorbent was packed into the sorption column. Before sorption, the sorbent was pretreated at 100 ºC in N_2 at a flow rate of 50 ml/min for 12 h to "clean" the sample. After cooling to the desired temperature, the simulated flue gas containing 15 % CO_2 and 4.5 % O_2 in N_2, which was purchased from GT&S Inc., was introduced into

sorption column at flow rate of 20 ml/min. When the outlet CO_2 concentration reached to the initial CO_2 concentration in the feed gas, it was switched to UHP N_2 (99.999 v%) at a flow rate of 50 ml/min and the sorbent bed temperature was increased to 100 ºC for desorption. The outlet gas was monitored by an on-line SRI 8610C gas chromatograph (GC) equipped with a molecular sieve 13X column, a silica-gel column and a thermal conductive detector (TCD). The results are presented in Figure 41.

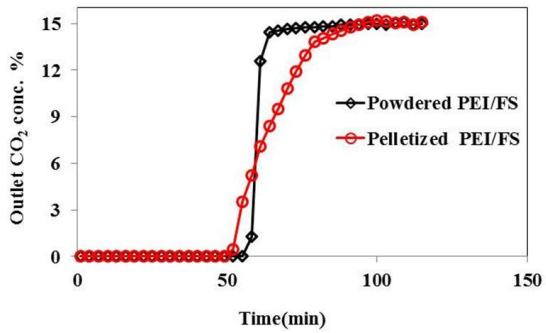

Figure 41. Breakthrough curves of CO_2 over the PEI/FS sorbent in fine powder (Black line) and in pellets (10-18 mesh, or 1-2 mm, Red line) at 75 °C for CO_2 capture from model flue gas containing 15% CO_2 in N_2.

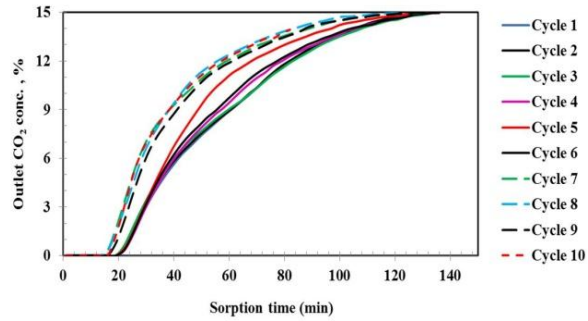

Figure 42. Breakthrough curves of CO_2 over the PEI/SBA-15 sorbent pellets (10-18 mesh, or 1-2 mm, 200 mL in total) at 75 °C for CO_2 capture model flue gas containing about 15% CO_2 and 4.5% O_2 in N_2 with a flow rate of 400 mL/min (a GHSV of ~120 h^{-1}).

The PEI/FS pellets can also work effectively to remove CO_2 from flue gas down to very low level and show up a high capacity, as shown in Figure 41. However, CO_2 broke through slightly earlier over PEI/FS pellets than that over the PEI/FS powder. At 75 ºC, the CO_2 breakthrough sorption capacity of powder PEI/FS is 135 mg-CO_2/g-sorbent. While the CO_2 breakthrough sorption capacity of pellet PEI/FS is 121 mg-CO_2/g-sorbent, which is 10 % lower than that of powder PEI/FS. The CO_2 saturation sorption capacity of pellet PEI/FS is 147 mg-CO_2/g-sorbent, which is close to that of powder PEI/FS, whose CO_2 saturation sorption capacity is 143 mg-CO_2/g-sorbent. It should also be noted that the sorption rate of pellet PEI/FS is slower than that of powder PEI/FS, as demonstrated by the breakthrough curves. To reach the saturation point, it took about 65 min for powder PEI/FS, whit it was about 100 min for pellet PEI/FS. It suggests making a pellet of PEI/FS sorbent could increase the internal diffusion barrier, thus results in a slower CO_2 sorption rate compared to the sorbent in powder form, which should be considered within the process design for the practical application. It should be mentioned that this phenomenon was not observed over PEI/SBA-15 sorbent, as described in our last report. It is probably because SBA-15 has stronger mechanic strength than the fumed silica used here.

With the proved data from the small column test, the 200 ml column (15 cm in Length, 5.08 cm in O.D. and 4.12 cm in I.D.) was packed with PEI/FS pellets (about 100 g, packing density is about 0.5 g/ml). Before sorption experiments, the sorbent was pretreated under 100 mL/min of nitrogen at 100 °C for 4 days by TGA to ensure the "clean" of the packed sorbent and stable mass of the sorbent material. Then, the weight of the column and the cleaned sorbent was measured. The simulated flue gas contain 15% CO_2 and 4.5% O_2 in N_2 was introduced at 400 ml/min under 75 °C and CO_2 concentration in the effluent was monitored by the on-line SRI 8610C GC. The obtained CO_2 breakthrough curve is also presented in Figure 42. Similar as the test in a small column, the scale-up column packed with PEI/FS pellets can also work effectively to remove CO_2 from flue gas down to very low level and show up a high capacity. On the basis of breakthrough curve, the sorption capacity can be calculated as of 113 mg-CO_2/g-sorbent, which is lower than the value obtained from the small scale test. This result indicates that the developed PEI/FS can be scaled up with about 20% loss in its initial capacity for CO_2 capture.

Additionally, we have also tested the regenerability of the PEI/FS pellets at this 200cc scale. The spent PEI/FS sorbent in pellets was regenerated at 100 °C by flowing 1000 ml/min of pure nitrogen overnight, then applied for CO_2 sorption again. The obtained CO_2 breakthrough curves of 10 cycles are

also presented in Figure 42 and sorption capacity as a function of regeneration cycle number is shown in Figure 43. As it can be seen, the capacity for the first 4 cycles is close, maintaining at 112 mg-CO_2/g-sorbent. A drop is observed at the 5th and 6th cycle, being 110 and 97 mg-CO_2/g-sorbent, respectively. Then, the sorption capacity maintains for the rest of cycles, indicating a good regenerability and relative high stability of PEI/FS sorbent pellets. Figure 44 shows the appearance of the PEI/FS sorbent material after 10 cycles of evaluation. For comparison, the image of PEI/FS pellets before CO_2 sorption is also presented. Clearly, after 10 cycles of CO_2 sorption-desorption, the PEI/FS pellets changed from white color to yellowish with some in brown, indicating the degradation of PEI polymer and/or PEI polymer getting out of the pore channels of fumed silica. The results show that it is important to further improve the thermal stability of the PEI/FS sorbent material for the practical application, which is now an important task of this project.

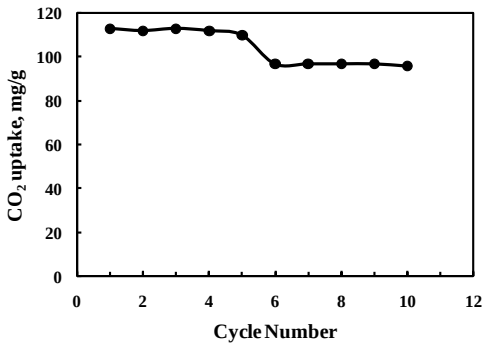

Figure 43. Breakthrough curves of CO_2 uptake as a function of cycle number during scale-up test over PEI/FS sorbent.

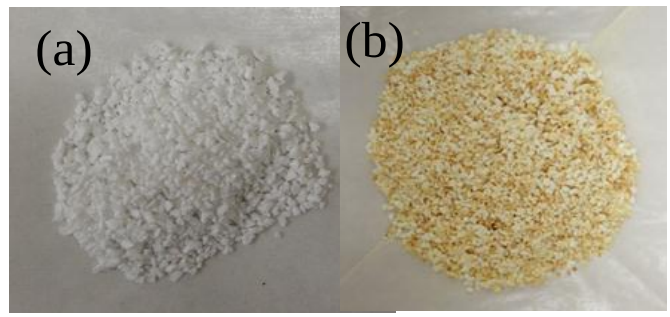

Figure 44. Appearance of PEI/FS pellets (10-18 mesh, i.e., 1-2 mm) (a) before and (b) after 10 cycles of CO_2 sorption-desorption.

4.6. Conducting a preliminary techno-economic analysis (Task 6)

One of the benefits of using solid sorbents for CO_2 capture relies in the reduction of the operational cost and especially heat requirements and costs related to corrosion. As proposed for project, we have conducted preliminary estimation on the energy consumption and material cost associate with the use of MBS for CO_2 capture.

4.6.1. Energy consumption estimation

In this project, a preliminary estimate of the heat requirements for MBS-2 and PEI-50/FS-M5 in comparison to amine scrubbing (30wt% MEA aqueous solution) has been evaluated compared. Table 17 lists the data considered for heat requirement evaluation. The values for MEA (30%wt) were obtained from the data reported by Kohl and Nielsen [6]. The heat capacity of PEI-50/FS-M5 and MBS-2 was averaged between the heat capacity of silica (SiO_2) and the heat capacity of PEI. The heat capacity of different forms of silica is reported to be between ~0.8 and 1 kJ/kg-K [7, 8] and is here considered to be 1 kJ/kg-K for both fumed silica and SBA-15. The heat capacity of the polymer was calculated according to the method reported by Maham et al. [9], where the contributions from four structural groups (CH2, NH, N and OH) are all considered. The molar capacity is therefore expressed as:

$$C_p = N_1C_p(CH2) + N_2C_p(NH) + N_3C_p(N) + N_4C_p(OH),$$

where N_x and $C_p(X)$ represent the number and the relative molar heat capacity contribution of the NH, N, CH2 and OH groups in a given alkanolamine molecule. Consequently, the heat capacity of the PEI polymer can be estimated to ~112 J/mol-K or ~2.6 J/g-K at 75 °C. The final heat capacity value for PEI-50/FS-M5 and MBS-2 was thus estimated to be ~1.8 J/g-K which is in agreement with values reported in the literature for amine functionalized solid sorbents [10] and very close to the value (1.6 J/g-K) reported by Ma et al. [11]. The heat of reaction was here approximated to 1436 kJ/kg-CO_2 that was obtained by Gray et al. for PEI impregnated on commercial fumed silica [12]. The heat requirements for the 30 wt%

MEA solution was adopted from the work by Abu-Zahra et al. [13], which is of 3.89 GJ/ton-CO_2 by considering the MEA solution with an amine lean loading of 0.242 mol-CO_2 per mole MEA and amine rich loading of 0.484 mol-CO_2 per mole MEA. The value is consistent with that reported in the literature [14].

Table 17. Operational and thermal data used for heat requirements estimates.

	MEA (30 wt%)	PEI-50/FS-M5	MBS-2	
T_{ads}	40	75	75	°C
T_{des}	120	100	100	°C
Heat capacity	3.89	1.8	1.8	kJ/kg-K
Density	1.005	0.43	0.17	g/ml
Integral heat of reaction	1919	1436	1436	kJ/kg-CO_2
Gravimetric capacity	75	133	140	mg/g
Volumetric capacity	75	57	24	mg/ml

To simplify the estimation for MBS-2 and PEI-50/FS-M5, the effect of moisture on the sorption capacity and heat requirement and the energy required for CO_2 compression have been neglected. The energy required for amine feeding is also neglected. Under the current assumptions and obtained data, the heat duty for MEA and MBS can be estimated. As shown in Figure 45, the heat requirement for the 30 wt% MEA solution was just below 4000 kJ/kg-CO_2. It was only about 2000 kJ/kg-CO_2 for MBS-2 and PEI-50/FS-M5. The energy consumption is two folds decrease using MBS instead of liquid MEA solution. The results obtained are comparable to those reported by Khatri et al. [7] for CO_2 capture by diamine-grafted SBA-15 of 1636 kJ/kg-CO_2, and compatible with the predictions of 50% reduction in heat requirements for the MBS in comparison to the commercial amine scrubbing process [11].

Furthermore, we have carried out the direct measurement of the thermal properties of MBS-2 and PEI-50/FS-M5 by TGA-DSC. Some preliminary attempts have been conducted using the DSC mode of the TA Q600 to determine the heat of reaction and heat capacity of PEI-50/FS-M5 as shown in Figure 46. Calibration was carried out using a sapphire for heat capacity and zinc for cell constant determination. The sample was first pretreated in N_2 at 100 °C. After 20 min at 75 °C, the 100% CO_2 stream was introduced. After 50 min of sorption, the temperature was slowly decreased to 30 °C. At 30 °C, the feed gas was switched to N_2 and the temperature was slowly risen (1 °C/min) to 110 °C. The heats obtained for sorption and desorption were very similar. The calculated heat of reaction during the sorption process was about 78 kJ/mol-CO_2 and the heat for desorption was measured to be 88 kJ/mol-CO_2.

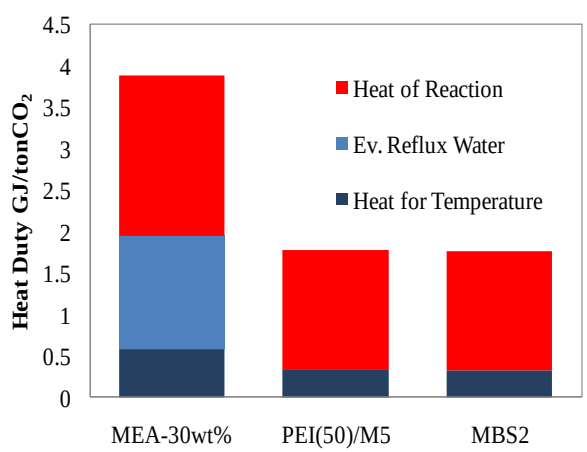

Figure 45. Heat requirements for the regeneration of the sorbents.

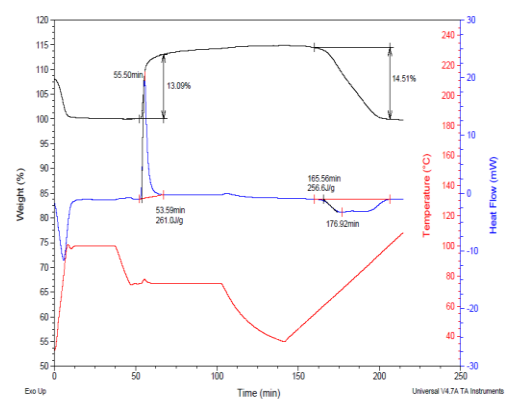

Figure 46. Weight (black), heat-flow (blue) and temperature (red) profiles during CO_2 sorption and desorption over PEI-50/FS-M5 sorbent.

4.6.2. Material cost estimation

As proposed, the major goal of this project is to develop a new generation of solid and regenerable polymeric molecular basket sorbent (MBS), which is more cost-effective than our early generation of MBS with a working capacity higher than 70 mg-CO_2/g-S. Within the project period, we have prepared several new MBSs using commercially available and cheap support materials including silica gel, fumed silica and carbon materials. All those MBSs have been examined for CO_2 capture and showed good CO_2 capacity. Here, we have conducted the economic analysis on the developed MBSs with the consideration of sorption capacity. The results are shown in Figure 47. The cost on kilograms basis was estimated from the material suppliers.

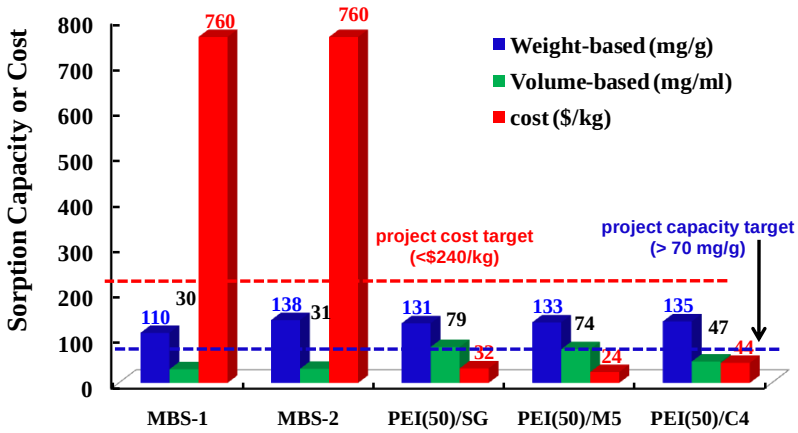

Figure 47. The comparison in the CO_2 sorption capacity and estimated material cost of the early generation and the new generation MBS developed in this project.

As it can be seen, the estimated preparation cost for PEI-50/SG, PEI-50/FS-M5 and PEI-50/C4 is $32, $24 and $44 per kilograms, while the estimated preparation cost of MBS-1 and MBS-2 reaches as high as $760/kg [15]. The preparation cost of the former is only about 3-6% of that of the latter. This is because the preparation cost of SBA-15 and MCM-41 accounts for more than 95% of the total preparation cost for MBS-1 and MBS-2. Thus, using a cheaper support material such as silica gel, fumed silica and/or carbon black, instead of MCM-41 and SBA-15 for MBS preparation could reduce the sorbent preparation cost by more than 90%, resulting in a significant decrease in the CO_2 capture cost. On the basis of CO_2 sorption capacity and the sorbent material preparation cost, the cost for CO_2 capture from the material aspect could be estimated. It is $6.9 and $5.5/g-$CO_2$ for MBS-1 and MBS-2, respectively. In contrast, it is only $0.24, $0.18 and $0.32/g-$CO_2$ for PEI/SG, PEI/M5 and PEI/C4, respectively.

It should also be mentioned that the new generation MBSs show not only cost-benefits, but also much higher volume-based CO_2 sorption capacity, especially for silica gel and fumed silica based MBS, which is about 2 times higher than that of MBS-1 and MBS-2. It is highly beneficial because higher volume-based CO_2 sorption capacity means significantly lower equipment size for the sorber using this type of sorbent material.

5. References

[1] Xu, X., et al., *Preparation and Characterization of Novel CO_2 "Molecular Basket" Adsorbents based on Polymer-modified Mesoporous Molecular Sieve MCM-41*. Microporous and Mesoporous Materials, 2003. **62** (1-2), p. 29-45.

[2] Wang, X.S., V.; Clark, J.; Ma, X.; Overbury, S.; Xu, X.; Song, C., *Infrared Study of CO_2 Sorption over "Molecular Basket" Sorbent Consisting of Polyethylenimine-Modified Mesoporous Molecular Sieve.* Journal of Physical Chemistry C, 2009, **113**, p. 7260-7268.

[3] Zhu T, Yang S, Choi DK, Row KH. Adsorption of carbon dioxide using polyethyleneimine modified silica gel. Korean J Chem Eng. 2010;27:1910–1915.

[4] Li, N.; Ma, X. L.; Zha, Q. F.; Kim, K.; Chen, Y. S.; Song, C. S. Maximizing the Number of Oxygen-Containing Functional Groups on Activated Carbon by Using Ammonium Persulfate and Improving the Temperature-Programmed Desorption Characterization of Carbon Surface Chemistry. Carbon 2011, 49, 5002

[5] Xu, X.C.; Song, C.S.; Miller, B.G.; Scaroni, A.W. Influence of moisture on CO_2 separation from gas mixture by a nanoporous adsorbent based on polyethylenimine-modified molecular sieve MCM-41. *Industrial & Engineering Chemistry Research*, **2005**. ***44****(21)*, 8113-8119.

[6] Kohl, A. L.; Nielsen, R. B., Gas Purification (5th Edition). Elsevier.

[7] Khatri, R. A.; Chuang, S. S. C.; Soong, Y.; Gray, M., Carbon Dioxide Capture by Diamine-Grafted SBA-15: A Combined Fourier Transform Infrared and Mass Spectrometry Study. Industrial & Engineering Chemistry Research 2005, 44 (10), 3702-3708.

[8] Bentz, D. P.; Flynn, D. R.; Kim, J. H.; Zarr, R. R., A slug calorimeter for evaluating the thermal performance of fire resistive materials. *Fire and Materials* **2006,** *30* (4), 257-270.

[9] Maham, Y.; G. Hepler, L.; E. Mather, A.; W. Hakin, A.; A. Marriott, R., Molar heat capacities of alkanolamines from 299.1 to 397.8 K Group additivity and molecular connectivity analyses. *Journal of the Chemical Society, Faraday Transactions* **1997,** *93* (9), 1747-1750.

[10] Satyapal, S.; Filburn, T.; Trela, J.; Strange, J., Performance and Properties of a Solid Amine Sorbent for Carbon Dioxide Removal in Space Life Support Applications. *Energy & Fuels* **2001,** *15* (2), 250-255.

[11] Ma, X.; Wang, X.; Song, C., A New Generation of "Molecular Basket" Sorbents (MBS) for Separation of CO2 and H2S from Various Gas Streams. 11th Annual SECA Workshop, Pittsburgh, PA, 2010.

[12] Gray, M. L.; Hoffman, J. S.; Hreha, D. C.; Fauth, D. J.; Hedges, S. W.; Champagne, K. J.; Pennline, H. W., Parametric Study of Solid Amine Sorbents for the Capture of Carbon Dioxide†. *Energy & Fuels* **2009,** *23* (10), 4840-4844.

[13] Abu-Zahra, M. R. M.; Schneiders, L. H. J.; Niederer, J. P. M.; Feron, P. H. M.; Versteeg, G. F., CO2 capture from power plants. Part I. A parametric study of the technicalperformance based on monoethanolamine. *International Journal of Greenhouse Gas Control* **2007,** *1* (1), 37-46.

[14] Asprion, N., CO2 post combustion capture by absorption. In *DECHEMA workshop on CO2*, Frankfurt, Germany, 2008.

[15] Wang, D.X., Sentorum-Shalaby, C., Ma, X.L., Song, C.S. High-Capacity and Low-Cost Carbon-Based "Molecular Basket" Sorbent for CO_2 Capture from Flue Gas. *Energy & Fuels*, 2011. **25**, p. 456-458

6. Publications and Presentations

Publications

[1] Dongxiang Wang, Cigdem Sentorum-Shalaby, Xiaoliang Ma, and Chunshan Song. High-Capacity and Low-Cost Carbon-Based "Molecular Basket" Sorbent for CO_2 Capture from Flue Gas. *Energy & Fuels*, **2011**, 25, 456-458.

[2] Zhonghua Zhang, Xiaoliang Ma, Dongxiang Wang, Chunshan Song, and Yonggang Wang. Development of Silica-Gel-Supported Polyethylenimine Sorbents for CO_2 Cpature from Flue Gas. *AIChE Journal* **2012**, 58, 2495-2502.

[3] Dongxiang Wang, Xiaoliang Ma, Cigdem Sentorum-Shalaby, and Chunshan Song. Development of Carbon-Based Molecular Basket Sorbent for CO_2 Capture. *Industrial & Engineering Chemistry Research*, **2012**, 51, 3048-3057.

[4] Xiaoxing Wang, Xiaoliang Ma, Vivane Schwartz, Jason Clark, Steven Overbury, Shuqi Zhao, Xiaochun Xu, and Chunshan Song. A Solid Molecular Basket Sorbent for CO_2 Capture from Gas Streams with Low CO_2 Concentration at Ambient Conditions. *Physical Chemistry Chemical Physics*, **2012**, 14 (4), 1485-1492.

[5] Xiaoxing Wang, Chunshan Song. Temperature-Programmed Desorption of CO_2 from Polyethylenimine-Loaded SBA-15 as Molecular Basket Sorbents. *Catalysis Today*, **2012**, 194, 44-52.

[6] Xiaoxing Wang, Xiaoliang Ma, Chunshan Song, Darren Locke, S. Siefert, R. E. Winans, J. Möllmer, M. Lange, A. Möller, R. Gläser. Molecular Basket Sorbents Polyethylenimine-SBA-15

for CO_2 Capture from Flue Gas: Characterization and Sorption Properties. Microporous and Mesoporous Materials, **2013**, 169, 103–111.

[7] Eric Fillerup, Xiaoxing Wang, Xiaoliang Ma, Chunshan Song. Utilization of polymer cross-linker to improve the thermal stability of "molecular basket" sorbents. *Preprints of Symposia – American Chemical Society, Division of Fuel Chemistry,* 55 (2), **2010**, pp.

[8] Xiaoliang Ma, Zhonghua Zhang, Jian Zhu, Xiaoxing Wang, Chunshan Song. CO_2 capture from the atmosphere using nano-porous-material-supported polyethylenimine sorbents. *Preprints of Symposia – American Chemical Society, Division of Fuel Chemistry,* 56 (1), **2011**, pp

[9] Xiaoxing Wang, Xiaoliang Ma, Vivane Schwartz, Jason Clark, Steven Overbury, Xiaochun Xu, Chunshan Song. "CO_2 Capture over Molecular Basket Sorbent: Sorption Mechanism Study" *Preprints of Symposia – American Chemical Society, Division of Fuel Chemistry,* 56 (2), **2011**, pp.

[10] Dongxiang Wang, Xiaoxing Wang, Xiaoliang Ma, Chunshan Song. CO_2 capture from flue gas using molecular basket sorbents with different supports. *Preprints of Symposia – American Chemical Society, Division of Fuel Chemistry,* 56 (2), **2011**, pp.

[11] Dongxiang Wang, Xiaoxing Wang, Xiaoliang Ma and Chunshan Song. CO_2 capture over molecular basket sorbent: Influence of three-dimensional structure. *Preprints of Symposia – American Chemical Society, Division of Fuel Chemistry,* 57 (2), **2012**, pp.

Presentations

[1] D.X Wang, X.X. Wang, X.L. Ma and C.S. Song. CO_2 capture over molecular basket sorbent: Influence of three-dimensional structure. 244th American Chemical Society meeting, Philadelphia, PA, Aug 19-23, 2012.

[2] E. Fillerup, D.X. Wang, X.X. Wang, C.S. Song. CO_2 Molecular Basket Sorbents: A Thermal Stability Study. *2012 NETL CO_2 Capture Science & Technology Meeting*. Pittsburgh, July 2012. [Poster]

[3] X.X. Wang, X.L. Ma, V. Schwartz, J.C. Clark, S.H. Overbury, X.C. Xu, C.S. Song. "CO_2 Capture over Molecular Basket Sorbent: Sorption Mechanism Study" 242nd *American Chemical Society Fall Meeting*. Denver, CO, August 28 – September 1, 2011.

[4] D.X. Wang, X.X. Wang, X.L. Ma, C.S. Song. CO_2 capture from flue gas using molecular basket sorbents with different supports. 242nd *American Chemical Society Fall Meeting*, Denver, CO, August 28 – September 1, 2011.

[5] X.X. Wang, D.X. Wang, E. Fillerup, E. Peduzzi, Z.H. Zhang, J.H. Guo, X.L. Ma, C.S. Song. CO_2 Capture Using Solid Molecular Basket Sorbents. *2011 NETL CO_2 Capture Science & Technology Meeting*. Pittsburgh, August 22-26, 2011.

[6] X.X. Wang, SQ Zhao, XL Ma, CS Song, Carbon dioxide sorption over molecular basket sorbents: a detailed TPD study. 22nd North American Catalysis Society meeting, Detroit, MI, June 2-10, 2011.

[7] X.X. Wang, S.Q. Zhao, X.L. Ma, C.S. Song. CO_2 capture from gas streams with low CO_2 concentrations using solid molecular basket sorbent. 241st *American Chemical Society Spring Meeting*. Anaheim, March 2011.

[8] X.L. Ma, Z.H. Zhang, J. Zhu, X.X. Wang, C.S. Song. CO_2 capture from the atmosphere using nano-porous-material-supported polyethylenimine sorbents. 241st *American Chemical Society Spring Meeting*. Anaheim, March 2011.

[9] X.L. Ma, X.X. Wang, C.S. Song. Advances and Challenges in Development of Amine-functionalized and Amine-immobilized Solid Sorbents for CO_2 Capture. *The International Chemical Congress of Pacific Basin Societies (PacifiChem 2010)*. Honolulu, December 2010.

[10] X.X. Wang, D.X. Wang, E. Fillerup, E. Peduzzi, Z.H. Zhang, X.L. Ma, C.S. Song. CO_2 Capture Using Solid Molecular Basket Sorbents. *2010 NETL CO_2 Capture Science & Technology Meeting*. Pittsburgh, September 2010.

[11] E. Fillerup, X.X. Wang, X.L. Ma, C.S. Song. Utilization of Polymer Cross-linker to Improve the Thermal Stability of Molecular Basket Sorbents. 240th *American Chemical Society Fall Meeting*. Boston, August 2010.

[12] X.X. Wang, X.L. Ma, C.S. Song. Novel Molecular Basket Sorbents (MBS) for CO_2 Capture from Flue Gas and Other Gas Streams. *DOE NETL SECA Technology Meeting*. Pittsburgh, May 2010 [Poster].

7. MILESTONE STATUS REPORT

ID	Project Milestone description	Project Duration Start: 9/1/2009 End: 8/31/2012												Planned Start Date:	Planned End Date:	Actual Start Date:	Actual End Date:	Comments (notes, explanation of deviation from plan)
		PY1				PY2				PY 3								
		Q1	Q2	Q3	Q4	Q5	Q6	Q7	Q8	Q9	Q10	Q11	Q12					
1	Provide primary results in development of MBS for CO_2 capture	■	■	■										9/1/2009	5/31/2010	9/1/2009	5/31/2010	**Complete**
2	Provide primary results in computational calculations		■	■	■									1/4/2010	9/30/2010	1/1/2010	9/30/2010	**Complete**
3	Complete the computational calculation and the development of MBS for CO_2 capture with working capacity of > 70 mg/g-S	■	■	■	■	■	■	■	■					9/1/2009	8/31/2011	9/1/2009	9/30/2011	**Complete**
4	Complete the improvement of the thermal stability of MBS									■	■	■	■	9/1/2011	8/31/2012	4/29/2011	8/31/2012	**Complete**
5	Complete the scale-up CO_2 sorption process using MBS						■	■	■					2/1/2011	8/31/2011	3/1/2011	9/30/2011	**Complete**
6	Prepare and provide the formulation of MBS and concept process for CO_2 capture from flue gas									■				8/1/2011	9/30/2011	6/1/2011	9/30/2011	**Complete**
7	Provide the quarterly technical & budgetary reports	■	■	■	■	■	■	■	■	■	■	■	■	quarterly	quarterly	1/1/2010	quarterly	**Complete**
8	Provide the final technical report including scale-up and economic analysis data												■	9/3/2012	11/30/2012	10/1/2012	11/30/2012	**Complete**

8. Milestones Status Description

Milestone 1. Provide primary results in development of MBS for CO_2 capture (9/1/2009 – 5/31/2010)

The primary results have been provided and this milestone was completed on time.

Milestone 2. Provide primary results in computational calculations (1/1/2010 – 9/30/2010)

The primary results have been provided and this milestone was completed on time.

Milestone 3. Complete the computational calculation and the development of MBS for CO_2 capture with working capacity of > 70 mg/g-S. (9/1/2009 – 9/30/2011)

With the efforts through this project, we have developed a new generation of MBS using cheap support material, commercially available fumed silica and silica gel materials. The sorption capacity of fumed silica and silica gel base MBS could be achieved as high as 140 mg/g-S. In addition, we have carried out computational calculation and the results showed that the addition of organic diacids such as oxalic acid could improve the thermal stability of new generation MBS, which leads to a new task and new Milestone 4 for this project. As of the date on 9/30/2011, this milestone has also been completed.

Milestone 4. Complete the improvement of the thermal stability of MBS (4/29/2011 – 8/31/2012)

To improve the thermal stability of the developed MBS, we have conducted two approaches: increasing the PEI molecular weight and cross-linking the PEI polymer. It was found that the use of PEI with high molecular weight is highly beneficial in terms of improving the thermal stability of MBS-2 materials for CO_2 capture. Within 10 and 20 repeated cycles, a reduction of about 80% and 90% in the loss of the sorbent capacity was successfully obtained by using PEI polymer with molecular weight of 1800 and wet conditions for CO_2 sorption and regeneration. Using oxalic acid to cross-link PEI, the sorption capacity decreased and the promotion effect on the thermal stability was only observed under wet conditions, but not significantly. The thermal stability of the OA cross-linked MBS-2(600) sorbent still needs to be improved further. As reported, this milestone has also been completed as of the date on 8/31/2012.

Milestone 5. Complete the scale-up CO_2 sorption process using MBS (3/1/2011 – 9/30/2011)

We have conducted the scale-up on PEI/SBA-15 sorbent as a base and on PEI/FS sorbent as newly developed and cost-effective material. The efforts showed that both PEI/SBA-15 and PEI/FS are scalable and showed a reasonable high capacity for CO_2 capture, being 135 and 113 mg/g-S, respectively. As reported, this milestone has also been completed as of the date on 9/30/2011.

Milestone 6. Prepare and provide the formulation of MBS and concept process for CO_2 capture from flue gas. (6/1/2011 – 9/30/2011)

Based on the capacity and sorption-desorption aspects of MBS materials, the concept process using the developed MBS for CO_2 capture from flue gas has been proposed and provided in the quarterly report. Please refer the 7th quarterly technical report. Consequently, this milestone is completed.

Milestone 7. Provide the quarterly technical & budgetary reports (1/1/2010 – 8/31/2012, quarterly)

As scheduled, the quarterly technical and budgetary reports are prepared and delivered on time. All the quarterly technical and budgetary reports have been submitted.

Milestone 8. Provide the final technical report including scale-up and economic analysis data (9/3/2012 – 10/31/2012)

As shown in this final report, the preliminary study on the scale-up and techno-economical analysis on the developed MBS materials has been performed and the results have been presented in the report. Consequently, this milestone has been completed.

9. Appendix – Supporting Figures

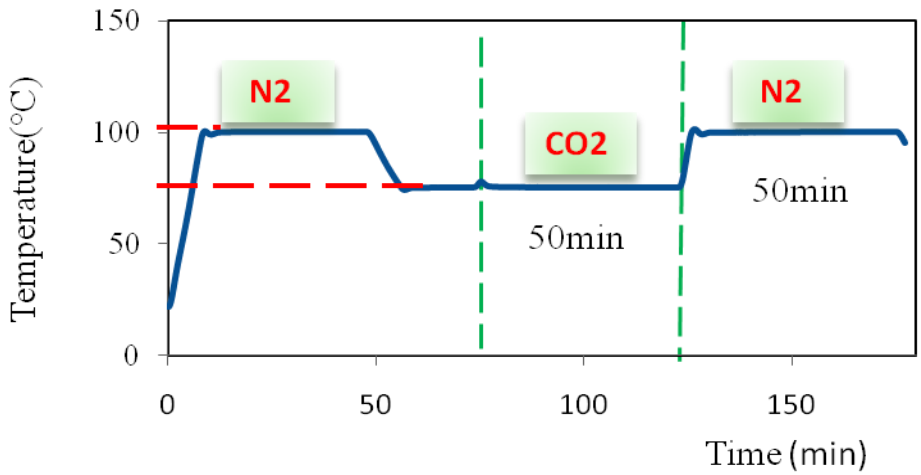

Figure S1. TGA temperature program for evaluation of CO_2 sorption-desorption performance of MBS.

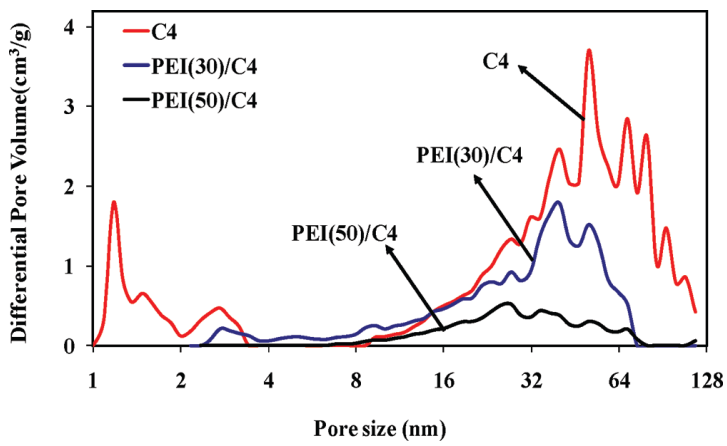

Figure S2. Pore size distribution of the parent C4 and PEI/C4 with different PEI loading.

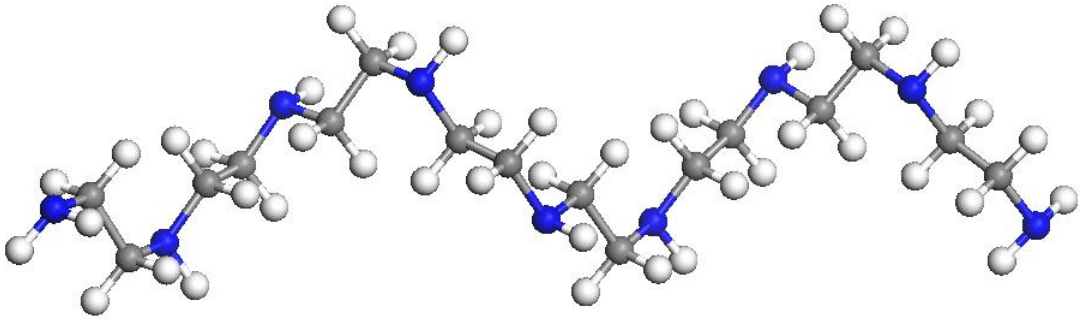

(a)

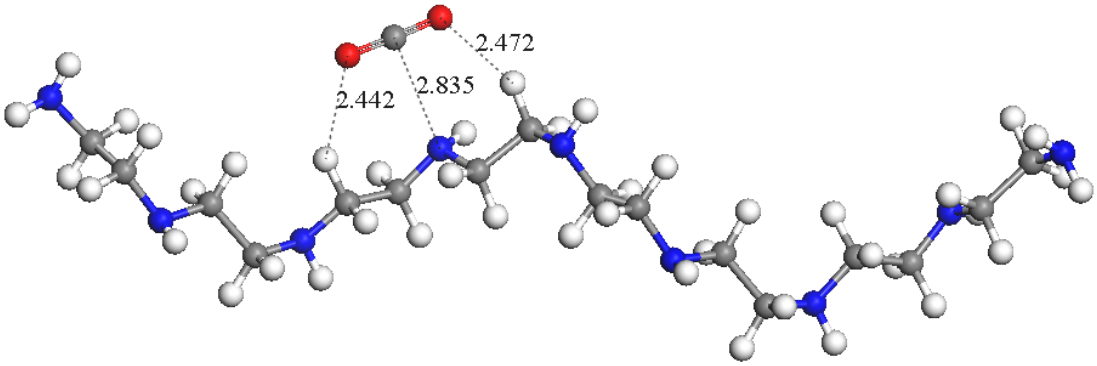

(b)

Figure S3. Structural configuration of (a) PEI and (b) CO_2 sorbed over PEI, calculated by AM1*. N atoms are depicted as blue spheres, C atoms are light grey spheres, H atoms are white spheres, O atoms are depicted as red spheres.

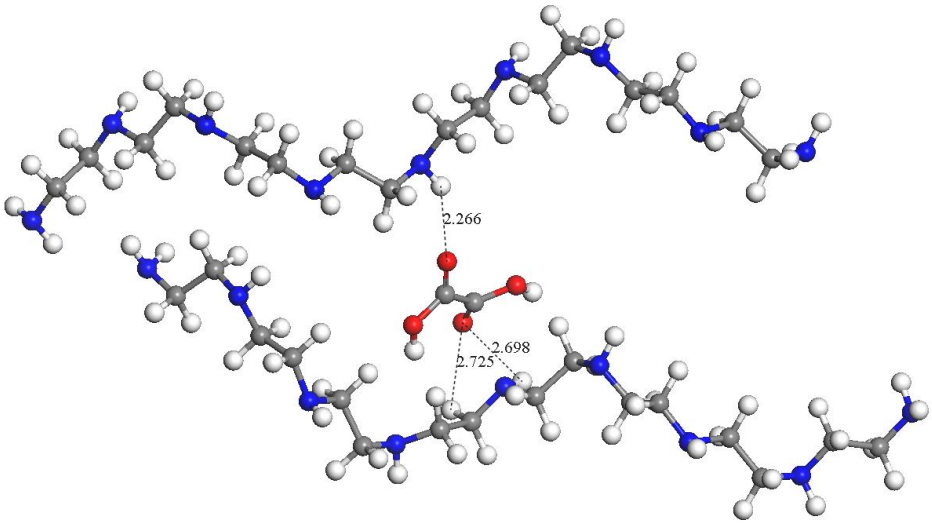

(a)

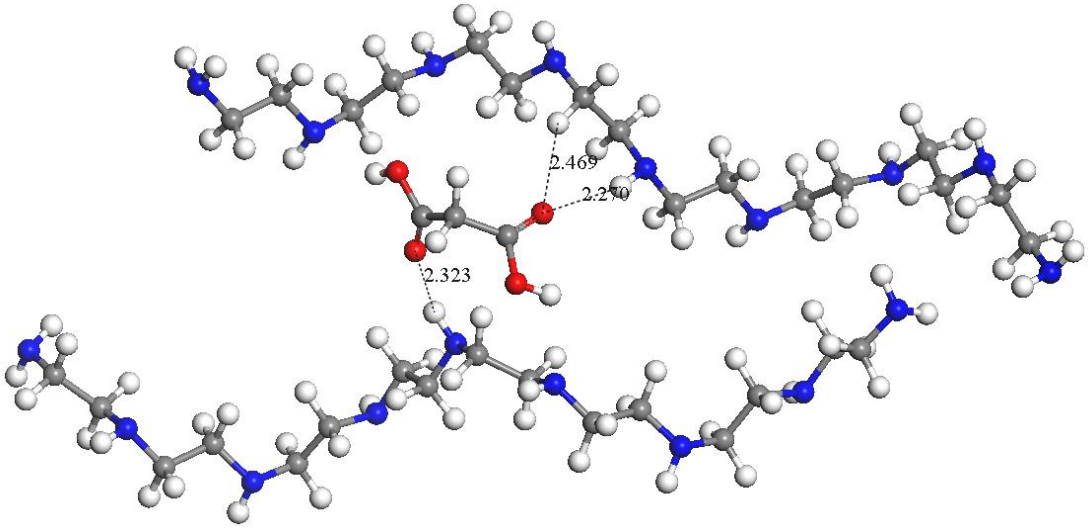

(b)

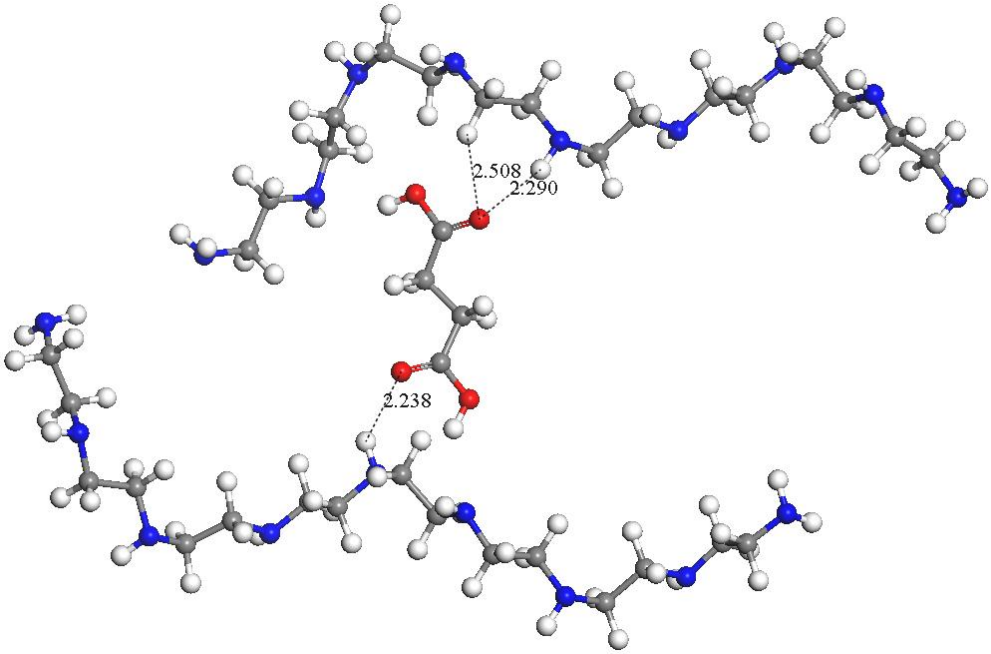

(c)

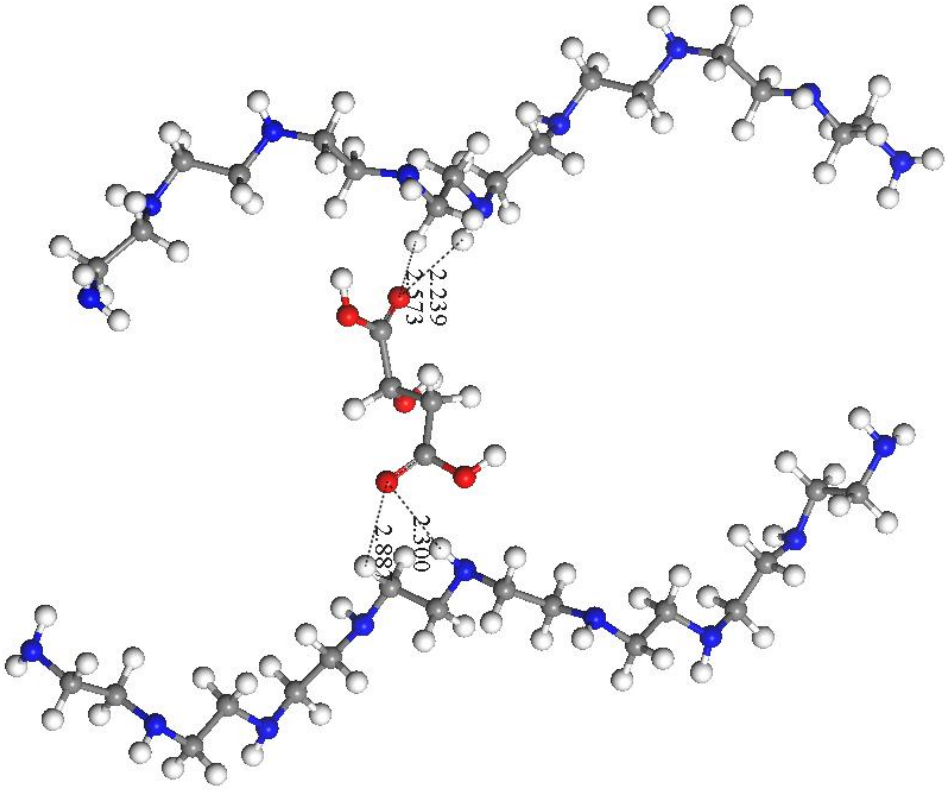

(d)

Figure S4. Configurations of cross-linked PEIs using (a) oxalic acid, (b) malonic acid, (c) succinic acid, and (d) DL-malic acid.

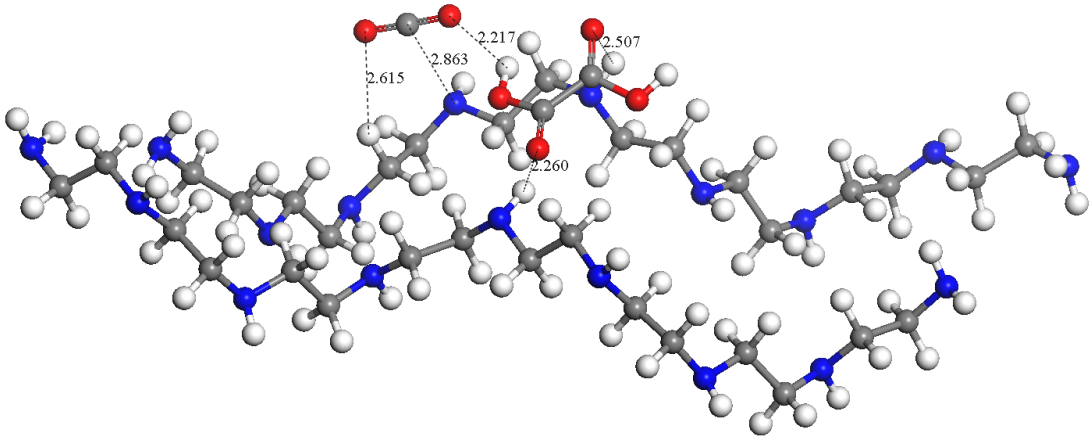

(a)

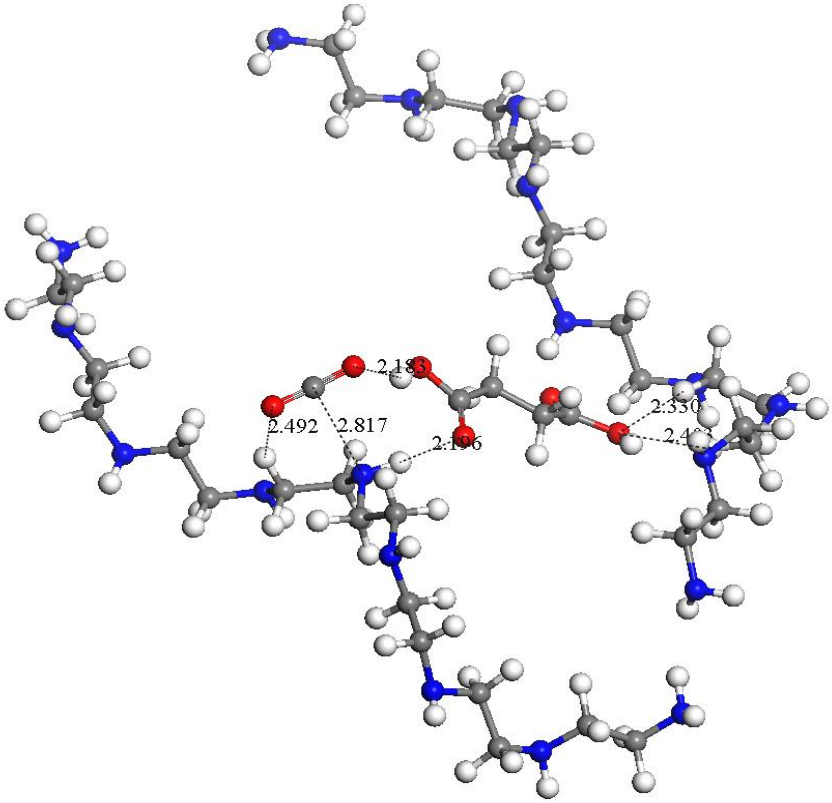

(b)

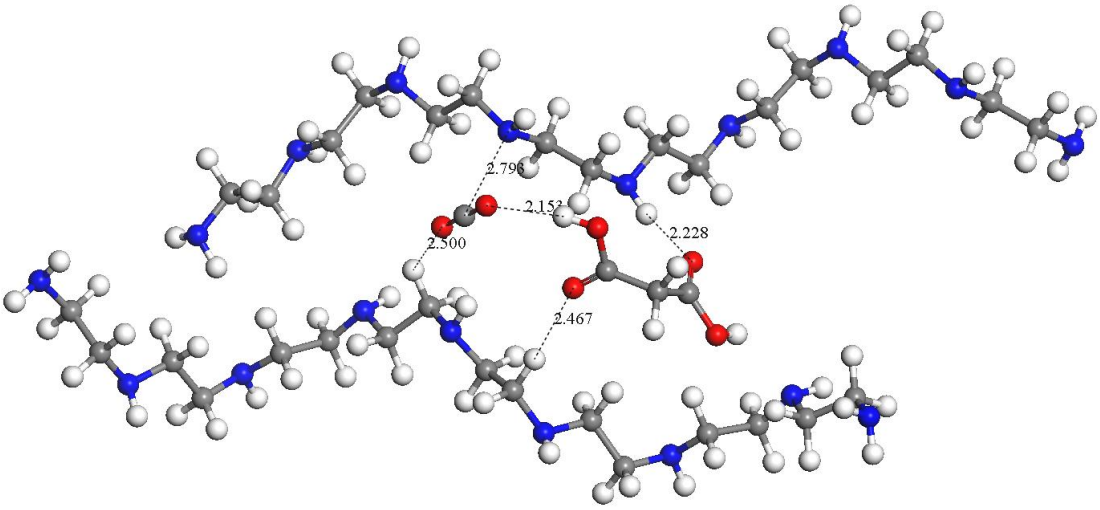

(c)

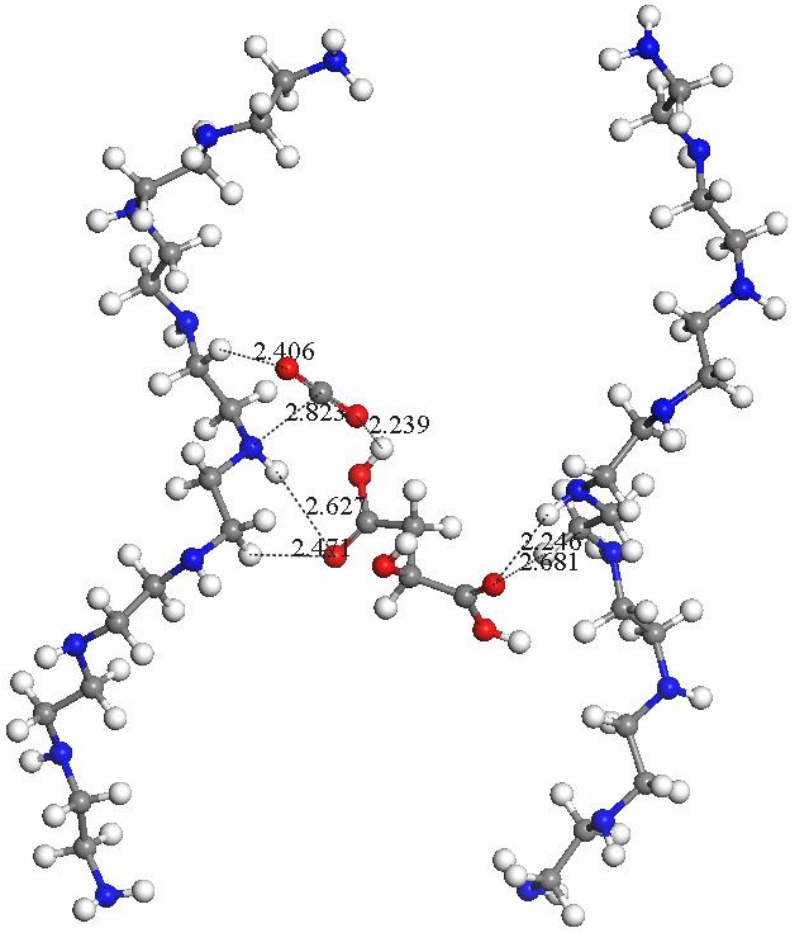

(d)

Figure S5. Configurations of CO_2 sorption on cross-linked PEIs using (b) malonic acid, (c) succinic acid, and (d) DL-malic acid.

COST PLAN/STATUS

Baseline Reporting Quarter	YEAR 1 Starts: 9/01/2009 Ends: 8/31/2010					YEAR 2 Starts: 9/01/2010 Ends: 8/31/2011					YEAR 3 Starts: 9/01/2011 Ends: 8/31/2012						
	Q1 - 09/09	Q2 - 12/09	Q3 - 03/10	Q4 - 06/10	YEAR 1 TOTAL	Q5 - 09/10	Q6 - 12/10	Q7 - 03/11	Q8 - 06/11	YEAR 2 TOTAL	Q9 - 9/11	Q10 - 12/11	Q11 - 3/12	Q12 - 6/12	YEAR 3 TOTAL	Q13 - 8/12	PROJECT TOTAL
Baseline Cost Plan																	
Federal Share	5,209.73	25,061.52	43,235.35	40,346.49	113,853.09	54,451.53	41,605.08	69,931.39	57,729.77	223,717.77	29,855.00	29,855.00	29,855.00	29,856.14	119,421.14		456,992.00
%	0.57	0.63	0.75	0.79	0.72	0.86	0.70	0.77	0.86	0.80	0.81	0.81	1.00	1.00	0.89		0.80
Non-Federal Share	4,009.91	14,755.88	14,071.46	10,742.12	43,579.37	8,990.88	17,836.85	20,338.48	9,528.90	56,695.11	7,012.00	7,012.52			14,024.52		114,299.00
%	0.43	0.37	0.25	0.21	0.28	0.14	0.30	0.23	0.14	0.20							0.20
Total Planned	9,219.64	39,817.40	57,306.81	51,088.61	157,432.46	63,442.41	59,441.93	90,269.87	67,258.67	280,412.88	36,867.00	36,867.52	29,855.00	29,856.14	133,445.66		571,291.00
Cumulative Baseline Cost	9,219.64	49,037.04	106,343.85	157,432.46		63,442.41	122,884.34	213,154.21	280,412.88		36,867.00	73,734.52	103,589.52	133,445.66			571,291.00
Actual Incurred Costs																	
Federal Share	5,209.73	25,061.52	43,235.35	40,346.49	113,853.09	54,451.53	41,605.08	69,931.39	68,771.33	234,759.33	12,639.77	5,481.50	20,199.14	49,967.23	88,287.64	20,091.94	456,992.00
%	0.57	0.63	0.75	0.79	0.72	0.86	0.70	0.77	0.81		0.65	1.00	1.00	1.00			
Non-Federal Share	4,009.91	14,755.88	14,071.46	10,742.12	43,579.37	8,990.88	17,836.85	20,338.48	16,612.69	63,778.90	6,940.73	-	-	-	6,940.73	-	114,299.00
%	0.43	0.37	0.25	0.21	0.28	0.14	0.30	0.23	0.19		0.35	-	-	-			
Total Incurred Costs - Qtrly	9,219.64	39,817.40	57,306.81	51,088.61	157,432.46	63,442.41	59,441.93	90,269.87	85,384.02	298,538.23	19,580.50	5,481.50	20,199.14	49,967.23	95,228.37		571,291.00
Cumulative Incurred Costs	9,219.64	49,037.04	106,343.85	157,432.46		63,442.41	122,884.34	213,154.21	298,538.23		19,580.50	25,062.00	45,261.14	95,228.37			
Variance																	
Federal Share	-	-	-	-		-	-	-	(11,041.56)		17,215.23	24,373.50	9,655.86	(20,111.09)			
Non-Federal Share	-	-	-	-		-	-	-	(7,083.79)		71.27	7,012.52	-	-			
Total Variance - Qtrly	-	-	-	-		-	-	-	(18,125.35)	-	17,286.50	31,386.02	9,655.86	(20,111.09)			
Cumulative Variance	-	-	-	-		-	-	-	(18,125.35)		(838.85)	30,547.17	40,203.03	20,091.94			

Variance Explanations: